Journal Pre-proof

Architecture and kinematics of the Famatinian deformation in the Sierra Grande de San Luis: A record of a collisional history at 33° S latitude

Augusto Morosini, Rodolfo Christiansen, Eliel Enriquez, Diego S. Pagano, Juan M. Perón Orrillo, Ariel Ortiz Suárez, Myriam P. Martínez, Brian L. Muñoz, Gabriel Ramos

PII: S0895-9811(20)30529-0

DOI: https://doi.org/10.1016/j.jsames.2020.102986

Reference: SAMES 102986

To appear in: *Journal of South American Earth Sciences*

Received Date: 8 April 2020

Revised Date: 14 October 2020

Accepted Date: 22 October 2020

Please cite this article as: Morosini, A., Christiansen, R., Enriquez, E., Pagano, D.S., Perón Orrillo, J.M., Suárez, A.O., Martínez, M.P., Muñoz, B.L., Ramos, G., Architecture and kinematics of the Famatinian deformation in the Sierra Grande de San Luis: A record of a collisional history at 33° S latitude, *Journal of South American Earth Sciences* (2020), doi: https://doi.org/10.1016/j.jsames.2020.102986.

Author statement

- All the guest editor suggestions were taken into account for the new presentation.
- The title was subtly modified.
- Some paragraphs were modified during the new corrections to improve grammar and spelling.

We are very grateful with the reviewers and editors, and we hope that with the modifications made we can satisfy expectations.

Sincerely,

Augusto. F. Morosini

Architecture and kinematics of the Famatinian deformation in the Sierra Grande de San Luis: a record of a collisional history at 33° S latitude

Augusto Morosini[1,2]*, Rodolfo Christiansen[3,4], Eliel Enriquez[1], Diego S. Pagano[1], Juan M. Perón Orrillo[1,2], Ariel Ortiz Suárez[1], Myriam P. Martínez[3], Brian L. Muñoz[1], Gabriel Ramos[1]

[1] Departamento de Geología – UNSL - San Luis, Argentina
[2] CCT - CONICET - San Luis, Argentina
[3] IGSV - UNSJ - San Juan, Argentina
[4] CCT - CONICET - San Juan, Argentina
*Corresponding author; e-mail: afmorosini@gmail.com
Departamento de Geología, Universidad Nacional de San Luis. Ejército de los Andes 950 (D5700HHW), San Luis, Argentina.
Phone: +54 (0266) 4520300 int. 2515

Abstract

An improved understanding of the evolution of the Famatinian basement in the Sierra Grande de San Luis (SGSL) in Argentina is presented. Combining geological, geophysical and petrological data, a 3D inversion model for the basement rocks and their shear zones in the study area was constructed. The inversion model and the ground data show that the main deformation mechanism that affected the metamorphic complexes is related to a significant number of shear zones which delineate the architecture of the basement. Results suggest that the regional scale shear system (~40 km wide and ~120 km long) and the internal structural elements of the different tectonic domains are the product of an important crustal shortening. A contractional tectonic framework related to the indentation of the Cuyania/Precordillera microcontinent on the western Gondwana margin is proposed to be the cause of the tectonic mechanisms that led to a pop-up megastructure in the western sector of the SGSL and the closing of the Famatinian backarc.

Keywords: Shear zone system, Tectonic evolution, Pop-up structure, Gravity/magnetic data, Structural analysis.

1. INTRODUCTION

The processes that affected the basement units in the Sierra Grande de San Luis (SGSL) have been the subject of extensive discussions in the last 20 years (e.g. Sims et al., 1998; von Gosen and Prozzi, 1998; Sato et al., 2003; Ortiz Suárez and Casquet, 2005; Delpino et al., 2007; 2016; Steenken et al., 2008; Morosini et al., 2014; Christiansen et al., 2019). These units represent the root of the Famatinian orogen, which was associated with a convergent plate motion at the Western Gondwana margin in Ordovician-Silurian times. Therefore, revealing the basement architecture is essential for the reconstruction of the paleotectonic setting. The systematic study of the shear zones that delineate the crustal geometry during tectonic processes is a fundamental step to understand the geodynamic processes that created the different orogenies in the world (e.g. Solar and Brown, 2001; Little et al., 2002; Goscombe et al., 2005; Chetty and Bhaskar Rao, 2006; Schulmann et al., 2008; Carosi et al., 2018).

The structural and kinematic features of the shear zones in the SGSL were studied in detail by von Gosen (1998a, b). This author interprets that the arrangement of the crustal blocks (or metamorphic complexes) in the southwestern sector of the study area was related to transpressive stress conditions due to a sinistral oblique contractional strain. Later, von Gosen and Prozzi (2005) observed dextral mylonitic zones as a result of a WNW-ESE shortening process, combining sinistral and dextral oblique contractional deformations in a conjugated system. On a regional tectonic scale, a collision model was suggested in which the Cuyania/Precordillera microcontinent acted as an indenter due to its shape (curved toward the exterior) conditioning the different orientations of the dextral and sinistral faults during the Late Ordovician-Early Devonian (von Gosen et al., 2002). Although very detailed studies about the shear zones were carried out by these authors, the architecture of southern SGSL was better understood after the construction of a three-dimensional model using the structural data with geophysical and petrophysical constraints (Christiansen et al., 2019).

The shear zones in the western portion of the SGSL were studied in this work, incorporating new structural and geophysical data of the northern sector, which were not considered in Christiansen et al. (2019). New evidence about the ductile deformation style and the tectonic setting during the Famatinian orogeny is presented in a three-dimensional model in order to establish the geodynamic evolution of the western proto-margin of Gondwana.

2. GEOLOGICAL SETTING

2.1. Regional context

Several Neoproterozoic to Paleozoic elements formed the Terra Australis Orogen along the South American Andes (Cawood, 2005). The late Cenozoic tectonics in the Andean foreland, known as the Pampean flat-slab of the Central Andes (Ramos et al., 2002), caused a great exposure to these elements developed during the Pampean and Famatinian cycles in the Sierras Pampeanas of Argentina.

The Pampean events (Aceñolaza and Toselli, 1976; Dalla Salda, 1987; Rapela et al., 1998; Escayola et al., 2007; Rapela et al., 2007; Ramos et al., 2014) occurred from the Ediacaran (~550 Ma) to the Stage 3 of the Cambrian (~515 Ma) (Siegesmund et al., 2010; Baldo et al., 2014). The most important outcrops of this orogenic cycle are recognized in the basement of the Sierras de Córdoba (Fig. 1). These events were developed in a context were a subduction-related magmatic arc was active between 550 and 525 Ma (Schwartz et al., 2008; Iannizzotto et al., 2013; Baldo et al., 2014; López de Luchi et al., 2018). A new short and intense tectono-thermal event followed the subduction stage, deforming and metamorphosing an accretionary prism in amphibolite to granulite facies, located on the western side of the arc at ~520 Ma (Tibaldi et al., 2008). Several hypotheses explain the origin of this orogeny: (a) the collision of a continental terrane named Pampia against the Río de la Plata Craton (Ramos, 1988), b) the subduction of a seismically active ocean ridge, or ridge-trench collision (Gromet et al., 2005; Schwartz et al., 2008), (c) the collision of a ridge against the Kalahari craton, subsequent collision of the Western Sierras Pampeanas block, and displacement by a transform fault to the Río de la Plata craton (Rapela et al., 2007), (d) the collision of an island arc with the Río de La Plata craton and subsequent Pampia terrain collision (Escayola et al., 2007; Steenken et al., 2010), e) the collision of an exotic Laurentian MARA block (acronym of Maz, Arequipa, Río Apa) again the Kalahari and Rio de la Plata cratons (Casquet et al., 2012, 2018), among others.

The Famatinian orogeny was originally defined by Aceñolaza and Toselli (1976) in order to group the tectono-sedimentary events that occurred during the Lower Paleozoic in the northwestern and central regions of Argentina. However, there is evidence that these events can be extended to the north up to the Venezuelan Andes, and to the south, until the central part of Patagonia (Ramos, 2018). The Famatinian magmatic arc is represented by excellent outcrops of Early Paleozoic batholiths, which were formed along the paleo-Pacific Gondwana margin, in the Sierra de Famatina (Toselli et al., 1996; Saavedra et al., 1998; Pankhurst et al., 1998). In the geodynamic context of Argentina, the Famatinian arc is genetically related to an east-dipping subduction zone and to a backarc metamorphic belt bordering the preceding peri-Gondwanan Pampean orogen (Otamendi et al., 2020). Southward of 28° south latitude, the orogenic exhumation can be considered an episode associated with the closure of the arc due to a continent-to-arc collision (Astini and Dávila, 2004; Cristofolini et al., 2014; Otamendi et al., 2020).

The Famatinian arc initiated at ~495 Ma when a subduction regime was re-established along the western margin of the Pampean orogen and was continuously active during the Early Ordovician (Pankhurst et al., 1998; Sims et al., 1997; Steenken et al., 2004; Cristofolini et al., 2014). This arc developed in a thick and wide sedimentary basin, which contained sediments from the erosion of the exhumed Pampean arc, and were deposited between ~530 and ~495 Ma, as the Meson Group, and the Negro Peinado, Achavil and San Luis Formations (Drobe et al., 2009; Cristofolini et al., 2012; Rapela et al., 2016; Perón Orrillo et al., 2019). Subduction-related magmatism in the Sierras Pampeanas segment ceased about ~465 Ma (Cristofolini et al., 2012; Ducea et al., 2015; Morosini et al., 2017; Otamendi et al., 2017). At this time, the Famatinian orogen began its intense construction, southward of 28° south latitude, so the arc and backarc were internally structured and differentially uplifted during the collision of the Laurentian-derived Cuyania/Precordillera microcontinent (Thomas and Astini, 1996; Benedetto, 2004; Otamendi et al., 2020) against the western margin of Gondwana (Astini and Davila, 2004; Ramos, 2004; Otamendi et al., 2009, 2017; Ducea et al., 2010, 2015; Ramos et al., 2010; Cristofolini et al., 2014). This continent-arc collision conditioned the different orientations of the fault trends during the Mid Ordovician-Early Devonian times (von Gosen et al., 2002; Astini and Dávila, 2004). Furthermore, this collision produced the current exposures of the Famatinian deep paleo-arc that show a continuous deepening from north to south (Otamendi et al., 2010; Tibaldi et al., 2013; Cristofolini et al., 2014) and from east to west (Camilletti et al., 2020). During the Famatinian belt construction, the deformation was regionally resolved in different ways; through large scale fold and thrust belts in the upper crust (Astini and Dávila, 2004), along major shear zones in the front and margins of the Famatinian paleo-arc (von Gosen and Prozzi, 1998, 2005; Höckenreiner et al., 2003; Cristofolini et al., 2014; Mulcahy et al., 2014), through large-scale west-verging shear zones located in the Pampean basement (Sims et al., 1997; Martino, 2003; Cristofolini et al., 2017; Semenov et al., 2019), and double-vergent structures developed in the paleo-backarc (Larrovere et al., 2017; Christiansen et al., 2019). Further, contraction at mid-crustal level in the paleo-backarc was predominately focused along west-verging reverse ductile shearing and folding (Finch et al., 2017; Larrovere et al., 2020).

The Achalian orogeny occurred during the Mid-Late Devonian (Sims et al., 1997) and produced, to a lesser extent, deformation in the area. The collision of the Chilenia terrane (Ramos et al., 1984) against the western margin of the Cuyania/Precordillera terrane, which was already amalgamated to Gondwana, caused reactivation of ancient shear zones and intra-plate plutonic activity (Sims et al., 1998; Steenken et al., 2008). This plutonism was widely distributed along the Sierras Pampeanas Orientales (southward of 27° S) and was associated with a stage of uplift and erosion (Sato et al., 2003; Llambías et al., 1998; Morosini et al., 2017) related to progressive delamination of the crust, accompanied by upwelling of the upper mantle from south to north (Grosse et al., 2009).

2.2. Local geology of the Sierra de San Luis

The SGSL is located in the southern sector of the Sierras Pampeanas (Caminos, 1979) and has approximately 160 km long and 80 km wide (Fig. 2). Three NNE trending metamorphic complexes integrate the SGSL: the Conlara (CMC), Pringles (PMC) and Nogolí (NMC) Metamorphic Complexes (Sims et al., 1997). In the southern sector, these units are separated by two low-grade metamorphic belts named San Luis Formation (SLF) (Prozzi and Ramos, 1988). In the north area, a medium-grade metamorphic unit called Las Higueras (Ortiz Suárez et al., 2009) separates the Conlara from the Pringles Metamorphic Complex. The presence of ductile shear zones between metamorphic units indicates tectonic contacts (von Gosen and Prozzi, 1998; Ortiz Suárez and Casquet, 2005; Christiansen et al., 2019).

The Conlara Metamorphic Complex is located in the eastern sector of the SGSL. It is subdivided into two metamorphic domains (Sims et al., 1997; Morosini et al., 2019; Christiansen et al., 2019), one is predominantly composed by schistose rocks, equivalent to the Las Aguadas Group (Ortiz Suárez, 1988), and the other is predominantly composed by migmatites, named San Martín Group (Enriquez et al., 2015). Las Aguadas Group comprises mid-grade metamorphic rocks (high-greenschist to low-amphibolite facies), which correspond to gneisses, quartz-feldspar schists (banded) and micaceous schists (Ortiz Suárez, 1998; Morosini et al., 2019). The San Martín Group comprises rocks of a higher metamorphic grade (high-amphibolite facies) and is mostly composed by migmatites (metatexites and diatexites), orthoamphibolites and to a lesser extent marbles and calc-silicate rocks (Llambías and Malvicini, 1982; Delakowitz et al., 1991; López de Luchi et al., 2003). The sedimentary protoliths of this complex are the oldest in the SGSL with maximum depositional ages of 580 Ma (Steenken et al., 2006; Drobe et al., 2009) or 550 Ma (Rapela et al., 2016), probably they are equivalent to the Puncoviscana series of the NW of Argentina (Drobe et al., 2009, 2011) (Fig. 3). Three deformational phases (Ortiz Suárez, 1988) with two folding stages (von Gosen and Prozzi, 1998) were recognized in the Conlara Metamorphic Complex. The third deformational phase was contemporaneous with the El Peñón granite intrusion, dated at 497 ± 8 Ma (SHRIMP U/Pb-Zrn, Steenken et al., 2006), indicating that at least part of the tectonic evolution of CMC occurred during the Upper Precambrian. The age of metamorphism remains unsolved for this complex; Whitmeyer and Simpson (2004) reported metamorphic ages of 470-482 Ma (U/Pb-monazite), while age of 564 ± 21 Ma (stepwise leaching Pb/Pb-garnet data) was published by Siegesmund et al. (2010).

The Nogolí Metamorphic Complex is located in the western sector of SGSL. It is composed of paragneisses, orthogneisses, migmatites, schists, orthoamphibolites, marble, calc-silicate rocks and banded iron layers (Ortiz Suárez, 1999; González et al., 2002, 2004; Carugno Durán and Ortiz Suárez, 2012). According to González et al. (2004) this complex is integrated by different metasedimentary units with distinctive metamorphic degrees, from rocks that reached anatexis in high amphibolite facies (metatexites and diatexites), to rocks without fusion (middle-greenschist facies), represented mainly by metapsammites and metapelites (Drobe et al., 2009). According to its deformation, two structural sets can be recognized within this complex: one is a relict NW foliation attributed to pre-Famatinian events and the other is a penetrative NNE foliation assigned to Famatinian events (Sato et al., 2003; González et al., 2004). The average metamorphic age for this complex is 467 ± 12 Ma (Ortiz Suárez, 1999; González et al., 2002; Sato et al., 2005; Steenken et al., 2006; Carugno Duran and Ortiz Suárez, 2012), indicating an Ordovician metamorphic climax (Famatinian) (Fig. 3). The maximum depositional age of the protoliths was defined at ~530 Ma by U/Pb in detrital zircons, and they have a provenance source from the Pampean and Brasiliano orogenies (Drobe et al., 2009).

The Pringles Metamorphic Complex is located in the central sector of the SGSL, and includes two units; a middle-grade metamorphic unit called Micaschist Group (MG) by von Gosen and Prozzi (1998), and a high-grade metamorphic unit which reaches granulite facies (Hauzenberger et al., 2001; Delpino et al., 2001, 2016; Ortiz Suárez and Casquet, 2005) named San José Complex (SJC) by Costa et al. (2001). The Micaschist Group is arranged along two belts on both sides of the San José Complex. The metamorphic conditions for this unit vary from high-greenschist to middle-amphibolite facies and represent middle crustal portions (von Gosen and Prozzi, 1998; Morosini et al., 2014). It is composed by micaceous and quartz-feldspar schists, quartzites and calc-silicates (Ortiz Suárez et al., 1992; von Gosen, 1998a, b). The San José Complex is principally composed of migmatites and paragneisses, and to a lesser extent, by amphibolites, granulites, orthogneisses and calc-silicate rocks, metamorphosed in high-amphibolite to granulite facies. The La Jovita-Las Águilas mafic-ultramafic Complex (Sato et al., 2003) is hosted by the San José Complex and is spatially related to an internal mylonitic zone called La Arenilla (Ortiz Suárez et al., 1992). The average metamorphic age of the Pringles Metamorphic Complex is 469 ± 22 Ma (Sims et al., 1998; Ortiz Suárez, 1999; Steenken et al., 2006) (Fig. 3). The maximum depositional age of the sedimentary protoliths is ~530 Ma, with provenance from a Pampean source (Sims et al., 1998; Steenken et al., 2006).

Las Higueras Complex, located in the northwest of SGSL, is integrated by metapelites, metasandstones, calc-silicates and metavolcanic rocks metamorphosed under low-amphibolite facies (Ortiz Suárez et al., 2009). It shows a penetrative NNE to NE axial plane foliation, which dips mainly to the NW and to a lesser extent, towards the SE (Ortiz Suárez et al., 2009). Hornfels were recognized in this unit caused by the intrusion of Devonian granitic plutons, like El Telarillo, El Hornito and La Población (Ortiz Suárez et al., 2009). This complex presents lithology similarities with the San Luis Formation, but probably with different tectonothermal evolution, which suggests a link with the Micaschist Group (Ortiz Suárez et al., 2009). However, it also presents some common features with Las Aguadas Group (schists of the Conlara Metamorphic Complex). The absolute age of metamorphism of this complex is still unknown.

The San Luis Formation is a metasedimentary unit composed of siliciclastic sedimentary successions metamorphosed under greenschist facies (Ortiz Suárez et al., 1992; von Gosen, 1998b). The most abundant protoliths recognized in this unit are mudstones, sandstones and conglomerates (Ortiz Suárez et al., 1992), along with scarce rhyolites and dacites that intruded as dikes and sills (von Gosen and Prozzi, 1998; Casquet et al., 2014; Perón Orrillo et al., 2019). This unit shows tight folds with hinge lines plunging slightly toward NNE. The axial planes are marked by sub-vertical NNE-trending phyllitic cleavage that dips either to the NW or to the SE (von Gosen, 1998b; von Gosen and Prozzi, 1998; Perón Orrillo et al., 2019). The absolute age of metamorphism for this unit remains unknown, but it is restricted to have occurred after the intrusion of metavolcanic rocks dated at 467.4 ± 5.1 Ma (Casquet et al., 2014) and related to the Famatinian magmatic arc stage during the early to middle Ordovician (von Gosen, 1998b). Maximum depositional age in the western belt straddles over the transition from the late Neoproterozoic (~555 Ma) to the early Cambrian (~530 Ma), whereas maximum depositional age in the eastern belt is late Cambrian (~515 Ma) (Perón Orrillo et al., 2019). Both belts of the San Luis Formation show U-Pb age distributions of detrital zircons with dominant peaks that are characteristic of the orogenic systems in the West Gondwanan landmasses (Perón Orrillo et al., 2019).

The SGSL is composed of about 20% plutonic rocks which have been widely studied and classified (Ortiz Suárez et al., 1992; Llambías et al., 1998; Sato et al., 2003; Brogioni et al., 2005, López de Luchi et al., 2007). Two Paleozoic magmatic events were recognized in the study area; a basic, intermediate and acidic Ordovician magmatism (~475 ± 11 Ma), associated with the development of the Famatinian arc/retro-arc (Sims et al., 1998; Sato et al., 2003; Steenken et al., 2006; Casquet et al., 2014; Morosini et al., 2017, 2019) and a Devonian (~398 ± 13 Ma) monzogranitic and monzonitic magmatism associated with the Achalian orogeny (Sims et al., 1997; Stuart-Smith et al. 1999; López de Luchi et al., 2002, 2007, 2017; Sato et al., 2003; Siegesmund et al., 2004; Morosini et al., 2017; Dahlquist et al., 2019) (Fig. 3).

The shear zones recognized in the SGSL are generally sub-parallel to a previous axial plane foliation developed during an intense folding by shortening and they were generated during the construction of Famatinian orogen that occurred between the late Ordovician and early Devonian (Whitmeyer and Simpson, 2004; Steenken et al., 2008; Christiansen et al., 2019). Studies by von Gosen (1998a) and Delpino et al. (2001) in the La Arenilla shear zone (the hottest of the SGSL) proposed that the kinematic indicators were formed by tectonic shortening with a small oblique sinistral component. Additionally, during the middle-late Devonian there was a reactivation of this shear zone in low greenschist-grade deformation (Sims et al., 1997; Steenken et al., 2008).

An inverted disposition of the metamorphism for the Pringles Metamorphic Complex, caused by a syn-metamorphic orogenic exhumation of high-pressure over low-pressure rocks was determined by Ortiz Suárez and Casquet (2005). According to these authors, the extrusion was caused by a combination of internal deformation on each metamorphic domain and sinistral-reverse displacements along ductile shear zones. Steenken et al. (2008), based on a petrological-structural analysis, proposed that the metamorphic fabrics (S_1) of the Pringles Metamorphic Complex were affected by two folding events (D_2 and D_3) related to the Ordovician approach and collision of the Cuyania/Precordillera terrane. According to Hauzenberger et al. (2001) the mafic-ultramafic intrusions of Las Aguilas were the heat sources that led to amphibolite and local granulite facies metamorphism in the Pringles Metamorphic Complex. Slightly before these events (at 510 Ma), the San Luis Formation was deposited, probably along with the sedimentary protoliths of the Nogolí and Pringles metamorphic complexes, but it was affected by a low metamorphism (von Gosen, 1998b). Drobe et al. (2009) proposed that after an extensional phase, related to deposition of the protoliths of the San Luis Formation, Pringles and Nogoli Metamorphic Complexes, the back arc basin was closed and folded, producing a differential uplift of the meta sedimentary units. This last event was a contractional stage in the Famatinian orogeny and was responsible for exposing and juxtaposing the high-grade metamorphic rocks of the Pringles Metamorphic Complex over the low grade metamorphic rocks of the San Luis Formation at the same crustal level.

The last work on this topic corresponds to Christiansen et al. (2019), which analyzed the main shear zones in the south-western sector of the SGSL and built a three-dimensional model of the area. These authors conclude that there is a large-scale doubly-vergent structure caused by a transpressional tectonic setting due to the collision between an allochthonous terrane (Cuyania/Precordillera) and the proto margin of Western Gondwana.

3. METHODOLOGY

In order to study the entire Sierra Grande de San Luis, the database used by Christiansen et al. (2019) was extended to the north, providing new geological, geophysical and petrophysical data. For the southern sector we used the entirely previous database (Christiansen et al., 2019), which consists of aeromagnetic, gravimetric, petrophysical, structural, and petrological data. This area has a higher concentration of information due to the easy accessibility to its outcrops and the high-density aeromagnetic database.

The northern sector was not covered by magnetic data because the achievable resolution was not sufficient for this type of study. However, magnetic susceptibility values were acquired in order to compare and contrast the ranges of values obtained for the same units in the southern sector. Faults and shear zones were characterized based on surface geological observations and their continuity at depth was obtained from a 3D model. Although the same gravity database as in the southern sector was used, this work shows 500 new gravity points and 34 new density values for the northern sector that were not exposed in previous publications.

3.1 Geological data

Structural data and rock samples for the northern sector were obtained during several field works, while the data for the southern sector was obtained from Christiansen et al. (2019). Structural data (foliations and lineations) were acquired on outcrops within and between units of different metamorphic grades with structural hand compasses. Measurement locations were carefully selected to represent the main shear zones structures. These data were plotted and processed statistically with Stereonet© 2011-2015 (Allmendinger et al., 2013; Cardozo and Allmendinger, 2013). Representative thin sections of oriented samples in different units and shear zones were petrographically analyzed under an optical microscope to determine microstructures, mineral associations and rock strain states (Simpson and de Paor, 1991; Passchier and Trouw, 2005).

3.2 Gravity data

Gravity anomaly grids were computed based on 886 stations covering an area bigger than the Sierra Grande de San Luis to avoid border effects (Fig. 4). Theoretical gravity was calculated using the International Gravity Formula 1967 and Bouguer gravity anomalies (Blakely, 1995) were calculated using an average rock density of 2.67 g/cm^3 (Hinze, 2003). The effects of earth curvature (LaFehr, 1991a, b) were corrected due to the size of the area considered for the study. Although the terrain effects are small, these were corrected following Nagy (1966) and Kane (1962), using local and regional DEMs with 90 m and 300 m resolutions, respectively. A terrain density of 2.67 g/cm^3 was considered in these corrections. The anomaly grid was obtained, applying kriging interpolation with a 1500 m cell size (Christiansen et al., 2015). Regional-residual separation was performed following Zeng et al. (2007), finding an optimum upward continuation height of 25 km. This separation resulted in representative wavelengths of up to 6 km depth (Jacobsen, 1987). For more information regarding the processing of gravimetric data, the reader is directed to Christiansen (2019).

3.3 Magnetic data

Total Magnetic Anomaly data are available only for the southern sector of the SGSL and was previously presented by Chernicoff and Ramos (2003) and Christiansen et al. (2019) (Fig. 5). It was acquired and pre-processed by Servicio Geológico Minero Argentino (SEGEMAR) along lines at average heights of 120 m in E-W direction and spaced every 500 m with N-S tie lines every 5000 m. Data spikes (high amplitude and short wavelength noise) were removed utilizing a non-linear filter (Naudy and Dreyer, 1968). The filtered data were gridded to a cell size of 160 m using a bi-directional gridding method. The resulting grids were compared with 125 ground magnetic stations (previously upwarded to 120 m) that were acquired over two E-W profiles in the southern sector of the SGSL. A shift in the TMA (Total Magnetic Anomaly) of 180 nT was detected and corrected. In order to obtain the residual TMA grid a Gaussian filter was applied with a cut-off wavelength of 24 km. This is consistent with a maximum depth of investigation of ~6 km. The northern area could not be explored with magnetic data with sufficient resolution to show the geological structures, so it was decided not to continue with the terrestrial magnetic analysis in this sector.

3.4 Density and magnetic susceptibility data

Rock samples were considered to analyze density values utilizing the method of double weighting with paraffin (Smithson, 1971), while the magnetic susceptibility values were measured in situ with portable equipment. The obtained values were averaged within a radius of 50 meters and assigned to the center of the locations. As a result, 34 density and 68 magnetic susceptibility values for the northern sector were added to the existing database (Christiansen et al., 2019). These data were used as a reference input for the petrophysical parameters in the initial 3D model (see section 3.5). Some discrepancies with respect to the same units in the southern sector may arise since the number of samples is very limited and the metamorphic grade varies within the area in parallel with the physical properties of the rocks (Best, 2003). Furthermore, there is a possible range of values of two to four orders of magnitude in the magnetic susceptibility for the same unit (Clark, 1997).

Moreover, the weathering of rocks diminishes these values due to the metastable nature of both magnetite and pyrrhotite at the surface of the Earth (Isles and Rankin, 2013). The complete list of samples is shown in Appendix A

3.5 Three dimensional litho-constrained inversion model

Geophysical inversion models provide useful insights into rock properties and geometry of the lithological units. Inversion and modelling methods carried out in this paper were implemented using the GeoModeller software developed by Intrepid Geophysics and BRGM (Calcagno et al., 2008; Guillen et al., 2008). This technique was specially designed for cases in which geology is known in scattered places on the surface. The ability to evaluate the petrophysical properties of the units by performing a deterministic search for least squares through the values proposed for each lithology is also of special interest.

Based on the theory of potential fields, this technique interpolates and extrapolates information considering the geological contacts, their orientation and the order of the stratigraphic column to create an initial 3D model to describe the geometry of the different lithological units. Then each unit is assigned statistically petrophysical properties, being defined by their mode, mean, standard deviation and distribution law. A potential-field approach is then used to adjust these models through litho-constrained joint inversion by comparing the measured gravimetric and magnetic data with those produced by the model. Once the initial model is achieved, certain limitations or values must be introduced to the restrictions that will be used by the inversion algorithm when modifying the properties and geometry of the units.

The non-deterministic method of inversion modifies one cell of the model during each iteration, within a range determined by the user, either in terms of geometry or rock property. The new obtained geophysical response is recomputed following the small change, and assessed against the field geophysical data. Results are given through likelihood statistics in the form of the most probable geological model and distributions of densities and magnetic susceptibilities for all its volume. For a detailed description of the methodology that led to the 3D litho-constrained inversion model the reader is directed to Christiansen (2019) and Christiansen et al. (2019). The complete inversion process for the northern zone is presented in Appendix B.

4. RESULTS

4.1. Structure and microstructure of the San Luis Shear System

The main structural feature in the Sierra Grande de San Luis is a ductile shear system, named by von Gosen and Prozzi (2005) as San Luis Shear System (SLSS). This system has a N15°

average strike and consists of several shear zones which transpose and alternate lithological units and structural domains. From east to west the principal shear zones are: 1) Río Guzmán, 2) San Martín, 3) Inti Huasi, 4) La Troya, 5) Quebrada Escondida, 6) La Arenilla, 7) San Pedro - El Volcán, 8) La Escalerilla, 9) Pancanta - La Carolina, 10) El Realito - Río de La Quebrada, and 11) Río de Los Bayos – Funes (Fig. 6). The main characteristics of the shear zones are described below and summarized in Table 1.

4.1.1. Río Guzman Shear Zone (RG-SZ)

The RG-SZ (Sims et al., 1997) represents the boundary between the Conlara Metamorphic Complex and the eastern belt of the San Luis Formation. The mylonitic/phyllonitic fabric is defined by the paragenesis of Qz+Chl+Ser±Mag, indicating low-grade deformation conditions (greenschist facies). The mylonitic foliation (S_{my}) has mainly steeply to vertical dips towards the ESE, while the stretching lineation (L_{my}) plunges towards the SSE (Figs. 2 and 6). Kinematic indicators such as S/C’ fabrics, σ-type clasts and asymmetric folds, indicate an oblique reverse-sinistral movement, with east-side-up. Ar/Ar-muscovite ages of 362 and 351 Ma (Sims et al., 1998) suggest a Devonian age for this shear zone.

4.1.2. San Martín Shear Zone (SM-SZ)

The SM-SZ extends northward of Las Chacras batholith and separates the Conlara Metamorphic Complex from Las Higueras Complex (Fig. 6). It is composed by at least three main belts with striking NNE-SSW that juxtapose different lithologies, which tend to increase in metamorphic grade to the east. The SM-SZ is composed of phyllonites and mylonites of schists. Overall, the S_{my} has an NNE strike with a steeply to subvertical ESE dip, while the L_{my} plunges towards the ENE. Kinematic indicators such as S-C structures, asymmetric sigma porphyroclasts and drag folds show reverse motion with a minor dextral component (Fig 7a). The mineral paragenesis in mylonitic rocks is Qz+Pl+Bt±Grt±Chl indicates greenschist facies metamorphic conditions.

4.1.3. Inti Huasi Shear Zone (IH-SZ)

The IH-SZ (Ortiz Suárez and Casquet, 2005) separates the eastern belt of the Micaschist Group (west) from the eastern belt of the San Luis Formation (east). This shear zone has a southern segment with N strike, and a northern segment with NE strikes (Fig. 6). It contains mylonites and phyllonites that overprint phyllites, micaceous schists, pegmatites and tonalites. The S_{my} dips W or NW, while the L_{my} plunges towards the NW. Drag folds, transposed structures by shear bands, S/C and S/C'-fabrics, σ-type clasts and mica fish, indicate a reverse sense (west-side-up) with a minor sinistral strike-slip component for this shear zone. Temperatures between ~350 and 450° C were interpreted due to the development of bulging (BGL) and subgrain rotation (SGR) recrystallisation microstructures in quartz.

4.1.4. La Troya Shear Zone (LT-SZ)

The LT-SZ (Ortiz Suárez and Casquet, 2005) separates the San José Complex from the eastern belt of the Micaschist Group (Fig. 2 and 6). The southern segment has a N strike with a slight concavity towards the east and dips towards the W or NW, whereas the northern segment has a general NE strike, and dips at a very high angle towards the NW. It is ramified into some minor synthetic splay shear belts in the Micaschist Group (Fig. 6). The LT-SZ deforms migmatites, gneisses, coarse-grained schists and few amphibolites, which present kinematic indicators such as asymmetric folds, S/C'-fabrics, boudin structures transposed by shear bands, σ-type clasts and mica fish. Ribbons of quartz with grain boundary migration (GBM) recrystallization indicate moderate to high-temperature deformation (~500-550° C). Likewise, the growth of new bands of sericite would be indicating reactivations at lower temperatures (Fig. 7b). In the southern sector, the L_{my} plunges to NW, and the shear was resolved through reverse movement (west-side-up) with a minor sinistral strike-slip component. In contrast, in the northern sector, the L_{my} is horizontal, with a maximum plunge of ~5° towards to N, indicating a sinistral strike-slip sense with a very little reverse component.

4.1.5. Quebrada Escondida Shear Zone (QE-SZ)

The QE-SZ separates the Las Higueras Complex from the San José Complex. It is composed by several branches striking NNE and located northwest of Las Chacras batholith (Fig. 6). QE-SZ is disrupted by this intrusion because in this area its strike is displaced in E-W direction by a clockwise rotation and all branches converge into one. This shear zone develops mylonites of schists, granites, tonalites, pegmatites, and migmatites, and to a lesser extent protomylonites and ultramylonites bands. The S_{my} strikes NE and dip to NW, and the L_{my} plunges towards the SW, although occasionally they dip with low-angles towards the NE. Kinematic indicators such as S-C' structures, drag folds, sigma clasts, mica fish, indicate reverse movements (west-side-up) with a minor dextral strike-slip component. Ribbons of quartz with grain boundary migration (GBM) recrystallization suggest a deformation temperature of ~500-550° C.

4.1.6. La Arenilla Shear Zone (LA-SZ)

The LA-SZ (Ortiz Suárez et al., 1992) extends more than 95 km in N-S direction within the San José Complex. In the central part, it comprises a single wide belt (~3 km), while to the north and south, it ramifies into wider branches (Figs. 2 and 6). This shear zone contains mylonites of gneisses, migmatites, pegmatites and mafic-ultramafic rocks. The S_{my} strikes N to NNE, with steep dips (>70°) towards the E or NW. The L_{my} is close to down dip (von Gosen y Prozzi, 1998; Delpino et al., 2007). In general terms, the LA-SZ shows reverse movement with a minor strike-slip sinistral component. The eastern block is the hanging wall when the S_{my} dips to the E (von Gosen and Prozzi, 1998; Delpino et al., 2001), while the western block is the hanging wall when the S_{my} dips towards the W (Morosini et al., 2014), giving rise to a horst pop-up structure. Nevertheless, in a small branch of this shear zone, oblique normal-sinistral movement was observed, but this is an exception to the general movement of the LA-SZ (Fig. 2). Metasedimentary mylonites have porphyroclastic texture with mantled σ-shape clasts of Pl, Kfs and Grt, and a recrystallized matrix of Bt, Sil, Ms and Qz (ribbons). Kfs and Pl porphyroclasts show deformed twinning, undulous extinction, recrystallized edges and fragmentation (shear-band type porphyroclasts). Leucosome pods with sigma-shape (Fig. 7c), asymmetrical drag-folds of stromatitic migmatite and S/C or S/C' fabrics are very common. Mafic mylonites have porphyroclastic texture or a compositional banded foliation (Fig. 7d). The σ-shape clasts of Pl, Amp, Opx or Grt hosted in matrix of Amp, Pl, Px, Bt and Op are a common feature of these rocks. Occasionally mafic mylonites have ultramylonite texture and a millimetric compositional banding with leucocratic granoblastic bands of Pl and mafic nematoblastic bands of Amp ± Px ± Op. The P-T conditions of the mylonitic event reached upper amphibolite facies at intermediate pressures (668-764º C, 630-690 MPa) (Delpino et al., 2007) and minimum temperature records indicate more than 600° C (Steenken et al., 2008). These authors also determined the age of 414 ± 10 Ma (K/Ar-biotite) in a Bt-Grt-Sil mylonite, which suggests tectonic activity during Silurian times. Likewise, within this shear zone, there are also thin overlapping bands with evidence of deformation at lower temperatures (greenschist facies) that indicate retrograde conditions during the exhumation (Delpino et al., 2007).

4.1.7. San Pedro - El Volcán Shear Zone (SP-EV-SZ)

The SP-EV-SZ (Ortiz Suárez, 1999; Morosini, 2011) separates the western belt of the Micaschist Group from the San José Complex. It comprises mylonites of migmatites, gneisses, micaceous and quartz schists, pegmatites and amphibolites. The S_{my} strikes from NE to NNW, and dips toward the E. The L_{my} plunges predominantly towards the SE. The kinematics indicators such as asymmetrically folded veins, σ-shape or synthetically faulted Kfs porphyroclasts (Fig. 7e), mica fish, bookshelf and pinch and swell structures of Kfs and Pl indicate reverse movement (east-side-up) with a minor sinistral strike-slip component. Therefore, the San José Complex was juxtaposed over the western belt of the Micaschist Group (Ortiz Suárez, 1999; von Gosen and Prozzi, 2005; Morosini et al., 2014). At its northern end, a later shearing, which developed a S_{my+1} foliation of NE strike, displaced and curved (clockwise rotation) the trajectories of the previous shear zones. The kinematic indicators show a dextral strike-slip motion for this ductile fault. Temperatures between ~450 and 550° C have been interpreted as evidenced by grain boundary migration (GBM) recrystallization of quartz, and feldspars (core and mantle microstructures). However, the presence of late retrograde microstructures is common, like bands of sericite, microfractures in feldspar, undulous extinction or BLG in quartz (Fig. 7f). These elements would be indicating a late reactivation close to ~300 ºC (greenschist facies).

4.1.8. La Escalerilla shear zone (LE-SZ)

The LE-SZ extends over 63 km with NNE general strike. It is located on the eastern boundary of the La Escalerilla pluton, which is between the western belts of the Micaschist Group and San Luis Formation (Figs. 2, 6 and 8a). The southern segment is curved and has a concave morphology towards the east with a strike that changes slowly from NNW to NE, while the northern segment is rectilinear with NNE strike. The S_{my} presents steep dips to the E, while the L_{my} plunges towards the SSE or SE. It is composed of mylonites of granites, quartzites and schists, and of phyllonites. The S_{my} in deformed granites is a high-temperature mylonitic to ultra-mylonitic lamination developed in amphibolite facies conditions (Steenken et al., 2008). Evidence of deformation temperatures over 550°C includes undulous extinction in plagioclase, subgrain rotation (SGR) recrystallisation and myrmekitization in microcline, and ribbons of quartz with grain boundary migration (GBM) recrystallisation (Fig. 8b). The presence of sericite indicates reactivation at lower temperatures. The S/C-fabric and σ-shape feldspar clasts in granitic mylonites, as well as asymmetric folds of veins in schists, indicate an oblique reverse-sinistral movement with east-side-up (von Gosen, 1998a, Steenken et al., 2008, Morosini and Ortiz Suárez, 2010). In the central sector the shear zone intersects several minor branches (10 m width) with NNW strikes, which are synthetic to the movement of the main branch. In these branches the L_{my} plunges gently towards the SSE, and σ-shape or imbricated K-feldspar porphyroclasts indicates sinistral strike-slip movement.

4.1.9. Pancanta - La Carolina Shear Zone (P-LC-SZ)

The P-LC-SZ is located within the western belt of the San Luis Formation. The main branch has an NNE strike with a near planar morphology. The S_{my} dips steeply toward NW, while the L_{my} plunges gently towards the SW. Kinematic indicators, such as σ and δ-shape clasts, drag folds, en echelon veins and S/C-fabric evidence an oblique dextral-reverse motion (Fig. 8c). It is mainly composed of phyllonites with domanial slaty cleavage, which is typical of shearing in low metamorphic grade rocks. Based on thermobarometric data, Morosini and Ortiz Suárez (2011) determined temperatures of ~450° C in the northern segment of this branch. The other branch strikes EW and it separates an isolated block of the Nogolí Metamorphic Complex from the San Luis Formation. Its S_{my} dips moderately toward N while the L_{my} plunges towards WNW. Kinematic indicators show oblique reverse-dextral motion.

4.1.10. El Realito - Río de La Quebrada Shear Zone (ER-RQ-SZ)

The ER-RQ-SZ (Sato et al., 2003) separates the Nogolí Metamorphic Complex from the Pringles Metamorphic Complex (in the northern part), from the western belt of the San Luis Formation (in the central part), and from the La Escalerilla pluton (in the southern part). It affects metamorphic rocks of different grades and some tonalitic and granitic plutons developing mylonites, phyllonites and protomylonites. It has a general NNE strike with local variations. In some places, it splits into several smaller anastomosed branches that form lozenges while in other places, it is intercepted by new lateral branches (González et al., 2006). Three distinctive segments can be recognized. The northern segment is divided into several parallel branches that border the El Realito pluton with an NNE strike, and vertical dips. In the central segment the S_{my} strikes NNE, dips steeply toward NW, and the L_{my} plunges towards NNW. The Gasparillo and San Miguel tonalitic plutons were thrust to the east over the western belt of San Luis Formation with an oblique sinistral sense (von Gosen, 1998a; Morosini, 2011). Along this segment, some minor branches intercept the main one. These minor shear zones display a S_{my} with N to NNW strike, steep dips to W or E, and the L_{my} has a gentle plunge to the N or NNW. A sinistral strike-slip movement is evidenced by the counterclockwise rotation of the main arm of the shear zone. In the southern segment the S_{my} strikes NNE and dips moderately toward ESE. The L_{my} dips towards the SE, and the kinematics indicators showed a reverse movement (east-side-up, Fig. 8d), with a minor sinistral strike-slip component. The preferred orientation of micas and amphibole prisms, σ and δ-shape clasts, mica fish, ribbons of quartz with dynamic recrystallization (SBR and GBM), core and mantle structures in Kfs porphyroclasts with undulate extinction and exsolution of perthites, and plagioclase with flexured twinning, are evidence of shearing in a wide range of temperatures between 450° and 550° C.

4.1.11. Río de Los Bayos - Funes Shear Zones (RB-F-SZ)

The RB-F-SZ are located within the Nogolí Metamorphic Complex (González et al., 2006). Due to their length and thickness they are the most important of 24 ductile shear bands in the area. The main characteristics are a trajectory of more than 30 km that form lozenges with N to NNE orientation (Fig. 6). The lithology of these shear zones varies from protomylonites and mylonites to ultramylonites and phyllonites of metasedimentary and mafic/felsic igneous protoliths (Fig. 8f). Its metamorphism differs from high to low thermal grade (Sato et al., 2003). Generally, the S_{my} is subvertical or steeply dipping towards the E or W, and the L_{my} plunges towards the S, SSE or NNW. Mica elongation, drag folds, S/C and S/C' fabrics and asymmetric porphyroclasts indicate dominance of sinistral oblique sense with tectonic transport to the NNW. However, the relationship of these shear zones with orogenic and late to postorogenic granitoids indicates repeated activation (Sato et al., 2003; González et al., 2006).

4.2. Deformational stages

Sets of structures were defined based on reliable overprinting criteria, such as a foliation (S_n) that has been folded (F_{n+1} folds) or cross-cutting relationship. We avoid using descriptive features like style, orientation, tightness of folds to correlate structural sets because it may change in outcrops of the same age. Although these descriptive features help to understand part of the deformation mechanisms, they are not reliable to define the succession of events (Passchier and Trouw, 2005). We define four deformational events that affected the rocks of the SGSL. Figure 9 shows the results of the main structural elements plotted in stereograms, while the main features are summarized in the Table 2. In addition, Figure 10 attempts to graphically simplify the complex structural sequence of each metamorphic unit.

A particular feature in the SGSL is that the first deformational phase (D_1) is associated with the development of a continuous or spaced foliation (S_1) defined by the growth of metamorphic minerals (slaty cleavage, schistosity, compositional banded, or stromatitic foliations), which are arranged parallel or subparallel to the S_0 sedimentary bedding. Naturally, the spatial dispositions of the S_1 foliation vary in each unit depending on the style of overprint generated by the subsequent deformation phases, but statistically they are more feasible to measure in planes with NNE to NE strikes (Fig. 9) because the contractional folding events were in WNW-ESE direction.

The second deformational phase (D_2) was responsible for generating an intense folding, widely visible in most outcrops of the SGSL (Figs. 10 and 11). This deformation phase (D_2) generated F_2 folds with S_2 axial planes of the average NNE strike. The S_2 are vertical or steeply inclined towards the WNW or ESE, depending on the sector (Fig. 9). In general, the B_2 hinge lines of the F_2 folds are gently or moderately plunging towards the NNE or SSW, and less frequently towards the SE. The amplitudes and lengths of the F_2 folds are variable and generally depend on the metamorphic degree and the structural domain that they represent (Figs. 10, and 11, and Table 2).

The D_3 deformational phase is related to the development of the San Luis Shear System, except in the Conlara metamorphic Complex where it represents the D_4 deformational phase. These NNE shear zones worked under non-coaxial stress regimes (Christiansen et al., 2019), generating rotations and fold of the previous fabrics of internal domains that surround the shear belts. Therefore, two set of structural fabrics are recognized for the D_3 deformational phase according to its strain. The most representative fabrics are the S_{3my} mylonitic foliation and its different associated structural elements (e.g. S-C, S-C' structures and drag folds) located within the shear belts (high-strain zone). The other set of structural elements is recognized within the internal domains (low-strain zone) surrounded by shears belts. In these domains, the superimposition of F_3 folds over F_2 folds produced interference patterns similar to type 3 of Ramsay (1967) (Fig 10).

The third deformation phase (D_3) also generated superposition of F_3 over F_2 folds in the Conlara Metamorphic Complex, developing type 3 interference patterns. But in this complex, unlike the rest of the units, there is not a clear spatial link between the development of these patterns and the presence of shear zones.

A fourth deformation phase (D_4) is related to the development of narrow NE or NW shear zones displacing the prior S_{3my} mylonitic surfaces (Fig. 10). The S_{4my} is not penetrative on a regional scale, and only developed along widely spaced belts (hundreds of meters to kilometers). Likewise, several shear zones associated with D_3 show low-temperature reactivations through discrete planes taking advantage of the prior deformation surfaces. These reactivations are also considered part of a fourth deformation phase (D_4), since they overprint to the previous ones. In the Las Higueras Complex a localized S_4 surface can be associated with the forced intrusion of the Devonian plutons.

4.3. Geophysical maps and inversion results

Residual Bouguer and magnetic anomaly maps show information about the density and magnetic susceptibility distribution in the upper part of the crust. These grids are obtained by the elimination of regional longer wavelength anomalies using frequency filters. The information provided by the combination of both methods facilitates the identification of structures and lithologies for the generation of an initial 3D model, which is then adjusted by inversion. The results are models that are consistent with the known surface geology and measured density and magnetic susceptibility values. Final models show the geometry in 3D and provide information about the distribution of petrophysical parameters below the surface.

4.3.1 Gravity anomaly maps

The residual Bouguer anomaly map (Fig. 12) displays a reasonable gravity variation according to the different types of lithologies in the SGSL. The clearest and most prominent signals are the negative anomalies produced by the large Devonian post-orogenic granitic plutons, such as Las Chacras, El Hornito, El Telarillo, La Población and San José del Morro. In the Nogolí and Pringles metamorphic complexes the maximum positive values are mainly associated with mafic-ultramafic rocks. Furthermore, a moderate positive anomaly is recognized in the northeastern sector of the Conlara Metamorphic Complex which is attributed to the mafic and intermediate rocks of the Rodeo Viejo pluton. The prominent positive anomaly values, which cover an area of approximately 500 km^2 and are located immediately to the west and northwest of the SGSL, suggest the presence of an important volume of sub-cropping mafic rocks belonging to the Famatinian magmatic arc axis. These rocks can be considered the southeastern continuation of the mafic units present in the Sierra de Valle Fértil - La Huerta (e.g. Otamendi et al., 2009), which are characterized by a strong positive gravimetric anomaly (Introcaso et al., 2004; Weidmann et al., 2016).

Although gravimetric information is consistent with surface lithology, in some places, data coverage is not homogeneous, and therefore, the spatial interpolation fails to represent real anomalies. Consequently, some geological features such as the Renca pluton, located in the eastern sector of the SGSL, do not show a significant negative anomaly as the rest of the Devonian post-orogenic plutons.

4.3.2 Magnetic anomaly maps

One of the most significant and contrasting properties among the lithological units of the SGSL is the magnetic susceptibility. Variations in this physical parameter produce strong magnetic anomalies (e.g. presence of mafic-ultramafic rocks). Due to the dipolar nature of the geomagnetic field, observed magnetic anomalies are asymmetric even when the source body distribution is symmetric. Therefore, for visualization purposes, residual magnetic data is presented after the reduction to the magnetic pole (RTP) filter is applied. This method removes anomaly asymmetry, assuming that the remnant magnetism is small. In this way, anomalies are situated above the causative bodies. Due to the lack of aeromagnetic data in the northern sector, a reduced to the magnetic pole (RTP) aeromagnetic map only for the southern SGSL is shown in Fig. 13.

The RTP map clearly shows a magnetic contrast between two first-order structural meridional domains in the metamorphic basement. In the western sector of the SGSL, where the Nogolí and Pringles Metamorphic Complexes and the San Luis Formation are located, magnetic anomalies are particularly prominent, thin, elongated and interspersed positive and negative values. These N-S trending features correspond to the structural patterns generated by the ductile shear zones and to the magnetic domain of the San Luis Shear System. In contrast, on the eastern sector, where the Conlara Metamorphic Complex is located, the RTP image does not show strong anomaly contrasts, except for the prominent signals caused by the Devonian granitic plutons, small Neogene volcanic domes and some minor linear features interpreted as modern faults. A common feature of Devonian granitic plutons is concentric positive magnetic anomalies in their edges that contrast with the internal zone and their host rock. These magnetic zoning represent internal lithological changes (Sims et al, 1997; Chernicoff and Ramos, 2003) and are probably produced by a difference in the content of magnetite in their facies.

Two main reasons explain the prominent magnetic signals in the western SGSL. One reason is related to the folding or shearing of rocks at moderate to high temperature, which generates a high concentration of magnetite in low-strain zones resulting in increased magnetic susceptibility (Isles and Rankin, 2013). These interpretations are documented in the Río Guzmán Shear Zone, where veins of remobilized quartz with intense magnetism are present. The other reason is associated to the mafic-ultramafic rocks in the San José Complex, which contain a high concentration of pyrrhotite and magnetite as primary and secondary minerals (e.g. Hauzenberger et al., 1997). The main negative magnetic anomalies are related to the La Escalerilla and San Miguel plutons, indicating, in general terms, their low magnetic susceptibilities compared to other units.

4.3.3 Inversion model

The creation of the 3D models and a subsequent inversion was carried out for the southern and northern sectors separately. The southern sector was covered by gravity and magnetic information, consequently, a joint inversion was made using both data sets. As a result, the most probable geological model and density and magnetic susceptibility cubes were obtained (Fig. 14). For a detailed explanation of the joint inversion process and the obtained 3D model in the southern sector, the reader is directed to Christiansen et al. (2019).

The initial model for the northern sector was constructed by geostatistical interpolation in order to obtain a reference lithological model. Stratigraphy and relationships between units were defined following geological field studies. Density values obtained from the field samples (section 3.4) were assigned to the lithological units. For those units without density data, the values were assigned following international tables taking lithology into account. Eight control profiles were defined perpendicular to the main structures on which to observe the units up to a depth of 6 km. This value corresponds to the research depth defined based on the residual gravity grids.

The initial model was adjusted on the profiles considering the gravity produced by the sections. The densities were then optimized using the least-squares technique and the gravimetric response was recalculated. The inversion of the data was carried out through 20 million iterations respecting the established stratigraphic order. A voxel size of 500x500x300 m (x-y-z) was used with a probability of change in the petrophysical properties of 50% and a probability of change in the geometry of the units of 50%.

Results for the northern sector (Fig. 15) indicate that the structures continue with the same trend as in the south with almost vertical contacts between the main units. Most of the analyzed shear zones project to the depth with the same inclination as the measured angles on the surface. The density distribution shows great surface variation, especially in the sediments. In general, it is observed that the results for the densities are very similar to those obtained in the laboratory with differences of 2.35% on average.

As a most distinctive feature, it can be noted that the San José Complex extends along the entire length of the model, reducing its width by the center. On the other hand, the Las Chacras Batholith presents great dimensions and its base would not exceed 4000 m depth. Considering the fault system and the arrangement of the lithological units, we can affirm that in this area, the double-vergent structure of regional-scale observed towards the south is maintained, although it would affect only the San José Complex and the Las Higueras Complex because the Micaschist Group and San Luis Formation do not continue to the north.

5. DISCUSSION AND INTERPRETATION

5.1. Architecture of the Sierra de San Luis

One of the most difficult tasks regarding geological modelling is to determine the continuation of structures and lithological units at depth. If the limits between the units of the SGSL are projected indefinitely according to the angles measured on the surface, very different profiles would be obtained comparing to the model presented here. A strong predominance of vertical or steep dip structures on the surface such as the San Luis Formation or the granitic and tonalitic plutons can be extremely thick, reaching depths of tens of kilometers, resulting in an unreal and unlikely design for the orogenic architecture. Considering the petrophysical properties and geophysical data, the boundaries between units acquire different inclinations at depth and therefore the model becomes more realistic.

The results of the surface structural survey reveal that most of the shear zones incline with angles greater than 60° (Fig. 6b). However, in the Pringles Metamorphic Complex the mylonitic foliations are practically vertical (90°) in its central sector (San José Complex) and gradually reduce its angles (~60°) towards both flanks (in the boundaries between Micaschist Group and San Luis Formation) (Fig. 2). In the western flank the foliation dips to the east, while in the eastern flank to the west. Generally, the stretching lineation (L_{my}) dips to the southeast when the shear zones dip to the east and towards the northwest when the S_{my}-planes are inclined to the west. Predominant kinematic indicators show (in both cases) reverse movements with a minor sinistral strike-slip component. This situation is compatible with a general non-coaxial compressive deformation. According to Goscombe and Gray (2009), the tectonic obliquity (β_σ) of an orogen can be determined from an average of the regional pattern of maximum stretching direction indicated by stretching lineations, thus defining a maximum stretching obliquity (β_L). The San Luis Shear System presents angles between the orogen strike (N15°) and the direction of the stretching lineation in the shear zones (β_L), indicating that the kinematic corresponds to a transpressional orogen of sinistral oblique (to high-angles) convergence with steep dips (Fig. 6).

The 3D litho-constrained inversion model shows the orogenic architecture of the SGSL up to a depth of 6 km (Fig. 16). Since most of the boundaries between lithological units are shear zones, the structural pattern of the entire shear system and the shape of each tectonic thrust sheet are outlined by the 3D shape of each lithological unit. According to the geophysical model, the architecture of the central part of the San Luis Shear System can be interpreted as a large-scale double-vergent megastructure. The inversion model also shows that most of the shear zones tend to intercept at depth to form a single belt of ductile deformation, which can be interpreted as a vertical extrusion channel (Figs. 16 and 17a, b).

The double-vergent pop-up structure has a central zone or high metamorphic grade core represented by the San José Complex that hosts mafic-ultramafic rocks. This central zone is flanked on both sides (in decreasing order of metamorphic grade) by the Micaschist Group (middle-grade) and the San Luis Formation (low-grade) (Figs. 16f and 17c). The elongated sigmoidal-shape of the La Escalerilla granitic pluton, located between the Micaschist Group and San Luis Formation (Figs. 16f and 18), is consistent with a deformed element within this transpressive shear system (von Gosen, 1998a; Morosini and Ortiz Suárez, 2010). In the northern sector of the SGSL, the San José Complex is directly in contact with the Nogolí Metamorphic Complex to the west and Las Higueras Complex to the east but maintains a wedge-shaped in cross-section that tapers towards the east.

The Nogolí and Conlara metamorphic complexes form the external substrate of the doubly-vergent structure. The Nogolí Metamorphic Complex lies below the western belt of the San Luis Formation, as well as the La Escalerilla and El Realito plutons (Figs. 16c and 18). The San Luis Formation was probably placed on top of the Nogolí Metamorphic Complex through an early decollement, which in turn acted as a ramp for the emplacement of the La Escalerilla pluton, and then was truncated by the El Realito - Río de la Quebrada Shear Zone (Fig 17c). Within the Nogolí Metamorphic Complex, mafic-ultramafic, tonalitic and granitic rocks are present on the surface and, according to the geophysical results, must also be present at depth.

Two metamorphic zones are recognized within the Conlara Metamorphic Complex. The San Martín Group (high-grade metamorphism) is in a central belt on the northeast edge of the model, as well as two oval-shaped sectors that would represent migmatic domes (Morosini et al., 2019) (Fig. 16). The zone of less metamorphic grade (Las Aguadas Group) is located between the previous ones and represents the superstructure of the Conlara Metamorphic Complex.

The eastern belt of the San Luis Formation and Las Higueras Complex are in contact with the western limit of the Conlara Metamorphic Complex. According to the field results this limit is a shear zone with steep dip towards the east. However, the 3D model indicates a sub-horizontal dip towards the western limit, which is intercepted at depth by the vertical Inti Huasi Shear Zone. This sub-horizontal boundary is interpreted as an east vergence decollement associated with the orogenic retro-wedge (Fig. 17) evidenced by the presence of asymmetric folds with eastern vergence in the San Luis Formation. Results suggest that these structures are detachment folds developed above a decollement during shortening in the D_2 deformational phase. Moreover, this surface together with the Inti Huasi, La Troya and Quebrada Escondida shear zones are interpreted as the limits of the thrust sheets that were extruded eastward and resulted in the stacking of the San José Complex over the Las Higueras Complex and the Micaschist Group, and of the Micaschist Group over the eastern belt of the San Luis Formation in the south area.

The interpreted basal detachment that placed the San Luis Formation and Las Higueras Complex in contact with the Conlara Metamorphic Complex was truncated sometime after the (F_2) folding by the younger west-verging and high-angle Río Guzmán and San Martín shear zones (Fig. 17c). Our interpretations suggest that the sedimentary protoliths of the San Luis Formation and the Las Higueras Complex were deposited to the west of the oldest protoliths of the Conlara Metamorphic Complex, and then during the Famatinian contractional stage were juxtaposed. For all these reasons, it is considered that the Conlara Metamorphic Complex acted as a backstop during the development of the pop-up megastructure.

5.2. P-T conditions of the units that integrate the double-vergent structure

The metamorphic evolution of the SGSL is complex and not yet fully understood. The data set of the metamorphic conditions (Fig. 19a and Table C1) shows the P-T peaks and the different metamorphic grades for the units that composed the double-vergent belt corresponding to: 1) high-amphibolite to granulite facies for the San José Complex, 2) low-to medium-amphibolite facies for the Micaschist Group, and 3) low-to high-greenschist facies for the San Luis Formation, all of them represent a Barrovian Series. The regional distribution of the metamorphic grade in the double-vergent megastructure has an NNE-SSW longitudinal pattern. The axis of higher temperature is coincident with the La Jovita - Las Águilas mafic-ultramafic belt (these rocks being also the deepest) located at the center of the double-vergent structure. The lower temperature and pressure zones correspond to both San Luis Formation belts, which flank the mafic-ultramafic belt on each side. These units are now located in a structural position below the high-grade units, with the Micaschist Group structurally inserted between them. The distribution of the metamorphic conditions and relation with the structure indicate an inverted arrangement of the metamorphism, produced by the thrust of deeper higher-temperature zones over more superficial and colder zones (Fig. 17c) (Ortiz Suárez, 1999; Ortiz Suárez and Casquet, 2005; Morosini et al., 2014).

Results indicate that the mylonitic temperature conditions of the shear zone in the area depend on the previous metamorphic conditions of each geological unit prior to the orogenic exhumation. For example, the San Luis Formation and the Micaschist Group are separated by shear zones with mylonitic temperatures in medium-greenschist facies. In contrast, the La Arenilla Shear Zone nucleated within the San José Complex, reached high-amphibolite facies. However, it is possible to distinguish in the La Arenilla Shear Zone greenschist facies mylonitic events, which are located at the boundaries of the pop-up core or reworking previous upper-amphibolite shear zones. This last observation indicates a superposition of high and low temperature ductile deformation events due to the cooling of the San José Complex during its decompression, and suggest a protracted contractional activity.

A paleo-depth profile perpendicular to the double-vergent megastructure calculated from the metamorphic climaxes (Fig. 19b) indicates maximum paleo-depths of 36 km for the high-grade metamorphic rocks in the internal domain (San José Complex) and 18 km for the external domain (San Luis Formation). This bell-shaped profile is consistent with the development of a vertical extrusion channel where the greatest amount of exhumation corresponds to the pop-up core. The vertical advection of the hot material in the pop-up structure (vertical channel flow of the Pringles Metamorphic Complex) is evidenced by the cooling paths determined with K-Ar ages in Hbl, Ms and Bt (Steenken et al., 2008). The average K-Ar isotopic closure ages for the Pringles Metamorphic Complex is approximately ~40 M.y. younger than in the Conlara Metamorphic Complex and in the northern portion of Nogolí Metamorphic Complex. Only in the Middle Devonian (~370 Ma) the metamorphic complexes reached temperatures of ~300 °C and were positioned next to each other as they are currently preserved (Fig. 19c). These data suggest a higher exhumation rate in the central part of the double-vergent structure (Pringles Metamorphic Complex) than rest of the SGSL units during the Famatinian orogeny.

5.3 Kinematic model of the orogenic section

The configuration of the metamorphic units and tectonic domains of the current upper crust in the study area (up to 6 km depth) are compatible with a double-vergent structure developed in the central sector of the SGSL (Figs. 16 and 17c). The exhumed units represent lower and middle levels of the crust during the Famatinian orogeny. The mega-structure involves the Pringles Metamorphic Complex, San Luis Formation and Las Higueras Complex, while the Conlara and Nogolí metamorphic complexes are the surrounding elements.

The structural style of the orogenic wedge developed in the western units of the SGSL (west to the Río Guzmán and San Martín shear zones) suggests that the Conlara Metamorphic Complex acted as a backstop (e.g. Byrne et al., 1993) during the development of the double-vergent transpressive belt (Fig. 20). Evidence of this interpretation is the provenance age patterns of detrital zircons, such as the maximum depositional ages determined in the Conlara Metamorphic Complex (Drobe et al., 2009; Rapela et al., 2016), which suggest that its protholits correspond to a prior sedimentation cycle, equivalent to the pre-Pampean Puncoviscana Series of the Argentine Northwest (see Rapela et al., 2016; Weinberg et al., 2018). This series was deposited in the fore-arc and/or trench of the west-facing Pampean arc before ~530 Ma and was structured during the Pampean orogeny between 537 and 524 Ma (Escayola et al., 2011). This sequence was probably part of the paleo-continent during the development of the Famatinian island arc located westward. Conversely, the sedimentary protoliths of the units located west of the Conlara Metamorphic Complex have detrital zircons of early Cambrian age. These sediments were deposited at the margin of the Pampean orogenic system during the middle and late Cambrian (Steenken et al., 2006; Drobe et al., 2009, Perón Orrillo et al., 2019), and are equivalent to the Negro Peinado and Achavil formations (Collo et al., 2009), the Mesón Group (Augustsson et al., 2011) and Valle Fértil metasediments (Cristofolini et al., 2012).

The predominant lithological and geophysical features in the Nogolí Metamorphic Complex suggest that it was the immediate eastern part of the Famatinian magmatic arc (exposed in the

Sierras de Valle Fértil - La Huerta, Ulapes and Chepes). This can be interpreted from the larger volume of Ordovician plutonic rocks or the prominent gravimetric anomaly located a few kilometers to the west of the SGSL (Fig. 12). An isostatic root rapidly developed synchronic with the Famatinian arc, and a voluminous and compositionally stratified igneous crust, immediately west of the Nogolí Metamorphic Complex, was developed before the orogenic stage between 488-465 Ma (Tibaldi et al., 2013; Ducea et al., 2015; Camilletti et al., 2020; Otamendi et al., 2020). During this period, in the backarc there was an uplift of the mantle isotherms that gave rise to a regional metamorphic event of low-to medium-pressure (Hauzenberger et al., 2001; Larrovere et al., 2011). This metamorphic event melted deeper crustal meta-sedimentary units and developed migmatic complexes, while on the surface the sedimentary protoliths of the La Cébila Formation were being deposited (Verdecchia et al., 2007). For these reasons, we interpret that the first deformational phase (D_1) that affected the Cambrian sedimentary protoliths in the SGSL imprinted its metamorphic fabrics in an extensional or neutral setting (?).

The beginning of the continent-arc collision due the accretion of the Cuyania/Precordillera microplate against Gondwana (Benedetto, 2004; Astini and Dávila, 2004; Ramos et al., 2004) caused that all units belonging to the Pringles and Nogolí metamorphic complexes, the San Luis Formation and Las Higueras Complex were imprisoned between the Famatinian arc and the Conlara Metamorphic Complex (backstop). These units were intensely deformed by the contraction during the closure of the Ordovician backarc basin (D_2 deformational phase). This deformation ultimately resulted in the extrusion and riding of high-grade metamorphic units of the Pringles Metamorphic Complex (San José Complex) above those of lower grade (San Luis Formation and Las Higueras Complex), and the imbrication of the structural domains in the Nogolí Metamorphic Complex (D_3 to D_4 deformational phases).

From the suture zone (Valle Fértil-Desaguadero lineament) to the high-grade metamorphic rocks of the San José Complex (pop-up core), the orogenic deformation probably has an imbricated west-vergence pro-wedge style, as it happens northwest of the study area (Fig. 20a). While eastward, from the San José Complex to the Conlara Metamorphic Complex, the shear zones with east-vergence corresponds to a retro-wedge developed over the Pampean paleo-orogen (backstop) (Fig. 20b). Within the Conlara Metamorphic Complex there is a predominantly western vergence structural style, and its eastern limit is the large western vergence Guacha Corral shear zone, that was reactivated during the Famatinian orogeny (Semenov et al., 2019).

5.4 Geotectonic implications in the construction of Famatinian orogen

The structural features related to the development of a double-vergent transpressive belt in the SGSL suggest that there was a significant shortening between 32° and 34° S latitude. As a result, a vertical exhumation of 36 km of the San José Complex in the core of a pop-up structure was produced. According to Schulmann et al. (2008) a rigid floor is required for the mechanism of vertical extrusion to be possible, represented by a strong sub-root mantle. In the orogenic model presented in this work, the overriding Famatinian arc and backarc became mechanically decoupled from the complementary lithospheric mantle and the whole main arc and backarc metasedimentary sequences experienced rapid uplift rates (Otamendi et al., 2020) (Fig. 20b). Furthermore, lithospheric mantle was mechanically decoupled from the backstop and horizontally displaced to the east toward the continent. For this reason, there were important activations in the old west-vergent shear zones located in the Sierras de Córdoba during the construction of the Famatinian orogen (e.g. Semenov et al., 2019).

The deformation style across the collided edge suggests that there was an indentation of the Cuyania/Precordillera microcontinent over the proto-margin of Gondwana (von Gosen and Prozzi, 2005; Christiansen et al., 2019). At least three lines of evidence indicate that the Cuyania/Precordillera microplate was an indenter: 1) the subcircular-shape of the first-order structural mega-lineament named Valle Fértil-Desaguadero, which according to geophysical studies corresponds to a suture (e.g. Giménez et al., 2000; Introcaso et al., 2004; Álvarez et al., 2016) (Fig. 20a); 2) a counter-clockwise rotation due to tectonic escape for the Western Puna block, located immediately in the northern sector of the indentation, interpreted through paleomagnetic data by Spagnuolo et al. (2011); and 3) the style of wrap-around deformation of the shear zones in the indented basement between 30°S and 34°S, which suggests that there was a radial field of the horizontal deviatoric stress vectors (Christiansen et al., 2019).

The disposition and kinematic features of the main shear zones recognized in the Famatinian orogen southwards of 28° south latitude (Fig. 20a), show that the shortening directions were more or less perpendicular to the strike of the shear zones (Otamendi et al., 2020, and references therein), suggesting an orthogonal convergence of the indenter over the paleo-continent. However, the local obliquity shown by the stress vectors with respect to the general strike of the orogen in the SGSL (Fig. 6) is interpreted as a consequence of the clockwise rotation of the vectors due to the convex morphology of the indenter in these latitudes (Christiansen et al., 2019). The peaks of metamorphic conditions reflected in the paleo-depths, and consequently, in the vertical flow of the material during the orogenesis (e.g. Goscombe and Gray 2009) suggest that the Famatinian orogen was not uniformly exhumed, neither latitudinally nor longitudinally (Otamendi et al., 2020). The differential exhumation can be explained by the morphology of an indenter conditioning the deformation style of the indented margin (e.g. Houseman and England, 1993; Nettesheim et al., 2018).

Determining the horizontal components of movement or the shortening driven by the indentation of the Cuyania/Precordillera microcontinent is one of the future challenges. However, with a preliminary model of indentation it is possible to deduce that the shortening should increase from north to south along of Sierras Pampeanas Orientales (Fig. 20a, c). The total volume of exhumed material due to indentation should be proportional to the amount of shortening at the same latitude. This interpretation is consistent with the increase in paleo-depths from north to south along the Famatinian orogen between 34° S and 27° S (Otamendi et al., 2020). At 33° S, this event produced the development of a transpressive double-vergent megastructure (pop-up) with vertical extrusion of deep crustal rocks (~36 km), and would represent one of the sectors with greater orogenic shortening.

6. CONCLUSIONS

The shear zones of the Sierra de San Luis record greenschist to amphibolite facies deformation conditions (between 350° and 760° C) with lithologies that vary from protomylonites, mylonites, ultramylonites and phyllonites of metasedimentary to mafic/felsic igneous protoliths. The disposition of the shear zones shows an anastomosed pattern in plan view, but the results of the 3D litho-constrained inversion model show that most of shear zones converge in one central zone, resulting in a double-vergent megastructure. The deeper and hottest rocks (San José Complex) in the Sierra de San Luis are in the core of this structure, while the lower temperature and pressure rocks (San Luis Formation) are located below this high-grade unit. The Micaschist Group is structurally inserted between the high and low-grade units. The current distribution of the metamorphic units indicates an inverted disposition of the metamorphism, where deeper and hottest zones overthrust the more superficial and colder units.

The angles between the general orogen strike and the direction of stretching lineations in the shear zones indicate that the kinematic corresponds to a transpressional orogen of sinistral oblique (to high-angles) convergence with steep dips. The structural evidence, aeromagnetic contrasts, 3D litho-constrained model, and background on the sedimentation and provenance ages in the Conlara Metamorphic Complex suggest that this unit acted as a backstop during the development of the double-vergent transpressive belt. In this context, the Famatinian magmatic arc (located immediately to the west of the Nogolí Metamorphic Complex) acted as a buoyant crustal element during the convergence with the ability to support larger amounts of stress than the rocks of the backarc (Nogolí and Pringles metamorphic complexes, Las Higueras Complex and San Luis Formation).

An important shortening occurred during the Famatinian orogeny at the Pampean segment latitude, increasing from north to south over the collided edge. This is in concordance with the hypothesis of an indentation of the Cuyania/Precordillera microplate on the Gondwana proto-margin. In the segment that covers the Sierra Grande de San Luis (33° S) the shortening was responsible for a huge orogenic extrusion (with double-vergent disposition) developed over the Famatinian backarc.

7. ACKNOWLEDGEMENTS

We are particularly grateful to the Universidad Nacional de San Luis through projects PROICO 03-1818 and PROIPRO 03-1718, Universidad Nacional Del Sur, Instituto Geofísico Sismológico Volponi, Grosso Group Company and Servicio Geológico Minero (SEGEMAR) for providing access to the geophysical data for academic purposes. The authors would also like to acknowledge the Consejo Nacional de Investigaciones Científicas y Técnicas (CONICET) and Intrepids (www.intrepid-geophysics.com/) for the GeoModeller academic license. The authors are also thankful for the thorough review of the manuscript by Dr. Fernando Hongn, and an anonymous reviewer. We are grateful to Dr. Mariano Larrovere (guest editor) for the final suggestions that allowed improving the text.

8. References

Aceñolaza, F., Aceñolaza, G., 2005. La Formación Puncoviscana y unidades estratigráficas vinculadas en el Neoproterozoico - Cámbrico temprano del Noroeste Argentino. Latin American Journal of Sedimentology and Basin Analysis, 12, 65-87.

Aceñolaza, F.G., Toselli, A.J., 1976. Consideraciones estratigráficas y tectónicas sobre el Paleozoico inferior del Noroeste Argentino. Congreso Latinoamericano de Geología, No. 2, pp. 755-766.

Allmendinger, R.W., Cardozo, N.C., Fisher, D., 2013. Structural Geology Algorithms: Vectors & Tensors: Cambridge, England, Cambridge University Press, 289 pp.

Álvarez, O., Lince Klinger, F. Sánchez, M., Weidmann, C., Ariza, J., Giménez, M., 2016. Modelos globales de gravedad GOCE y EGM2008: su utilidad y complementariedad en la exploración geofísica. Revista de la Asociación Geológica Argentina, 73(1), 134-148.

Astini, R.A., Dávila F.M., 2004. Ordovician back arc foreland and Ocloyic thrust belt development on the western Gondwana margin as a response to Precordillera terrane accretion. Tectonics, 23, TC4008, DOI:10.1029/2003TC001620.

Augustsson, C., Rüsing, T., Adams, C.J., Chmiel, H., Kocabayoğlu, M., Büld, M., Zimmermann, U., Berndt, J., Kooijman, E., 2011. Detrital quartz and zircón combined: the production of mature sand with short transportation paths along the Cambrian West Gondwana margin, northwestern Argentina. Journal of Sedimentary Reseach, 81, 284-298.

Baldo, E., Rapela, C.W., Pankhurst, R.J., Galindo, C., Casquet, C., Verdecchia, S., Murra, J., 2014. Geocronología de las Sierras de Córdoba: revisión y comentarios. In: Martino, R.D., Guereschi, A.B., (Eds.), Geología y Recursos Naturales de la provincia de Córdoba, Asociación Geológica Argentina, 19º Congreso Geológico Argentino, Relatorio 1, 845-868, Córdoba.

Benedetto, J.L., 2004. The allochthony of the Argentine Precordillera ten years later (1993–2003), a new paleobiogeographic test of the microcontinental model. Gondwana Research, 7, 1027-1039.

Best, M.G., 2003. Igneous and Metamorphic Petrology, 729 pp. Oxford Blackwell Science.
Blakely, R.J., 1995. Potential Theory in Gravity & Magnetic Applications. 441 pp. Cambridge University Press. ISBN: 052141508X.

Blakely, R.J., 1995. Potential theory in gravity & magnetic applications. In: 441 pp. Press, Cambridge University 052141508X.

Brogioni, N., Parrini, P., Pecchioni, E., 2005. Petrología del magmatismo de arco predeformacional en el cordón del Realito y la Zona norte del Plutón La Escalerilla. Sierra de San Luis. Revista de la Asociación Geológica Argentina, 60 (3): 495-412.

Byrne, D.E., Wang, W.-H., Davis, D.M., 1993. Mechanical role of backstops in the growth of forearcs, Tectonics, 12, 123-144.

Calcagno, P., Chiles, J.P., Courrioux, G., Guillen, A., 2008. Geological modelling from field data and geological knowledge Part I. Modelling method coupling 3D potentialfield interpolation and geological rules. Physics of the Earth and Planetary Interiors, 171, 147-157.

Camilletti, G., Otamendi, J., Tibaldi, A., Cristofolini, E., Leisen, M., Romero, R., Barra, F., Armas, P., Barzola, M., 2020. Geology, petrology and geochronology of Sierra de Valle Fértil - La Huerta batholith: Implications for the construction of a middle-crust magmatic-arc section. Journal of South American Earth Sciences, 97, 102423.

Caminos, R., 1979. Sierras Pampeanas Noroccidentales. Salta, Tucumán, Catamarca, La Rioja y San Juan. In: Turner J.C.M., (Ed.), Geología Regional Argentina, Academia Nacional de Ciencias, 225-291, Córdoba.

Cardozo, N., Allmendinger, R.W., 2013. Spherical projections with OSXStereonet: Computers & Geosciences, v. 193-205, DOI: 10.1016/j.cageo.2012.07.021.

Carosi, R., Montomoli, Ch., Iaccarino, S., 2018. 20 years of geological mapping of the metamorphic core across Central and Eastern Himalayas. Earth-Science Reviews, 177, 124-138.

Carugno Durán, A., Ortiz Suárez, A., 2012. Metamorfitas de baja presión en la sierra de Socoscora, San Luis, y sus implicancias regionales. Revista de la Asociación Geológica Argentina, 69(2), 185-192.

Casquet, C., Pankhurst, R.J., Galindo, C., Rapela, C., Fanning, M., Baldo, E., Dahlquist, J., González Casado, J., Colombo, F., 2012. A history of Proterozoic Terranes in Southern South America: from Rodinia to Gondwana. Geoscience Frontiers, 3, 137-145.

Casquet, C., Baldo, E., Galindo, C. Pankhurst, R.J., Rapela, C.W., Fanning, M.C., 2014. Las vulcanitas de la Formación San Luis (Sierra de San Luis, Argentina): Nueva edad (SHRIMP) y geoquímica isotópica (Sr - Nd). 18° Congreso Geológico Argentino, Actas, S21-8, Córdoba.

Casquet, C., Dahlquist, J.A., Verdecchia, S.O., Baldo, E.G., Galindo, C., Rapela, C.W., Pankhurst, R.J., Morales, M.M., Murra, J.A., Fanning, C.M., 2018. Review of the Cambrian Pampean orogeny of Argentina; a displaced orogen formerly attached to the Saldania Belt of South Africa? Earth-Science Reviews, 177, 209-225.

Cawood, P.A., 2005. Terra Australis Orogen: Rodinia breakup and development of the Pacific and Iapetus margins of Gondwana during the Neoproterozoic and Paleozoic. Earth-Science Reviews, 69 (3-4), 249-279.

Chernicoff, C. J., & Ramos, V. A. (2003). El basamento de la sierra de San Luis: nuevas evidencias magnéticas y sus implicancias tectónicas. Revista de la Asociación Geológica Argentina, 58(4), 511-524.

Chetty, T.R.K., Bhaskar Rao, Y.J., 2006. The Cauvery Shear Zone, Southern Granulite Terrain, India: A crustal-scale flower structure. Gondwana Research, 10, 77–85.

Christiansen, R., Rodriguez, A., Martinez, P., Lince Klinger, F., 2015. Avances en el tratamiento estadístico de datos gravimétricos de las sierras de San Luis y Comechingones, importancia del grillado en procesamientos posteriores. Geoacta, 40(2), 76-86.

Christiansen, R., 2019. Estudios gravi-magnetométricos de la Sierra Grande de San Luis. Inversión conjunta litorrestringida y modelado en 3D. (Doctoral thesis, Universidad Nacional de San Juan, San Juan, Argentina). Available from the Universidad Nacional de San Juan repository. DOI: 10.13140/RG.2.2.11134.84806

Christiansen, R., Morosini, A., Enriquez, E., Muñoz, B.L., Lince klinger, F., Martinez, M.P., Ortiz Suárez, A., Kostadinoff, J., 2019. 3D litho-constrained inversion model of southern Sierra Grande de San Luis: new insights into the Famatinian tectonic setting. Tectonophysics, 756, 1-24.

Clark, D.A., 1997. Magnetic petrophysics and magnetic petrology: aids to geological interpretation of magnetic surveys. AGSO Journal of Australian Geology and Geophysics, 17, 83–104.

Collo, G., Astini, R., Cawood, P.A., Buchan, C., Pimentel, M., 2009. U–Pb detrital zircon ages and Sm–Nd isotopic features in low-grade metasedimentary rocks of the Famatina belt: implications for late Neoproterozoic–early Palaeozoic evolution of the proto-Andean margin of Gondwana. Journal of the Geological Society of London, 166, 303-319.

Costa, C., Gardini, C., Chiesa, J., Ortiz Suárez, A., Ojeda, G., Rivarola, D., Tognelli, G., Strasser, E., Carugno Durán, A., Guerstein, P., Sales, D., Vinciguerra, 2001. Hoja Geológica 3366-III San Luis, provincias de San Luis y Mendoza. Instituto de Geología y Recursos Minerales, Servicio Geológico-Minero Argentino (SEGEMAR), Boletín Nº 293, pp 104, en CD, ISSN Nº 1667-1988.

Cristofolini, E.A., Otamendi, J.E., Ducea, M.N., Pearson, D.M., Tibaldi, A.M., Baliani, I., 2012. Detrital zircon U–Pb ages of metasedimentary rocks from Sierra de Valle Fértil: entrapment of Middle and Late Cambrian marine successions in the deep roots of the Early Ordovician Famatinian arc. Journal of South American Earth Sciences, 37, 77-94.

Cristofolini, E.A., Otamendi, J.E., Walker Jr., B.A., Tibaldi, A.M., Armas, P., Bergantz, G.W., Martino, R.D., 2014. A Middle Paleozoic shear zone in the Sierra de Valle Fértil, Argentina: Records of a continent-arc collision in the Famatinian margin of Gondwana. Journal of South American Earth Sciences, 56, 170-185.

Cristofolini, E.A., Otamendi, J.E., Martino, R.D., Tibaldi, A.M., Armas, P., Barzola, M., 2017. Faja de cizalla Las Lajas: petrografía, estructura interna e implicancias tectónicas, extremo sur de la Sierra de Comechingones, Provincias de Córdoba y San Luis. Revista de la Asociación Geológica Argentina, 74(3), 295-314.

Cruciani, G., Franceschelli, M., Groppo, C., Brogioni, N., Vaselli, O., 2008. Formation of clinopyroxene + spinel and amphibole + spinel symplectites in coronitic gabbros from the Sierra de San Luis (Argentina): a key to post-magmatic evolution. Journal of Metamorphic Geology, 26 (7), 759-774.

Cruciani, G., Franceschelli, M., Brogioni, N., 2011. Mineral re-equilibration and P-T path of metagabbros, Sierra de San Luis, Argentina: insights into the exhumation of a mafic-ultramafic belt. European Journal of Mineralogy, 23, 591-608.

Cruciani, G., Franceschelli, M., Brogioni, N., 2012. Early stage evolution of the mafic-ultramafic belt at La Melada, Sierra de San Luis, Argentina: P-T constraints from metapyroxenite pseudosection modelling. Journal of South American Earth Sciences, 37, 1-12.

Dahlquist, J.A., Macchioli Grande, M., Alasino, P.H., Basei, M.A., Galindo, C., Moreno, J.A., Morales Camera, M.M., 2019. New geochronological and isotope data for the Las Chacras – Potrerillos and Renca batholiths: A contribution to the Middle-Upper Devonian magmatism in the pre-Andean foreland (Sierras Pampeanas, Argentina), SW Gondwana. Journal of South American Earth Sciences, 93, 348-363.

Dalla Salda, L., 1987. Basement tectonics of the southern Pampean Ranges, Argentina. Tectonics, 6(3), 249-260.

Delakowitz, B., Höll, R., Hack, M., Brodtkorb, M., Stärk, H., 1991. Geological and geochemical studies of the Sierra del Morro-Oeste (San Luis Province, Argentina): meta-sediments and meta-volcanics from a probable back-arc setting. Journal of South American Earth Sciences, 4, 189-200.

Delpino, S., Dimieri, L., Bjerg, E., Kostadinoff, J., Mogessie, A., Hoinkes, G., Hauzenberger, Ch., Felfernig, A., 2001. Geometrical analysis and timing of structures on mafic-ultramafic bodies and high-grade metamorphic rocks, Sierras Grandes of San Luis, Argentina. Journal of South American Earth Science, 14(1), 101-112.

Delpino, S.H, Bjerg, E.A., Ferracutti, G.R., Mogessie, A., 2007. Counterclockwise tectonometamorphic evolution of the Pringles Metamorphic Complex, Sierras Pampeanas of San Luis (Argentina). Journal of South America Earth Science, 23, 147-175.

Delpino, S., Rueda, M., Urraza., I., Grasemann, B., 2016. Microstructural development in ductile deformed metapelitic–metapsamitic rocks: A case study from the greenschist to granulite facies megashear zone of the Pringles Metamorphic Complex, Argentina. In: Mukherjee, S., Mulchrone, K.F (eds), Ductile Shear Zones: From micro-to macro-scales, First Edition. Ltd. Published 2016 by John Wiley & Sons, Ltd., 224-248.

Drobe, M., López de Luchi, M.G., Steenken, A., Frei, R., Naumann, R., Wemmer, K., Siegesmund., 2009. Provenance of the Late Proterozoic to Early Cambrian metaclastic sediments of the Sierra de San Luis (Eastern Sierras Pampeanas) and Cordillera oriental, Argentina. Journal of South American Earth Sciences, 28, 239-262.

Drobe, M., López de Luchi, M.G., Steenken, A., Wemmer, K., Naumann, R., Frei, R., Siegesmund., 2011. Geodynamic evolution of the Eastern Sierras Pampeanas (Central Argentina) based on geochemical, Sm–Nd, Pb–Pb and SHRIMP data. International Journal of Earth Science, (Geol Rundsch), 100, 631-657.

Ducea, M.N., Otamendi, J., Bergantz, G.W., Jianu, D., Petrescu, L., 2015. Constraints on the origin of the Ordovician Famatinian – Puna Arc. In: In: DeCelles, P.G., Ducea, M.N., Carrapa, B., Kapp, P. (Eds.), Geodynamics of a Cordilleran Orogenic System: The Central Andes of Argentina and Northern Chile, Geological Society of America Memoir 212. pp. 125–139.

Ducea, M.N., Otamendi, J.E., Bergantz, G., Stair, K., Valencia, V., Gehrels, G., 2010. Timing constraints on building an intermediate plutonic arc crustal section: U–Pb zircon geochronology of the Sierra Valle Fértil, Famatinian arc, Argentina. Tectonics, 29, TC4002.

Enriquez, E., González, L., Zavaroni, G., Ortiz Suárez, A., Muñoz, B., 2015. Geología del basamento de la región Los Piquillines-San Martín, provincia de San Luis. 3° Simposio sobre Petrología Ígnea y Metalogénesis Asociada. Resúmenes, 62-63, General Roca, Río Negro.

Escayola, M.P., Pimentel, M.M., Armstrong, R., 2007. Neoproterozoic backarc basin: sensitive high-resolution ion microprobe U-Pb and Sm-Nd isotopic evidence from the Eastern Pampean Ranges, Argentina. Geology, 35, 495-498.

Escayola, M.P., van Staal, C.R., Davis, W.J., 2011. The age and tectonic setting of the Puncoviscana Formation in northwestern Argentina: An accretionary complex related to Early Cambrian closure of the Puncoviscana Ocean and accretion of the Arequipa-Antofalla block. Journal of South American Earth Sciences, 32(4), 438-459.

Finch, M.A., Weinberg, R.F., Hasalová, P., Becchio, R., Fuentes, M.G. Kennedy, A., 2017. Tectono-metamorphic evolution of a convergent back-arc: the Famatinian orogen, Sierra de Quilmes, Sierras Pampeanas, NW Argentina. Geological Society of America Bulletin, 129, 1602-1621.

Giménez, M.E., Martínez, M.P., Introcaso, A., 2000. A Crustal model based mainly on gravity data in the area between the Bermejo basin and the Sierras de Valle Fértil- Argentina. Journal of South American Earth Sciences, 13, 275-286.

González, P., Sato, A., Basei, M., Vlach, S., Llambías, E., 2002. Structure, metamorphism and age of the Pampean-Famatinian Orogenies in the Western Sierras de San Luis. 15° Congreso Geológico Argentino (El Calafate), Actas 2, 51-56, Buenos Aires.

González, P.D., Sato, A.M., Llambías, E.J., Basei, M.A.S., Vlanch, S., 2004. Early Paleozoic structural and metamorphic evolution of western Sierra de San Luis, in relation to the accretion of Cuyania. Gondwana Research, 7, 1157-1170.

González, P., Sato, A., Llambías, E., 2006. Geologías de las fajas de deformación dúctil del oeste de la Sierra de San Luis. 13º Reunión de Tectónica, Resúmenes: p. 29, San Luis.

Goscombe, B., Gray, D., 2009. Metamorphic response in orogens of different obliquity, scale and geometry. Gondwana Research, 15, 151-167. DOI:10.1016/j.gr.2008.07.005.

Goscombe B., Gray D., Carson C., Groenewald, B., Scrimgeour I., 2005. Classification of metamorphic gradients and their utilization as indicators of tectonic regimes. Geological Society of Australia, Specialist Group in Tectonics and Structural Geology, Conference abstracts, Townsville.

Gromet, L.P., Otamendi, J.E., Miró, R., Demichelis, A.H., Schwartz, J.J., Tibaldi, A.M., 2005. The Pampean orogeny: ridge subduction of continental collision? Gondwana 12: Geological and Biological Heritage of Gondwana, Abstracts, 185, Mendoza.

Grosse, P., Söllner, F., Báez, M.A., Toselli, A.J., Rossi, J.N., de la Rosa, J.D., 2009. Lower Carboniferous post-orogenic granites in central-eastern Sierra de Velasco, Sierras Pampeanas, Argentina: U-Pb monazite geochronology, geochemistry and Sr-Nd isotopes. International Journal of Earth Sciences, 98, 1001-1025.

Guillen, A., Calcagno, P., Courrioux, G., Joly, A., Ledru, P., 2008. 3D realistic modelling of geology from field data and geological knowledge, part II – modelling validation using of gravity and magnetic data inversion. Physics of the Earth and Planetary Interiors, 171, 158-169.

Hauzenberger, C.A, Mogessie, A., Hoinkes, G., Bjerg, E.A, Kostadinoff, J., Delpino, S., Dimieri, L., 1997. Platinum group minerals in the basic to ultrabasic complex of the Sierras de San Luis, Argentina. In: Papunen, H. (ed) Mineral deposits: research and explorations - where do they meet? Balkema, Rotterdam, pp 439-442.

Hauzenberger, C., Mogessie, A., Hoinkes, G., Felfernig, A., Bjerg, E., Kostadinoff, J., Delpino, S., Dimieri, L., 2001. Metamorphic evolution of the Sierras de San Luis, Argentina: granulites facies metamorphism related to mafic intrusions. Mineralogy and Petrology, 71, 95-126.

Hinze, W.J., 2003. Bouguer reduction density, why 2.67? Geophysics, 68(5), 1559-1560.

Höckenreiner, M., Söllner, F., Miller, H., 2003. Dating the TIPA shear zone, an Early Devonian terrane boundary between the Famatinian and Pampean systems (NW Argentina). Journal of South American Earth Sciences, 16, 45-66.

Houseman, G., England, P., 1993. Crustal thickening versus lateral expulsion in the Indian-Asian continental collision. Journal of Geophysical Research, 98, B7, 12233-12249.

Iannizzotto, N.F., Rapela, C.W., Baldo, E.G., Galindo, C., Fanning, C.M., Pankhurst, R.J., 2013. The sierra norte - ambargasta batholith: late ediacaran - early cambrian magmatism associated with Pampean transpressional tectonics. Journal of South American Earth Sciences, 42, 127-143.

Introcaso, A., Martínez, M.P., Giménez, M., Ruiz, F., 2004. Geophysical study of the Valle Fértil lineament between 28°45′S and 31°30′S: boundary between the Cuyania and Pampia terranes. Gondwana Research, 7(4), 1117-1132.

Isles, D.J., Rankin, L.R., 2013. Geological Interpretation of Aeromagnetic Data. Australian Society of Exploration Geophysicists, Perth, Australia, 4-21.

Jacobsen, B.H., 1987. A case for upward continuation as a standard separation filter for potential-field maps. Geophysics, 52(8), 1138-1148.

Kane, M.F., 1962. A comprehensive system of terrain corrections using a digital computer. Geophysics, 27(4), 455-462.

LaFehr, T.R., 1991a. Standardization in gravity reduction. Geophysics, 56(8), 1170-1178.

LaFehr, T.R., 1991b. An exact solution for the gravity curvature (Bullard B) correction. Geophysics, 56(8), 1179-1184.

Larrovere, M.A., de los Hoyos, C.R., Toselli, A.J., Rossi, J.N., Basei, M.A.S., Belmar, M.E., 2011. High T/P evolution and metamorphic ages of the migmatitic basement of northern Sierras Pampeanas, Argentina: characterization of a mid-crustal segment of the Famatinian belt. Journal of South American Earth Sciences, 31(2-3), 279-297.

Larrovere, M.A., Suzaño, N., Ratschbacher, B.C., Sola, A., Alasino, P.H., Fuentes, M.G., Weinberg, R.F., Paterson, S.R., Becchio, R., Finch, M.A., 2017. Las fajas de cizalla dúctil del basamento ígneo-metamórfico del NOA. In: Muruaga C., Grosse P. (eds.), Ciencias de La Tierra y recursos naturales del NOA. Relatorio del XX Congreso Geológico Argentino, S.M. de Tucumán, 579-601.

Larrovere, M.A., de los Hoyos, C.R., Willner, A.P., Verdecchia, S.O., Baldo, E.G., Casquet, C., Basei, M.A., Hollanda, M.H., Rocher, S., Alasino, P.H., Moreno, G.G., 2020. Mid-crustal deformation in a continental margin orogen: structural evolution and timing of the Famatinian Orogeny, NW Argentina. Journal of the Geological Society, 177(2), 233-257.

Little, T.A., Holcombe, R.J., Ilga, B.R., 2002. Kinematics of oblique collision and ramping inferred from microstructures and strain in middle crustal rocks, central Southern Alps, New Zealand. Journal of Structural Geology, 24, 219-239.

Llambías, E.J., Malvicini, L., 1982. Geología y génesis de los yacimientos de tungsteno de las Sierras del Morro, Los Morrillos y Yulto, provincia de San Luis. Revista de la Asociación Geológica Argentina, 37, 100-143.

Llambías, E., Sato, A.M., Ortiz Suárez, A., Prozzi, C., 1998. The granitoids of the sierra de San Luis. Geological Society of London. Special Publication Nº 142. In: Pankhurst, R.J., Rapela, C.W., (eds), The Proto-Andean Margin of Gondwana. Geological Society of London, Special Publication, 142, 325-341.

López de Luchi, M., Hoffmann, A., Siegesmund, S., Wemmer, K., Steenken, A., 2002. Temporal constraints on the polyphase evolution of the Sierra de San Luis. Preliminary report based on biotite and muscovite cooling ages. 15° Congreso Geológico Argentino, Actas 1, 309-315. El Calafate.

López de Luchi, M.G., Cerredo, M.E., Siegesmund, S., Steenken, A., Wemmer, K., 2003. Provenance and tectonic setting of the protoliths of the metamorphic complexes of Sierra de San Luis. Revista de la Asociación Geológica Argentina, 58(4), 525-540.

López de Luchi, M.G, Siegesmund, S., Wemmer, K., Steenken, A., Naumann, R., 2007. Geochemical constraints on the petrogenesis of the Paleozoic granitoids of the Sierra de San Luis, Sierras Pampeanas, Argentina. Journal of South American Earth Sciences, 24, 138-166.

López de Luchi, M.G., Siegesmund, S., Wemmer, K., Nolte, N., 2017. Petrogenesis of the postcollisional Middle Devonian monzonitic to granitic magmatism of the Sierra de San Luis, Argentina. Lithos, 288-289, 191-213.

López de Luchi, M.G., Martínez Dopico, C.I., Wemmer, K., Siegesmund, S., 2018. Untangling the neoproterozoic-early Paleozoic tectonic evolution of the eastern sierras Pampeanas hidden in the isotopical record. In: Siegesmund, S., Basei, M., Oyhantçabal, P., Oriolo, S. (Eds.), Geology of Southwest Gondwana. Regional Geology Reviews. Springer, pp. 433–466.

Martino, R.D., 2003. Las fajas de deformación dúctil de las Sierras Pampeanas de Córdoba: Una reseña general. Revista de la Asociación Geológica Argentina, 58(4), 549-571.

Morosini, A., 2011. El Granito La Escalerilla, Provincia de San Luis. Ph.D. thesis. Universidad Nacional de San Luis. 434 p. (unpublished).

Morosini, A., Ortiz Suárez, A., 2010. La deformación famatiniana del granito La Escalerilla, Sierra de San Luis. Revista de la Asociación Geológica Argentina, 67(4), 481-493.

Morosini, A., Ortiz Suárez, A., 2011. El metamorfismo de contacto del granito La Escalerilla en el área de La Carolina, San Luis. Revista de la Asociación Geológica Argentina, 68(2), 279-291.

Morosini, A., Ortiz Suárez, A., 2013. Inversión metamórfica asociada al emplazamiento de granitos sincolisionales en la sierra de San Luis. 11º Congreso de Mineralogía y Metalogenia. Universidad Nacional de San Juan. Acta 1, 321-326. San Juan.

Morosini, A., Enriquez, E., Ortiz Suárez, A., Ramos, G., Carugno Durán, A., Ulacco, J., 2014. Hipótesis de extrusión vinculada a la inversión metamórfica del Complejo Metamórfico Pringles, Sierra de San Luis. 19° Congreso Geológico Argentino, Actas, S21-38, Córdoba.

Morosini, A., Ortiz Auárez, A., Otamendi, J., Pagano, D., Ramos, G., 2017. La Escalerilla pluton, San Luis Argentina: The orogenic and post-orogenic magmatic evolution of the famatinian cycle at Sierras de San Luis. Journal of South American Earth Sciences, 73, 100-118.

Morosini, A., Enriquez, E., Pagano, D.S., Orozco, B., Ulacco, J., Tibaldi, A., Cristofolini, E., Muñoz, B., Ortiz Suárez, A., Sánchez, E., Icazatti, F., Gil, R., Crespo, E., Ramos, G., 2019. Las Cañas plutonic complex: Geodynamic implications during the Famatinian orogenic magmatism in northeast of Sierra de San Luis, Argentina. Journal of South American Earth Sciences, 93, 313-347.

Mulcahy, S., Roeske, S., McClelland, W., Ellis, J., Jourdan, F., Renne, P., Vujovich, G.I., 2014. Multiple migmatite events and cooling from granulite facies metamorphism within the Famatina arc margin of northwest Argentina. Tectonics, 33, 1-25.

Nagy, D., 1966. The gravitational attraction of a right rectangular prism. Geophysics, 31(2), 362-371.

Naudy, H., Dreyer, H., 1968. Non-linear filtering applied to aeromagnetic profiles. Geophysical Prospecting, 16(2), 171–178.

Nettesheim, M., Ehlers, T.A., Whipp, D.M., Koptev, A., 2018. The influence of upper-plate advance and erosion on overriding plate deformation in orogen syntaxes. Solid Earth, 9, 1207-1224.

Ortiz Suárez, A., 1988. El basamento de Las Aguadas, provincia de San Luis. Revista de la Asociación Argentina de Mineralogía, Petrología y Sedimentología, 19(1-4), 13-24.

Ortiz Suárez, A., 1999. Geología y petrología del área de San Francisco del Monte de Oro, San Luis. Ph.D. thesis. Facultad de Ciencias Físico-Matemáticas y Naturales, Universidad Nacional de San Luis. (unpublished).

Ortiz Suárez, A., Prozzi, C., Llambías, E., 1992. Geología de la parte Sur de la Sierra de San Luis y granitoides asociados, Argentina. Revista de estudios geológicos, 48, 269-277.

Ortiz Suárez, A., Casquet, M. C., 2005. Inversión metamórfica en el orógeno famatiniano de la Sierra de San Luis, Argentina. Geogaceta, 38, 231-234.

Ortiz Suárez, A., Grosso Cepparo, P., Gómez Figueroa, J., Erroz, M., Montenegro, T., 2009. Geología del Basamento en el extremo noroeste de la Sierra de San Luis. Revista de la Asociación Geológica Argentina, 64 (3), 481-492.

Otamendi, J.E., Vujovich, G.I., de la Rosa, J.D., Castro, A., Tibaldi, A., Martino, R., Pinotti, L., 2009. Geology and petrology of a deep crustal zone the Famatinian paleoarc, Sierras Valle Fértil – La Huerta, San Juan, Argentina. Journal of South American Earth Sciences, 27, 258-279.

Otamendi, J.E., Pinotti, L.P., Basei, M.A.S., Tibaldi, A.M., 2010. Evaluation of petrogenetic models for intermediate and silicic plutonic rocks from the Sierra de Valle Fértil-La Huerta, Argentina: petrologic constraints on the origin of igneous rocks in the Ordovician Famatinian-Puna paleoarc. Journal of South American Earth Sciences, 30, 29-45.

Otamendi, J.E., Ducea, M.N., Cristofolini, E.A., Tibaldi, A.M., Camilletti, G.C., Bergantz, G.W., 2017. U-Pb ages and Hf isotope compositions of zircons in plutonic rocks from the central Famatinian arc, Argentina. Journal of South American Earth Sciences, 76, 412–426.

Otamendi, J.E., Cristofolini, E.A., Morosini, A., Armas, P., Tibaldi, A.M., Camilletti, G.C., 2020. The geodynamic history of the Famatinian arc: a record of exposed geology over the type section (latitudes 27º- 33º south). Journal of South American Earth Sciences, 100 (102558), 1-22.

Pankhurst, R.J., Rapela, C.W., Saavedra, J., Baldo, E., Dahlquist, J., Pascua, I., Fanning, C.M., 1998. The Famatinian magmatic arc in the central Sierras Pampeanas: an Early to Mid-Ordovician continental arc on the Gondwana margin. In: Pankhurst, R.J., Rapela, C.W. (Eds.), The Proto-andean Margin of Gondwana, Geological Society, London, vol. 142. Special Publication, 343-368.

Passchier, C.W., Trouw, R.A.J., 2005. Microtectonics (second ed.), Springer–Verlag, Berlin, p. 133.

Perón Orrillo, J.M., Romero, R., Otamendi, J., Morosini, A., Rivarola, D., Barra, F., Leisen, M., Ortiz Suárez, A., 2019. Depositional age and provenance in the San Luis Formation, Sierras Pampeanas, Argentina: evidence from detrital zircon studies. Journal of South American Earth Sciences, 94 (102228), 1-17.

Prozzi, C., Ramos, G., 1988. La formación San Luis. I Jornadas de Trabajo de Sierras Pampeanas. San Luis. Actas 1, San Luis.

Ramos, V.A., 1988. Late Pretorozoic-Early Paleozoic of South America: a collisional history. Episodes, 11, 168-174.

Ramos, V.A., 2004. Cuyania, an exotic block to Gondwana: review of a historical success and the present problems. Gondwana Research, 7(4), 1009-1026.

Ramos, V.A., 2010. The tectonic regime along the Andes: Present-day and Mesozoic regimes. Geological Journal, 45: 2-25.

Ramos, V.A, 2018. The Famatinian orogen along the protomargin of Western Gondwana: evidence for a nearly continuous Ordovician magmatic arc between Venezuela and Argentina. In: The Evolution of the Chilean-Argentinean Andes. Springer, pp. 133-161.

Ramos, V.A, Jordan, T., Allmendinger, R., Kay, S., Cortés, J., Palma, M., 1984. Chilenia: un terreno alóctono en la evolución paleozoica de los Andes Centrales. 10° Congreso Geológico Argentino, Actas 2, 84-106.

Ramos, V.A., Cristallini, E.O., Pérez, D.J., 2002. The Pampean flat-slab of the Central Andes. Journal of South American Earth Sciences, 15, 59-78.

Ramos, V.A., Martino, R.D., Otamendi, J.E., Escayola, M.P., 2014. Evolución geotectónica de las Sierras Pampeanas Orientales. In: Martino, R.D., Guereschi, A.B., (Eds.), Geología y Recursos Naturales de la provincia de Córdoba, Asociación Geológica Argentina, 19º Congreso Geológico Argentino, Relatorio 1, 965-977, Córdoba.

Ramsay, J.G., 1967. Folding and Fracturing of Rocks. McGraw-Hill, New York, 568.

Rapela, C.W., Pankhurst, R.J., Casquet, C., Baldo, E., Saavedra, J., Galindo, C., Fanning, C.M., 1998. The Pampean Orogeny of the southern proto-Andes: Cambrian continental collision in the Sierras de Córdoba. In: Pankhurst, R.J., Rapela, C.W., (eds), The Proto-Andean Margin of Gondwana. Geological Society, London, Special Publication, 142, 181-217.

Rapela, C.W., Pankhurst, R.J., Casquet, C., Baldo, E., Saavedra, J., Galindo, C., Fanning, C.M., 2007. The Pampean Orogeny of the southern proto-Andes: Cambrian continental collision in the Sierras de Córdoba. Earth-Science Reviews, 142, 181-217.

Rapela, C.W., Verdecchia, S.O., Casquet, C., Baldo, E,G., Galindo, C., Murra, J.A., Dahlquist, J.A., 2016. Identifying Laurentian and SW Gondwana sources in the Neoproterozoic to Early Paleozoic metasedimentary rocks of the Sierras Pampeanas: Paleogeographic and tectonic implications. Gondwana Research, 32, 193-212.

Saavedra, J., Toselli, A., Rossi, J., Pellitero, E., Durand, F., 1998. The Early Palaeozoic magmatic record of the Famatina System: a review. In: Pankhurst RJ, Rapela CW (eds.), The Proto-Andean Margin of Gondwana: Geological Society, London, Special Publication, 142, 283-295.

Sato, A.M., González, P.D., Llambías, E.J., 2003. Evolución del orógeno Famatiniano en la Sierra de San Luis: magmatismo de arco, deformación y metamorfismo de bajo a alto grado. Revista de la Asociación Geológica Argentina, 58(4), 487-504.

Sato, A.M., Gonzalez, P., Basei, M.A.S., 2005. Los ortogneises granodioríticos del Complejo Metamórfico Nogolí, Sierra de San Luis. In: 16 Congreso Geológico Argentino, Actas 1, 33-40. La Plata.

Schulmann, K., Lexa, O., Štípská, P., Racek, M., Tajčmanová, L., Konopásek, J., Edel, J. -B., Peschler, A., Lehmann, J., 2008. Vertical extrusion and horizontal channel flow of orogenic lower crust: key exhumation mechanisms in large hot orogens? Journal of Metamorphic Geology, 26, 273-297.

Schwartz, J.J., Gromet, L.P., Miró, R., 2008. Timing and duration of the calc-alkaline arc of the Pampean orogeny: implications for the late neoproterozoic to Cambrian evolution of western Gondwana. Journal of Geology, 116, 39–61.

Semenov, I., Weinberg, R., Taylor, R., Jourdan, F., 2019. Prolonged movement on a > 10-km-wide thrust during early Paleozoic orogeny in the Gondwana margin of NW Argentina. Tectonics, 38(8), 3210-3236.

Siegesmund, S., Steenken, A., López de Luchi, M.G., Wemmer, K., Hoffmann, A., Mosch, S., 2004. The Las Chacras-Potrerillos batholith (Pampean Ranges, Argentina): structural evidences, emplacement and timing of the intrusion. International Journal of Earth Sciciences (Geol Rundsch), 93, 23-43.

Siegesmund, S., Steenken, A., Martino, R.D., Wemmer, K., López de Luchi, M.G., Frei, R., Guereschi, A., 2010. Time constraints on the tectonic evolution of the Eastern Sierras Pampeanas (Central Argentina). International Journal of Earth Sciences, 99(6), 1199-1226.

Sims, J.P., Stuart-Smith, P.G., Lyons, P., Skirrow, R.G., 1997. “Report on 1:250.000 scale Geological and Metallogenic Maps, Sierras de San Luis and Comechingones. Prov. of San Luis and Córdoba”.

Sims, J., Ireland, T., Camacho, A., Lyons, P., Pieters, P., Skirrow, R., Stuart-Smith, P., Miró, R., 1998. U-Pb, Th-Pb and Ar-Ar geochronology from the southern Sierras Pampeanas, Argentina: implications for the Paleozoic tectonic evolution of the western Gondwana margin. In: Pankhurst, R.J., Rapela, C.W., (eds), The Proto-Andean Margin of Gondwana. Geological Society, London, Special Publication, 142, 256-281.

Simpson, C., De Paor, D., 1991. Deformation and kinematic of high strain zones. Annual GSA meeting. Short course notes. 116 p.

Smithson, S.B., 1971. Densities of metamorphic rocks. Geophysics, 36(4), 690-694.

Solar, G.S., Brown, M., 2001. Deformation partitioning during transpression in response to Early Devonian oblique convergence, northern Appalachian orogen, USA. Journal of Structural Geology, 23, 1043-1065.

Spagnuolo, C.M., Rapalini, A.E., Astini, R.A., 2011. Reinterpretation of the Ordovician rotations in NW Argentina and Northern Chile: a consequence of the Precordillera collision? International Journal of Earth Sciences (Geol Rundsch), 100, 603-618. https://doi.org/10.1007/s00531-010-0578-2.

Steenken, A., López de Luchi, M.G., Siegesmund, S., Wemmer, K., Pawlig, S., 2004. Crustal provenance and cooling of the basement complexes of the Sierra de San Luis: an insight into the tectonic history of the proto-Andean margin of Gondwana. Gondwana Research, 7, 1171–1195.

Steenken, A., Siegesmund, S., López de Luchi, M.G., Frei, R., Wemmer, K., 2006. Neoproterozoic to early Palaeozoic events in the Sierra de San Luis: implications for the Famatinian geodynamics in the Eastern Sierras Pampeanas (Argentina). Journal of Geological Society, 163, 965–982.

Steenken, A., Siegesmund, S., Wemmer, K., López de Luchi, M.G., 2008. Time constraints on the Famatinian and Achalian structural evolution of the basement of the Sierra de San Luis (Eastern Sierras Pampeanas, Argentina). Journal of South American Earth Sciences, 25(3), 336-358.

Steenken, A., López de Luchi, M.G., Martínez Dopico, C., Drobe, M., Wemmer, K., Siegesmund, S., 2010. The Neoproterozoic-early Paleozoic metamorphic and magmatic evolution of the Eastern Sierras Pampeanas: an overview. International Journal of Earth Sciences, 1-24 pp., DOI:https://doi.org/10.1007/s00531-010-0624-0.

Stuart-Smith, P., Camacho, A., Sims, J., Skirrow, R., Lyons, P., Pieters, P., Black, L., Miro, R., 1999. Uranium-lead dating of felsic magmatic cycles in the southern Sierras Pampeanas, Argentina: implications for the tectonic development of the proto-Andean Gondwana margin. In: Ramos, V.A., Keppie, J.D. (Eds.), Laurentia-gondwana before Pangea, vol. 336. Geological Society of America, pp. 87-114. Special Paper.

Thomas, W.A., Astini, R.A., 1996. The Argentine precordillera: a traveler from the Ouachita embayment of North American Laurentia. Science, 273(5276), 752-757.

Tibaldi, A.M., Otamendi, J.E., Gromet, L.P., Demichelis, A.H., 2008. Suya Taco and Sol de Mayo mafic complexes from Eastern Sierras Pampeanas, Argentina: evidence for the emplacement of primitive OIB like magmas into deep crustal levels at a late stage of the Pampean orogeny. Journal of South American Earth Sciences, 26, 172-187.

Tibaldi, A.M., Otamendi, J.E., Cristofolini, E.A., Baliani, I., Walker Jr., B.A., Bergantz, G.W., 2013. Reconstruction of the Early Ordovician Famatinian arc through thermobarometry in lower and middle crustal exposures, Sierra de Valle Fértil, Argentina. Tectonophysics, 589, 151-166.

Toselli, A.J., Durand, F., Rossi, J.N., Saavedra, J., 1996. Esquema de evolución geotectónica y magmática Eopaleozoica del Sistema de Famatina y sectores de Sierras Pampeanas. Actas 13° Congreso Geológico Argentino, Actas 5, 443-462.

Verdecchia, S.O., Baldo, E.G., Benedetto, J.L., Borghi, P.A., 2007, The First shelly faunas from metamorphic rocks of the Sierras Pampeanas (La Cébila Formation, Sierra de Ambato, Argentina): age and paleogeographic implications: Ameghiniana, 44(2), 493-498.

Verdecchia, S.O., Collo, G., Zandomeni, P.S., Wunderlin, C., Ferhmann, M., 2019. Crystallochemical indexes and geothermobarometric calculations as a multiproxy approach to P-T condition of the low-grade metamorphism: the case of the San Luis Formation, Eastern Sierras Pampeanas of Argentina. Lithos, 324–325, 385–401.

von Gosen, W., 1998a. Transpressive deformation in the southwestern part of the Sierras de San Luis (Sierras Pampeanas, Argentina). Journal of South American Earth Sciences, 11(3), 233-264.

von Gosen, W., 1998b. The Phyllite and Micaschist Group with associated intrusions in the Sierras de San Luis (Sierras Pampeanas/Argentina) - structural and metamorphic relations. Journal of South American Earth Sciences, 11(1), 79-109.

von Gosen, W., Prozzi, C., 1998. Structural Evolution of the Sierra de San Luis (Eastern Sierras Pampeanas, Argentina): implications for the proto-andean Margin of Gondwana. In: Pankhurst, R.J., Rapela, C.W., (eds), The Proto-Andean Margin of Gondwana. Geological Society, London, Special Publication, 142, 235-258.

von Gosen, W., Prozzi, C., 2005. Deformation of an Early Paleozoic magmatic arc related to terrane collision: Sierra de San Luis (Eastern Sierras Pampeanas, Argentina), Neues Jahrbuch für Geologie und Paläontologie, 238(1), 107-160.

von Gosen, W., Loske, W., Prozzi, C., 2002. New isotopic dating of intrusive rocks in the Sierra de San Luis (Argentina): implications for the geodynamic history of the Eastern Sierras Pampeanas. Journal of South American Earth Sciences, 15, 237-250.

Weidmann, C., Giménez, M., Lince Klinger, F., Alvarez, O., 2016. Anomalous values of gravity and magnetism in the western margin of Gondwana. Tectonophysics, 667, 1-15.

Weinberg, R.F., Becchio, R., Farias, P., Suzaño, N., Sola, A., 2018. Early Paleozoic accretionary orogenies in NW Argentina: Growth of West Gondwana. Earth-Science Reviews, 187, 219-247.

Whitmeyer, S.J., Simpson, C., 2004. Regional deformation of the Sierra de San Luis, Argentina: Implications for the Paleozoic development of western Gondwana. Tectonics, 23, 1-16. DOI: 10.1029/2003TC001542.

Zeng, H., Xu, D., Tan, H., 2007. A model study for estimating optimum upward-continuation height for gravity separation with application to a Bouguer gravity anomaly over a mineral deposit, Jilin province, northeast China. Geophysics, 72(4), 145-150.

Figure captions

Fig. 1: Geological map of the pre-Carboniferous units in the western margin of Gondwana at the Sierras Pampeanas and Northwest Argentina (modified from Aceñolaza and Aceñolaza, 2005; Steenken et al., 2006; Collo et al., 2009; Drobe et al., 2009; Augustsson et al., 2011; Rapela et al., 2016; Perón Orrillo et al., 2019; Otamendi et al., 2020, and others).

Fig. 2: Geological-structural map of the SGSL showing the distribution of metamorphic and magmatic units. A) Area covered by Christiansen et al. (2019). B) Area with new information presented in this work.

Fig. 3: Compilation of ages reported for the SGSL. 1) Sims et al. (1998); 2) Steenken et al. (2006); 3) Morosini et al. (2017); 4) Sato et al. (2003); 5) Casquet et al. (2014); 6) Sims et al. (1997); 7) Stuart-Smith et al. (1999); 8) Siegesmund et al. (2004); 9) Whitmeyer and Simpson (2004); 10) Carugno Duran and Ortiz Suárez (2012). 11) Sato et al. (2005). 12) González et al. (2002). 13) Morosini et al. (2019). 14) Siegesmund et al. (2010). 15) Ortiz Suárez (1999). 16) López de Luchi et al. (2002). 17) Dahlquist et al. (2019). 18) Drobe et al. (2009, 2011). 19) Rapela et al. (2016). 20) Perón Orrillo et al. (2019).

Fig. 4: Gravimetric grids of the study area. 1) Geological map of the study area. 2) Complete Bouguer Anomaly. 3) Regional Bouguer Anomaly. 2) Residual Bouguer Anomaly. A) Area covered by Christiansen et al. (2019). B) Area with new information presented in this work. Black dots represent gravity stations.

Fig. 5: Magnetic grids of the study area. 1) Geological map of the study area. 2) Total Magnetic Anomaly. 3) Regional Magnetic Anomaly. 2) Residual Magnetic Anomaly. A) Area covered by Christiansen et al. (2019). B) Area with new information presented in this work. Black dots represent the magnetic control stations.

Fig. 6: a) Map of the San Luis Shear System. b) Plot of variables describing the first-order geometry of orogenic system based on dips of shear zones (θ) and obliquity of the stretching direction respect to the orogen strike (β_L) (Modified from Goscombe and Gray, 2009). The black square and the cross correspond to the mean value with its standard deviation of the exposed structures, and represent of the gross geometry orogen. c) Cross sections of the San Luis Shear System (based on the results of the litho-constrained model).

Fig. 7: a) Field photography showing drag-folds in the San Martin Shear Zone. Floor view perpendicular to S_{my} and oblique to L_{my}. b) Photomicrography of the La Troya Shear Zone showing a mica fish with sericite recrystallized along the rims in mylonites. Section parallel to the L_{my} and normal to the S_{my} in cross-polarized light. c) Field photography showing a σ-shape leucosome pod in the La Arenilla Shear Zones. Floor view perpendicular to S_{my} and oblique to L_{my}. d) Field photographs showing a mesoscopic sinistral lozenge developed in mafic mylonites of the La Arenilla Shear Zone. e) Field photography showing a synthetically fragmented Kfs porphyroclast in a mylonitic pegmatite of San Pedro-El Volcán Shear Zone. View perpendicular to S_{my} and parallel to L_{my}. f) Photomicrography showing a plagioclase porphyroclast in a mylonite of the San Pedro-El Volcán Shear Zone. Two stages of deformation can be recognized, first a moderate to high temperature deformation is evidenced in the development of ribbons of Qz with GBM-recrystallization. Then, a lower temperature deformation is evidenced by sericite-rich bands, BLG-recrystallization of Qz and microfractures on Pl. Section parallel to the L_{my} and normal to the S_{my} in cross-polarized light.

Fig. 8: a) Field photography showing a southward view of the La Escalerilla Shear Zone. The view is perpendicular to both S_{my} and L_{my}. b). Photomicrography showing dynamic recrystallization (SGR) on a Kfs porphyroclast and myrmekitization belonging to a granitic mylonite of the La Escalerilla Shear Zone. Quartz ribbons with GBM recrystallisation are also observed. View perpendicular to the S_{my} in cross-polarized light. c) Field photography showing an asymmetric (σ-shape) boudin of quartz in a mylonitic schist of the Pancata-La Carolina Shear Zone. Floor view perpendicular to S_{my} and parallel to L_{my}. d) Field photography showing a mylonite of gneiss in the El Realito - Río de La Quebrada Shear Zones. North view perpendicular to the S_{my} and parallel to L_{my}. e) Photomicrography of the El Realito - Río de La Quebrada Shear Zone showing a mica fish with small recrystallised muscovite grains along the rims and ribbons of quartz in mylonites. Some of the quartz ribbons contain strongly elongated single crystals, formed by grain boundary migration (GBM) within the ribbon. Section parallel to the L_{my} and normal to the S_{my} in cross-polarized light. f) Field photography showing boudinage of felsic dikes intruded in mafic mylonites from the Río de los Bayos – Funes Shear Zone. North view perpendicular to S_{my}.

Fig. 9: Stereographic projections of planar and linear structures observed in the different lithological units of the SGSL. S_0 is the sedimentary bedding. S_1, S_2, S_3, S_{3my} and S_{4my} are foliation planes associated to deformational phases. L_{3my} is the stretching lineation associated to S_{3my} mylonitic foliation. B_2 and B_3 are hinge lines. Diagrams are shown as pole densities using the Kamb

contouring method of Stereonet© 2011-2015 (Allmendinger et al., 2013; Cardozo and Allmendinger, 2013).

Fig. 10: Interpretive diagrams of structural fabrics developed during the deformation phases.

Fig. 11: Photographs showing internal structural features of each lithological unit of the SGSL. a) Centimetric type 3 interference pattern in migmatites of Conlara Metamorphic Complex. b) Decimetric type 3 interference pattern in migmatites of Nogolí Metamorphic Complex. Corresponds to an internal domain limited by two shear belts. c) Fold (F_2) in migmatites of the San José Complex (PMC). d) Crenulation cleavage in the Micaschist Group (PMC). The S_2 foliation is defined by cleavage domains (flanks of microfolds) and microlithons (fold hinge areas) that preserved the S_1 schistosity. These characteristics are more common in areas near to the hinge of decametric folds. e) Decimetric layer of a folded meta-sandstone in Las Higueras Complex. f) Flank of a meso fold (F_2) in meta-turbidites of the eastern San Luis Formation belt.

Fig. 12: Residual Bouguer map of the study area obtained by upward continuation. Dark dots represent the locations of the geophysical stations. The yellow, blue, and magenta circles indicate different density ranges determined in laboratory samples. Numbers indicate the shear zones: 1) Río Guzmán, 2) San Martín, 3) Inti Huasi, 4) La Troya, 5) Quebrada Escondida, 6) La Arenilla, 7) San Pedro - El Volcán, 8) La Escalerilla, 9) Pancanta - La Carolina, 10) El Realito - Río de La Quebrada, and 11) Río de Los Bayos - Funes.

Fig. 13: a) Reduced to the pole residual anomaly map of the southern SGSL. In thin white lines the contour of the SGSL, plutons and shear zones. Numbers indicate the shear zones: 1) Río Guzmán, 2) San Martín, 3) Inti Huasi, 4) La Troya, 5) Quebrada Escondida, 6) La Arenilla, 7) San Pedro - El Volcán, 8) La Escalerilla, 9) Pancanta - La Carolina, 10) El Realito - Río de La Quebrada, and 11) Río de Los Bayos - Funes. The yellow, blue, and magenta circles indicate magnetic susceptibility ranges determined in outcrops. b) Total magnetic anomalies (TMA) image superimposed on a digital elevation model (SRTM). 4V vertical exaggeration. There is a clear contrast in the magnetic signal between the San Luis Shear System and the Conlara Metamorphic Complex. The limit occurs along the rectilinear Río Guzmán Shear Zone.

Fig. 14: Results of the inversion model for the southern sector. a) 3D model for the southern sector. b) Distribution of the geological units in the control sections. c) Final density cube. d) High density

values. e) Final magnetic susceptibility cube. f) High magnetic susceptibility values. Modified from Christiansen (2019) and Christiansen et al. (2019).

Fig. 15: Results of the inversion model for the northern sector. a) 3D model for the northern sector. b) Distribution of the geological units in the control sections. c) Final density cube. d) High density values. Modified from Christiansen (2019).

Fig. 16: 3D inversion model of the SGSL. a) Entire set of units. b) All units without sedimentary cover. c) Model without the Pringles Metamorphic Complex, Las Higueras Complex and San Luis formation. The bodies of mafic-ultramafic rocks in the San José Complex (central area of the double-vergent structure) are shown. d) Model without the Conlara and Nogolí metamorphic complexes and the plutonic rocks. e) Model showing the magmatic rocks. f) 3D view of the double-vergent structure (northward). The units are individualized and separated from each other for a better visualization.

Fig. 17: a) Three-dimensional shape of the eastern San Luis Formation and structural relationships with the other units. b) 3D morphology of the eastern San Luis Formation with the structural interpretation of its internal domain. c) Interpretation of the non-outcroping limits of the double-vergent structure. The interpretation on the left is only compatible with the characteristics observed to the north of the inflection zone of the La Escalerilla pluton.

Fig. 18: a) Map of the southwestern sector of the SGSL showing the transpressive deformation in the La Escalerilla pluton during the construction of the San Luis Shear System. b) Different views of the three-dimensional shape of the La Escalerilla pluton. c) Interpretative geological profile based on the 3D model and structural surface data. Numbers indicate the shear zones: 6) La Arenilla, 7) San Pedro - El Volcán, 8) La Escalerilla, 9) Pancanta - La Carolina, 10) El Realito - Río de La Quebrada, and 11) Río de Los Bayos - Funes.

Fig. 19: a) P-T diagram and location of the thermobarometry samples. b) Paleo-depth profile (in km) calculated according to the data set. The data were projected on a line of equal latitude from the original position of each sample, and considering an approximately N-S arrangement of isobars. Numbers indicate the shear zones: 1) Río Guzmán, 3) Inti Huasi, 4) La Troya, 6) La Arenilla, 7) San Pedro - El Volcán, 8) La Escalerilla, 9) Pancanta - La Carolina, 10) El Realito - Río de La Quebrada, and 11) Río de Los Bayos - Funes. c) Average paths of K-Ar ages determined for Hbl,

Ms and Bt for the Conlara Metamorphic Complex (CMC), Pringles Metamorphic Complex (PMC) and northern portion of the Nogolí Metamorphic Complex (NMC) (taken from Steenken et al., 2008).

Fig. 20: a) Map of the main shear zones in the Sierras Pampeanas Orientales (modified from Otamendi et al., 2020, and reference therein). 1) San Luis Shear System. 2) Guacha Corral, Pachango and Los Túneles shear zones (Sierra de Córdoba). 3) Río Las Cañas and Ulapes shear zones (Sierra de Chepes and Ulapes). 4) Valle Fértil - La Huerta and La Arenosa shear zones (Sierra de Valle Fértil - La Huerta). 5) Paganzo shear zone (Sierra de Paganzo). 6) Cordón de la Cumbre and Chuschin shear zones (Sierra de Famatina). 7) Señor de la Punta - El Candelero, Antinaco - Sanagasta, La Horqueta and Paluqui shear zones (Sierra de Velasco). 8) La Florida and TIPA shear zones (Sierras de Fiambalá, Tinogasta and Paimán). 9) La Chilca (Sierra de Ambato). The yellow arrows represent an interpretation shortening percentages for different latitudes, based on the different distances between the suture area and the backstop. b) Schematic images of the Famatinian geotectonic evolution in the studied segment. 1) construction of the Famatinian island arc (and backarc). 2) collision of the Cuyania/Precordillera microcontinent and construction of the Famatinian orogen (At this time the double-vergent structure of the SGSL was created). c) Interpretation of the collisional scenario and palaeo-setting elements. 1) before the indentation of the Cuyania/Precordillera microplate. 2) after the indentation. The indenter morphology determined the deformation style (exhumation and shortening). In this schematic model, the protrude of the indenter is approximately equivalent to the shortening produced. In addition, an interpretation of how the indenter morphology produces rotations of the horizontal deviatoric stresses on the indented margin is shown.

Table 1: Main characteristics of the shear zones in the SGSL.

Shear Zone	Extension length / width	S_{my} strike / dip	L_{my} dip dir. / dip	Sense of movement	Deformation conditions	Affected units
Río Guzmán (1)	60 km / ~800 m	N15°/ 80°SE (average)	~170°/ 65° (average)	oblique reverse-sinistral	~450-350°C greenschist facies	Las Aguadas Group (hanging wall). Eastern San Luis Formation (footwall).
San Martín (2)	35 km / ~400 m	N15°/75°SE (average)	~85°/ 50° (average)	oblique reverse-dextral	~550°-450°C high-greenschis facies	Las Aguadas Group (hanging wall). Las Higueras Complex (footwall).
Inti Huasi (3)	60 km / ~400 m	~N5°/ 55°W (southern part) ~N30°/ 84°NW (northern part)	~275°/ 70° (southern part) ~320°/ 70°NW (central part)	reverse (southern part) oblique reverse-sinistral (central and northern part)	~450-350°C greenschist facies	Eastern Micaschist Group (hanging wall). Eastern San Luis Formation (footwall).
La Troya (4)	62 km / ~400 m	~N40°/ 84°NW (northern part) ~N0°/ 55°W (southern part)	~10°/ 5° (northern part) ~290°/ 52° (southern part)	sinistral strike-slip (northern part) oblique reverse-sinistral (southern part)	~550-500°C high-greenschis facies	San José Complex (hanging wall). Eastern Micaschist Group (footwall).
Quebrada Escondida (5)	30 km / ~500 m	N40°/68°NW	~235°/ 46° (average)	oblique reverse-dextral	~550-500°C high-greenschis facies	San José Complex (hanging wall). Las Higueras Complex (footwall).
La Arenilla (6)	105 km / 400 m to 3 km (depends on the branch)	~N12º / >70°E or >70°W (depends on the branch)	290° or 110°/ >70° (depends on the branch)	oblique reverse-sinistral (general movement), one branch has oblique normal-sinistral movement.	~760-600°C amphibolite facies (initial conditions of deformation) ~450°C greenschist facies (retrograde conditions)	Internal shear zone of the San José Complex. Form a horst pop-up
San Pedro – El Volcán (7)	93 km / ~300 m	~N10º / ~73°E	~160°/ ~60° (south stretch) ~280°/ 5° (north end)	oblique reverse-sinistral (south stretch) dextral strike-slip (north end)	~550-450°C high-greenschis facies	San José Complex (hanging wall). Western Micaschist Group (footwall).
La Escalerilla (8)	63 km / ~400 m (main branch) ~7 km / ~30 m (synthetic branches)	~N10º / ~65°E (average of main branch) ~N345º / ~80°SW or NE (synthetic branches)	~155°/ ~50° (main branch) ~5°/ ~155 (synthetic branches)	oblique reverse-sinistral (main branch) sinistral strike-slip (synthetic branches)	~600-550°C amphibolite facies (initial conditions of deformation)	Western Micachist Group (hanging wall). Western San Luis Formation and La Escalerilla pluton (footwall)

Pancanta – La Carolina (9)	38 km / ~200 m (main branch) 5 km / ~100 m (secondary branch)	~N25°/ ~80NW (main branch) ~N85°/ ~77°N (secondary branch)	~220°/ ~30° (main branch) ~280°/ ~50° (secondary branch)	oblique reverse-dextral to dextral strike-slip (both branches)	~450°C greenschist facies	The main branch is located within the Western San Luis Formation. The secondary branch separates the San Luis Formation from a block of Nogolí Metamorphic Complex.
Realito – Río de La Quebrada (10)	82 km / ~500 m (for each branch)	~N15°/ ~88°W (northern part) ~N25°/ 65°-80°NW (central part) ~N20°/ 58°-70°SE (southern part)	~270°/ 80° (northern part ~340°/ 40° (central part) ~120°/ 45° (southern part)	oblique reverse-dextral (northern part) oblique reverse-sinistral (central and southern part)	~550°-450°C high-greenschis facies	In the north: Nogolí Metamorphic Complex (hanging wall). Western San Luis Formation and Micaschist Group (footwall). In the south: La Escalerilla pluton (hanging wall). Nogolí Metamorphic Complex (footwall).
Río de Los Bayos - Funes (11)	50 km / ~500 m (for each branch)	~N10°/ 80°E or 80W (subvertical)	~180°/ 44° (southern part) 345°/ 53° (northern part)	oblique reverse-sinistral (predominance in high temperature deformation)	amphibolite facies (initial conditions) to greenschist facies (retrograde deformation)	Internal shear zones of the Nogolí Metamorphic Complex.

Table 2. Fabric summary of the different deformational stages in the units of the SGSL.

Deformation phases	Conlara Metamorphic Complex	Nogolí Metamorphic Complex	Pringles Metamorphic Complex	Las Higueras Complex	San Luis Formation
D1	S_1 schistosity or compositional banded parallel to the S_0 sedimentary bedding.	S_1 schistosity or stromatitic banded parallel to the S_0 sedimentary bedding.	S_1 schistosity or compositional banded parallel to S_0 sedimentary bedding.	S_1 schistosity or slaty cleavage parallel or subparallel to S_0 sedimentary bedding.	S_1 slaty cleavage parallel or subparallel to S_0 sedimentary bedding.
D2	Open to isoclinal F_2 folds, predominantly asymmetric, of class 1C and 2. S_2 foliations represented by NNE axial plane surfaces are upright to moderately incline, predominantly toward east. B_2 hinges lines are horizontal to moderately plunging toward NE, SE and SSW (Fig. 9a).	Isoclinal to tight decametric to metric F_2 folds, of class 1C and 3. The S_2 axial plane foliation has of NE or NW strike, with high-angle dipping towards the NW or SE. The B_2 fold axes plunge moderately towards the NE, E or S (Fig. 9b).	Tight to isoclinal asymmetric F_2 folds, with predominantly cylindrical hinges (Fig. 11c). B_2 hinge lines plunge moderately to NNE or SSW (Fig. 9c). The S_2 axial surfaces have NNE strike, are upright or steeply inclined toward WNW or ESE (in San José Complex), or moderately inclined (in Micaschist Group).	Tight to open F_2 folds of class 1C and 3 (Fig. 11e), with B_2 axes vertical or steeply plunging toward N, NE or W. The S_2 crenulation schistosity strikes NE or NNE, and have moderately to steeply incline predominantly toward the NW, but also toward the SE (Fig. 9d).	Tight to closed decametric F_2 folds, predominantly asymmetric, of class 1C and 3. Z, S and M minor folds are present in all scales (Fig. 11f). S_2 (crenulation cleavage) is upright or steeply inclined toward west or east. The B_2 hinge lines plunge gently towards the NNE and SSW (Fig 9e).
D3	Spaced and non-penetrative S_3 axial plane with NW, NNE and NE strike, generally related to open to close F_3 folds, which overprint tight or isoclinal F_2 folds. B_3 hinge axes incline randomly (Fig. 9a), and its greater dip direction dispersion probably is due to the fact that the F_3 folds have been recognized in isolated and spaced outcropping. Complex interference patterns (variants of type 3) are recognized at different scales (Fig. 11a).	Associated to the SLSS. It is represented by S_{3my} mylonitic surfaces with NNE strike. Local overprinting F_3 folds (open to tight) over F_2 folds. The both B_2 and B_3 hinge lines are parallel with moderately to steeply plunging toward the NNE or NE, and evidence type 3 interference patterns (Fig. 11b). The S_3 hinge plane has NNE to NE strike, steeply inclined towards NW or SE (Fig. 9b). F_3 folds are located in internal domains (of various hundred meters scale) limited by parallel shear branches.	Associated to SLSS. The S_{3my} is upright or steeply inclined toward WNW or ESE (Fig. 9c). A not penetrative S_3 surface, represented by a localized crenulation cleavages striking NE to NNW and dipping to the NW or NE, is associated with the development of S_{3my} foliations. B_3 drag-fold axes associated with S_{3my} foliation dip toward NNE or SW. Also vertical sheath folds are common at some sites.	Associated to SLSS. Metric S_{3my} shear planes have NNE strike and steeply inclined toward WNW or ESE (Fig. 9d). F_3 drag-folds and occasionally a S_3 crenulation cleavage with steep dip to the E are associated with the S_{3my} shears.	Associated to the SLSS. The S_{3my} shear planes strikes NNE, and dip steeply to the ESE or WNW (Fig. 9e). An S_3 crenulation foliation is associated with developed of localized F_3 drag-folds with B_3 hinge axes gently plunging toward S or N. Sometimes type 3 interference patterns (highly localized and only on the metric scale) are observed within folded domains limited by discrete shear belts. These are produced by the superposition of F_3 over F_2 folds.
D4	Discrete S_{4my} shear planes associated to SLSS, mainly in its western boundary, in contact to Las Higueras Complex and eastern belt of San Luis Formation.	Discrete, widely spaced (hundreds of meters), and underpowered (metric) shear zones, which intercept and displace high temperature S_{3my} shear zones. S_{4my} foliations usually show NW strikes, and sinistral strike-slip movement.	Non-penetrative and spaced S_{4my} shear belts with NE strikes and steeply inclined towards NW or SE (Fig. 9c). These shears displace the S_{3my} shear zones through dextral strike-slip sense.	Non-penetrative and spaced S_{4my} shear belts with NE strikes. Local S_4 crenulation surfaces developed due to the forced emplacement of the Devonian plutons. The S_4 surfaces are parallel to the edges of the plutons.	Non-penetrative and spaced S_{4my} shear belts with NE strikes and steeply inclined towards NW or SE (Fig. 9e). These shears displace the S_{3my} shear zones through dextral strike-slip sense.

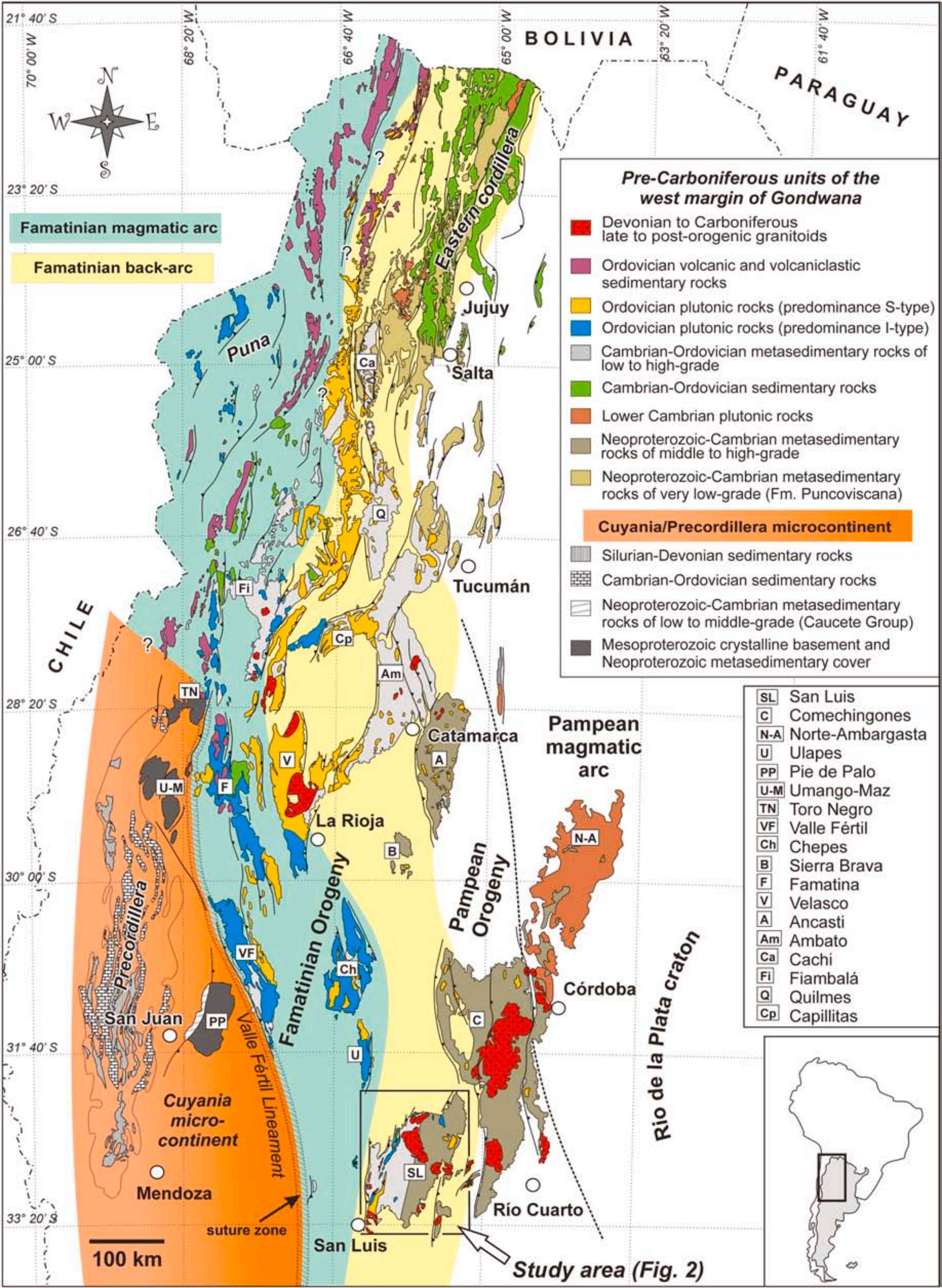

BOLIVIA
PARAGUAY
CHILE
Famatinian magmatic arc
Famatinian back-arc
Pre-Carboniferous units of the west margin of Gondwana
Devonian to Carboniferous late to post-orogenic granitoids
Ordovician volcanic and volcaniclastic sedimentary rocks
Ordovician plutonic rocks (predominance S-type)
Ordovician plutonic rocks (predominance I-type)
Cambrian-Ordovician metasedimentary rocks of low to high-grade
Cambrian-Ordovician sedimentary rocks
Lower Cambrian plutonic rocks
Neoproterozoic-Cambrian metasedimentary rocks of middle to high-grade
Neoproterozoic-Cambrian metasedimentary rocks of very low-grade (Fm. Puncoviscana)
Cuyania/Precordillera microcontinent
Silurian-Devonian sedimentary rocks
Cambrian-Ordovician sedimentary rocks
Neoproterozoic-Cambrian metasedimentary rocks of low to middle-grade (Caucete Group)
Mesoproterozoic crystalline basement and Neoproterozoic metasedimentary cover
SL San Luis
C Comechingones
N-A Norte-Ambargasta
U Ulapes
PP Pie de Palo
U-M Umango-Maz
TN Toro Negro
VF Valle Fértil
Ch Chepes
B Sierra Brava
F Famatina
V Velasco
A Ancasti
Am Ambato
Ca Cachi
Fi Fiambalá
Q Quilmes
Cp Capillitas
21° 40' S
23° 20' S
25° 00' S
26° 40' S
28° 20' S
30° 00' S
31° 40' S
33° 20' S
70° 00' W
68° 20' W
66° 40' W
65° 00' W
63° 20' W
61° 40' W
Puna
Eastern cordillera
Jujuy
Salta
Tucumán
Catamarca
La Rioja
Córdoba
Río Cuarto
San Luis
San Juan
Mendoza
Pampean magmatic arc
Pampean Orogeny
Famatinian Orogeny
Precordillera
Valle Fértil Lineament
Cuyania micro-continent
Rio de la Plata craton
suture zone
100 km
Study area (Fig. 2)

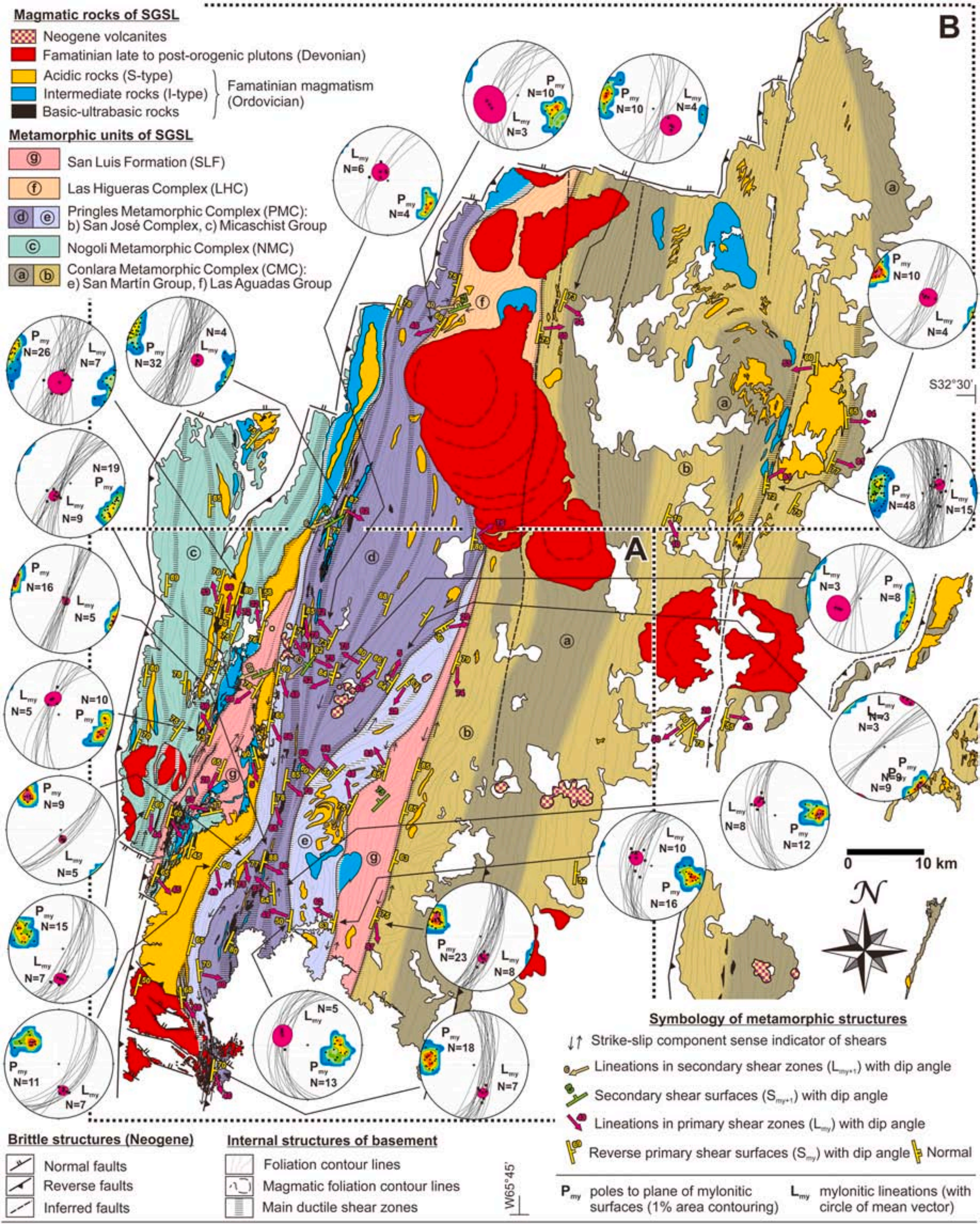

Magmatic rocks of SGSL
Neogene volcanites
Famatinian late to post-orogenic plutons (Devonian)
Acidic rocks (S-type)
Intermediate rocks (I-type)
Basic-ultrabasic rocks
Famatinian magmatism (Ordovician)
Metamorphic units of SGSL
San Luis Formation (SLF)
Las Higueras Complex (LHC)
Pringles Metamorphic Complex (PMC): b) San José Complex, c) Micaschist Group
Nogoli Metamorphic Complex (NMC)
Conlara Metamorphic Complex (CMC): e) San Martín Group, f) Las Aguadas Group
B
A
S32°30'
W65°45'
0 10 km
N
Symbology of metamorphic structures
Strike-slip component sense indicator of shears
Lineations in secondary shear zones (Lmy+1) with dip angle
Secondary shear surfaces (Smy+1) with dip angle
Lineations in primary shear zones (Lmy) with dip angle
Reverse primary shear surfaces (Smy) with dip angle
Normal
Pmy poles to plane of mylonitic surfaces (1% area contouring)
Lmy mylonitic lineations (with circle of mean vector)
Brittle structures (Neogene)
Normal faults
Reverse faults
Inferred faults
Internal structures of basement
Foliation contour lines
Magmatic foliation contour lines
Main ductile shear zones

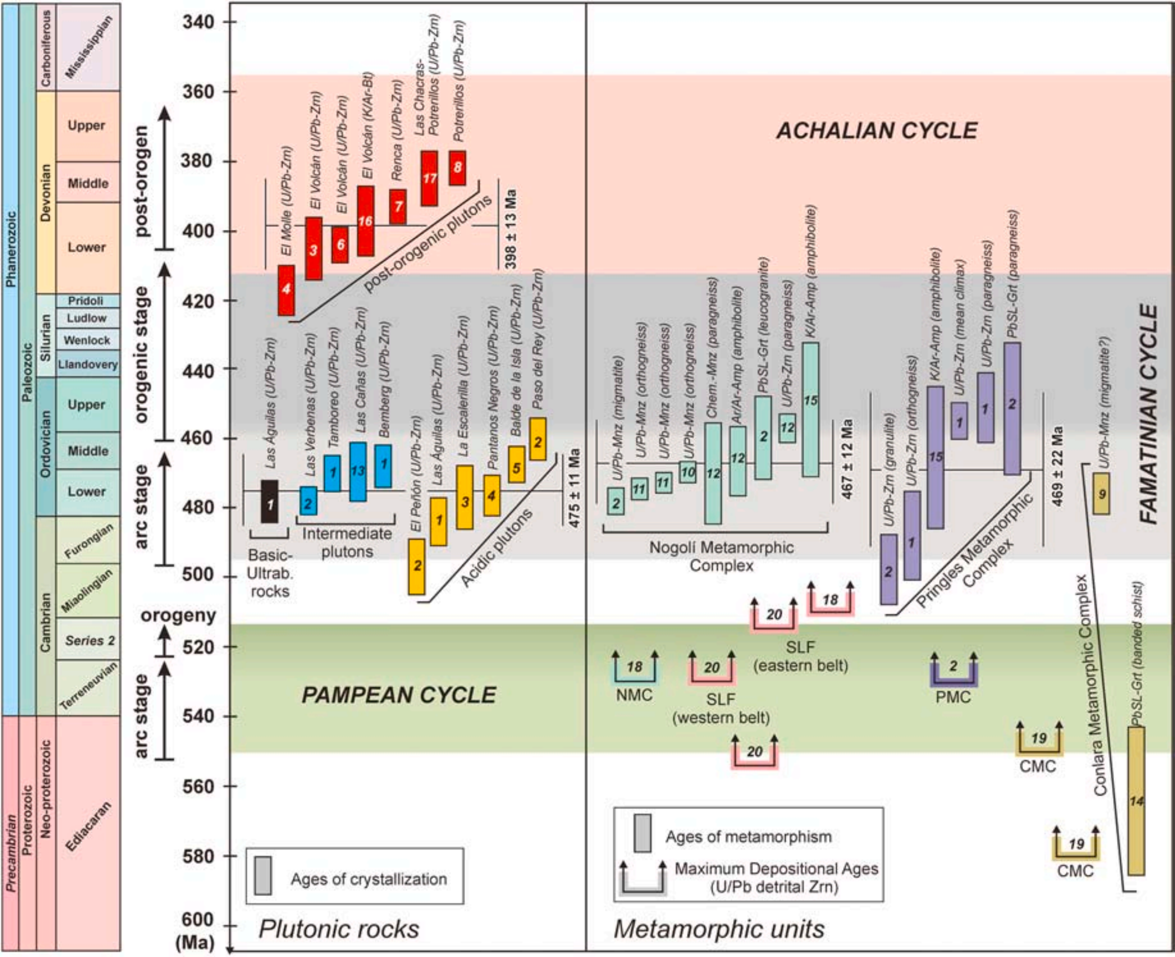

Phanerozoic
Paleozoic
Precambrian
Proterozoic
Neo-proterozoic
Carboniferous
Mississippian
Devonian
Upper
Middle
Lower
Silurian
Pridoli
Ludlow
Wenlock
Llandovery
Ordovician
Upper
Middle
Lower
Cambrian
Furongian
Miaolingian
Series 2
Terreneuvian
Ediacaran
post-orogen
orogenic stage
arc stage
orogeny
arc stage
340
360
380
400
420
440
460
480
500
520
540
560
580
600
(Ma)
ACHALIAN CYCLE
FAMATINIAN CYCLE
PAMPEAN CYCLE
El Molle (U/Pb-Zrn)
El Volcán (U/Pb-Zrn)
El Volcán (U/Pb-Zrn)
El Volcán (K/Ar-Bt)
Renca (U/Pb-Zrn)
Las Chacras-Potrerillos (U/Pb-Zrn)
Potrerillos (U/Pb-Zrn)
post-orogenic plutons
398 ± 13 Ma
Las Águilas (U/Pb-Zrn)
Las Verbenas (U/Pb-Zrn)
Tamboreo (U/Pb-Zrn)
Las Cañas (U/Pb-Zrn)
Bemberg (U/Pb-Zrn)
El Peñón (U/Pb-Zrn)
Las Águilas (U/Pb-Zrn)
La Escalerilla (U/Pb-Zrn)
Pantanos Negros (U/Pb-Zrn)
Balde de la Isla (U/Pb-Zrn)
Paso del Rey (U/Pb-Zrn)
475 ± 11 Ma
Basic-Ultrab. rocks
Intermediate plutons
Acidic plutons
U/Pb-Mnz (migmatite)
U/Pb-Mnz (orthogneiss)
U/Pb-Mnz (orthogneiss)
U/Pb-Mnz (orthogneiss)
Chem.-Mnz (paragneiss)
Ar/Ar-Amp (amphibolite)
PbSL-Grt (leucogranite)
U/Pb-Zrn (paragneiss)
K/Ar-Amp (amphibolite)
467 ± 12 Ma
Nogolí Metamorphic Complex
U/Pb-Zrn (granulite)
U/Pb-Zrn (orthogneiss)
K/Ar-Amp (amphibolite)
U/Pb-Zrn (mean climax)
U/Pb-Zrn (paragneiss)
PbSL-Grt (paragneiss)
469 ± 22 Ma
Pringles Metamorphic Complex
U/Pb-Mnz (migmatite?)
Conlara Metamorphic Complex
PbSL-Grt (banded schist)
SLF (eastern belt)
SLF (western belt)
NMC
PMC
CMC
CMC
Ages of crystallization
Ages of metamorphism
Maximum Depositional Ages (U/Pb detrital Zrn)
Plutonic rocks
Metamorphic units

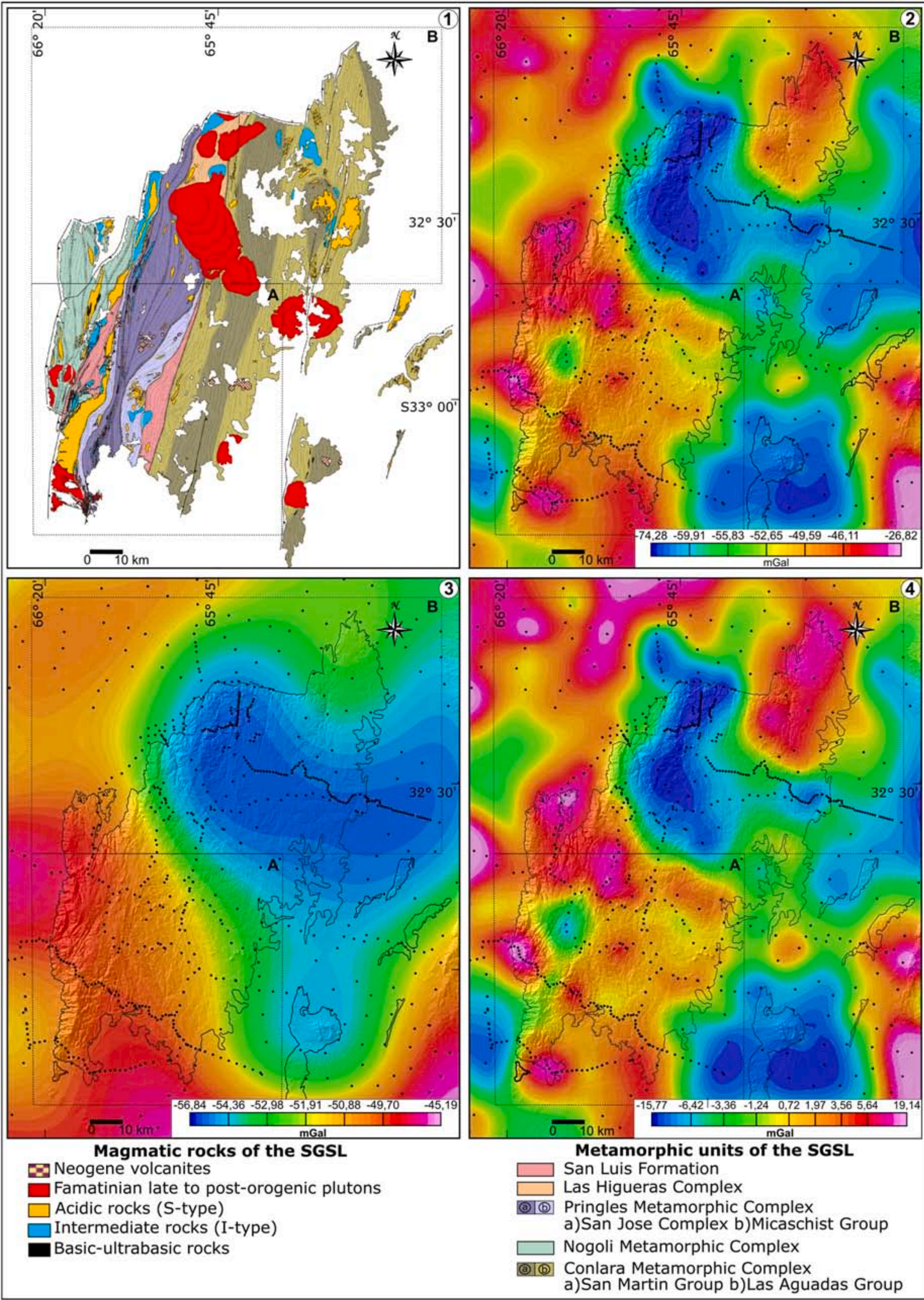
1
2
3
4
66° 20'
65° 45'
32° 30'
S33° 00'
A
B
0 10 km
-74,28 -59,91 -55,83 -52,65 -49,59 -46,11 -26,82
mGal
-56,84 -54,36 -52,98 -51,91 -50,88 -49,70 -45,19
mGal
-15,77 -6,42 -3,36 -1,24 0,72 1,97 3,56 5,64 19,14
mGal
Magmatic rocks of the SGSL
Neogene volcanites
Famatinian late to post-orogenic plutons
Acidic rocks (S-type)
Intermediate rocks (I-type)
Basic-ultrabasic rocks
Metamorphic units of the SGSL
San Luis Formation
Las Higueras Complex
Pringles Metamorphic Complex
a)San Jose Complex b)Micaschist Group
Nogoli Metamorphic Complex
Conlara Metamorphic Complex
a)San Martin Group b)Las Aguadas Group

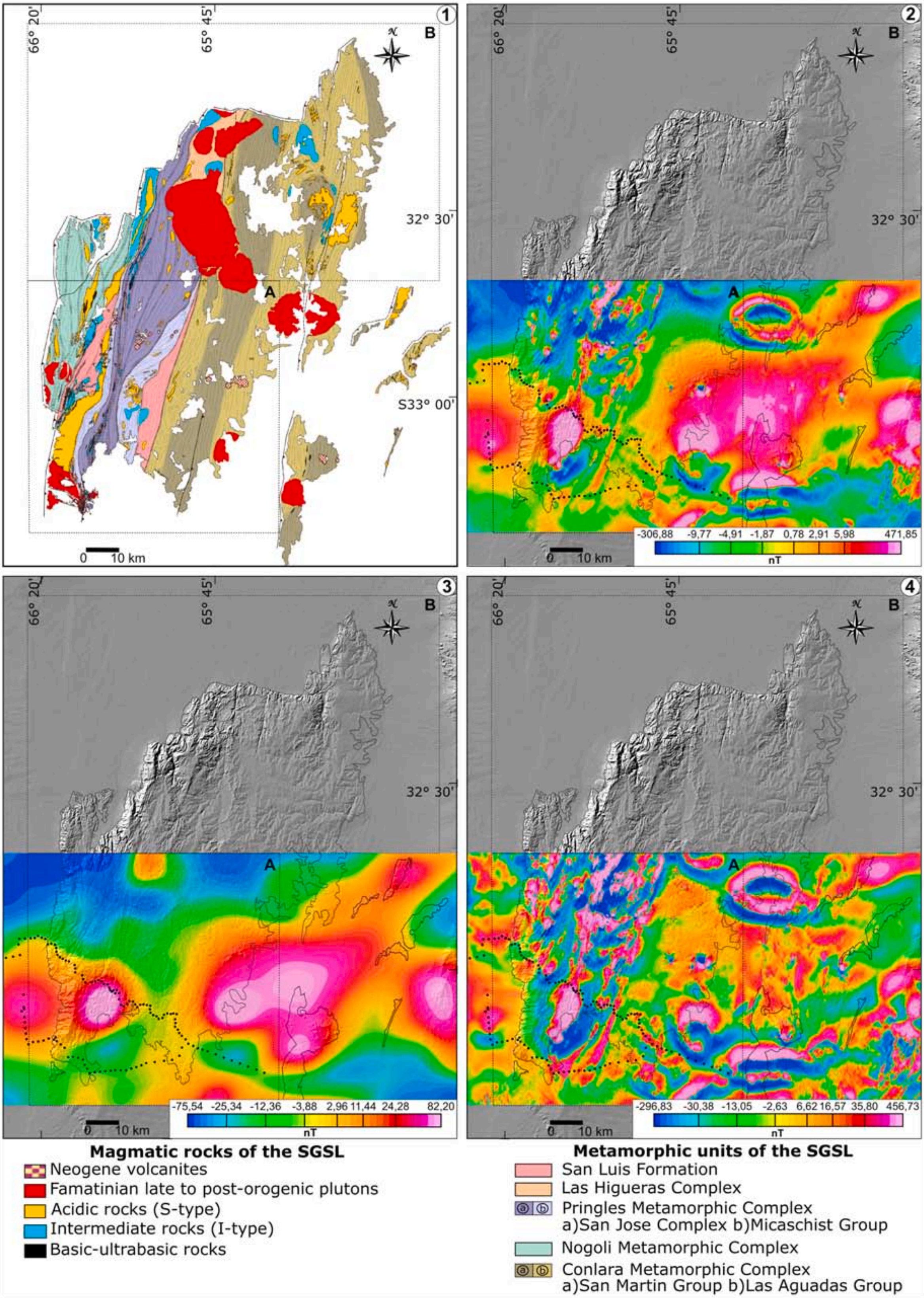
1
2
3
4
66° 20'
65° 45'
32° 30'
S33° 00'
A
B
0 10 km
-306,88 -9,77 -4,91 -1,87 0,78 2,91 5,98 471,85
nT
-75,54 -25,34 -12,36 -3,88 2,96 11,44 24,28 82,20
nT
-296,83 -30,38 -13,05 -2,63 6,62 16,57 35,80 456,73
nT
Magmatic rocks of the SGSL
Neogene volcanites
Famatinian late to post-orogenic plutons
Acidic rocks (S-type)
Intermediate rocks (I-type)
Basic-ultrabasic rocks
Metamorphic units of the SGSL
San Luis Formation
Las Higueras Complex
Pringles Metamorphic Complex
a)San Jose Complex b)Micaschist Group
Nogoli Metamorphic Complex
Conlara Metamorphic Complex
a)San Martin Group b)Las Aguadas Group

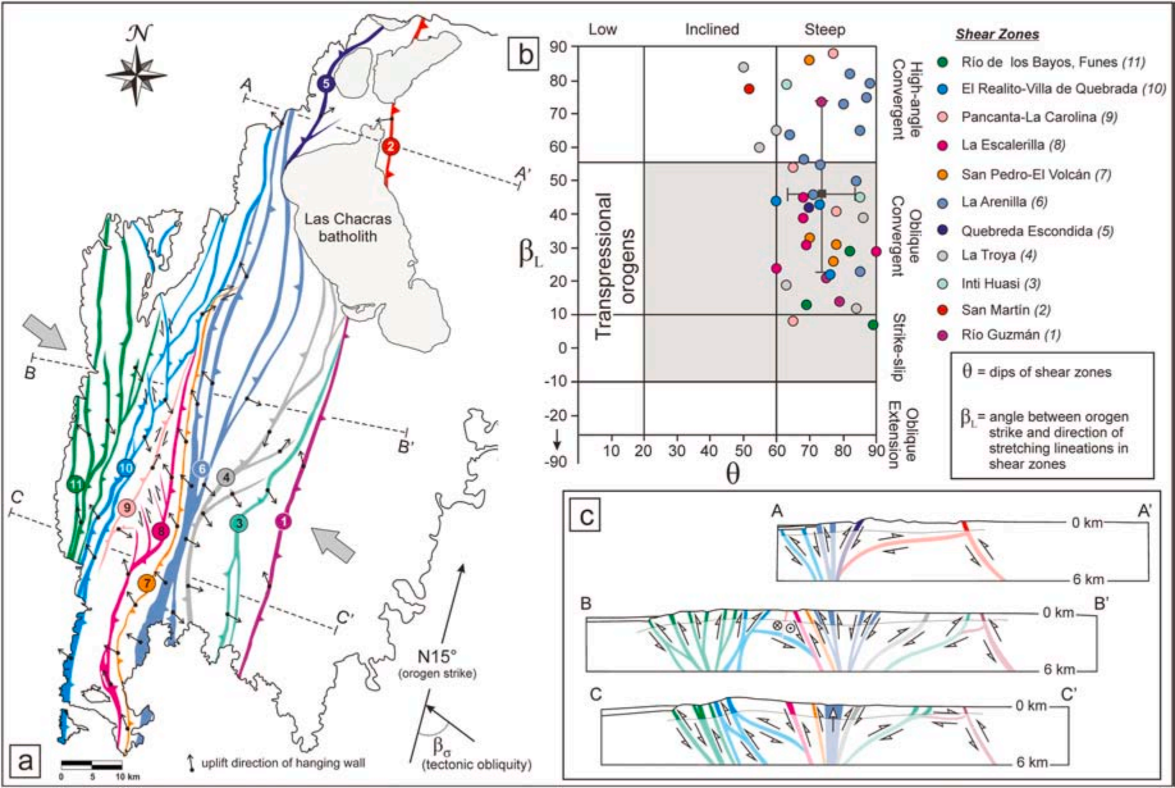

N
A
A'
B
B'
C
C'
Las Chacras batholith
N15° (orogen strike)
βσ (tectonic obliquity)
uplift direction of hanging wall
0 5 10 km
a
b
Low
Inclined
Steep
High-angle Convergent
Oblique Convergent
Strike-slip
Oblique Extension
Transpressional orogens
βL
θ
Shear Zones
Río de los Bayos, Funes (11)
El Realito-Villa de Quebrada (10)
Pancanta-La Carolina (9)
La Escalerilla (8)
San Pedro-El Volcán (7)
La Arenilla (6)
Quebreda Escondida (5)
La Troya (4)
Inti Huasi (3)
San Martín (2)
Río Guzmán (1)
θ = dips of shear zones
βL = angle between orogen strike and direction of stretching lineations in shear zones
c
0 km
6 km

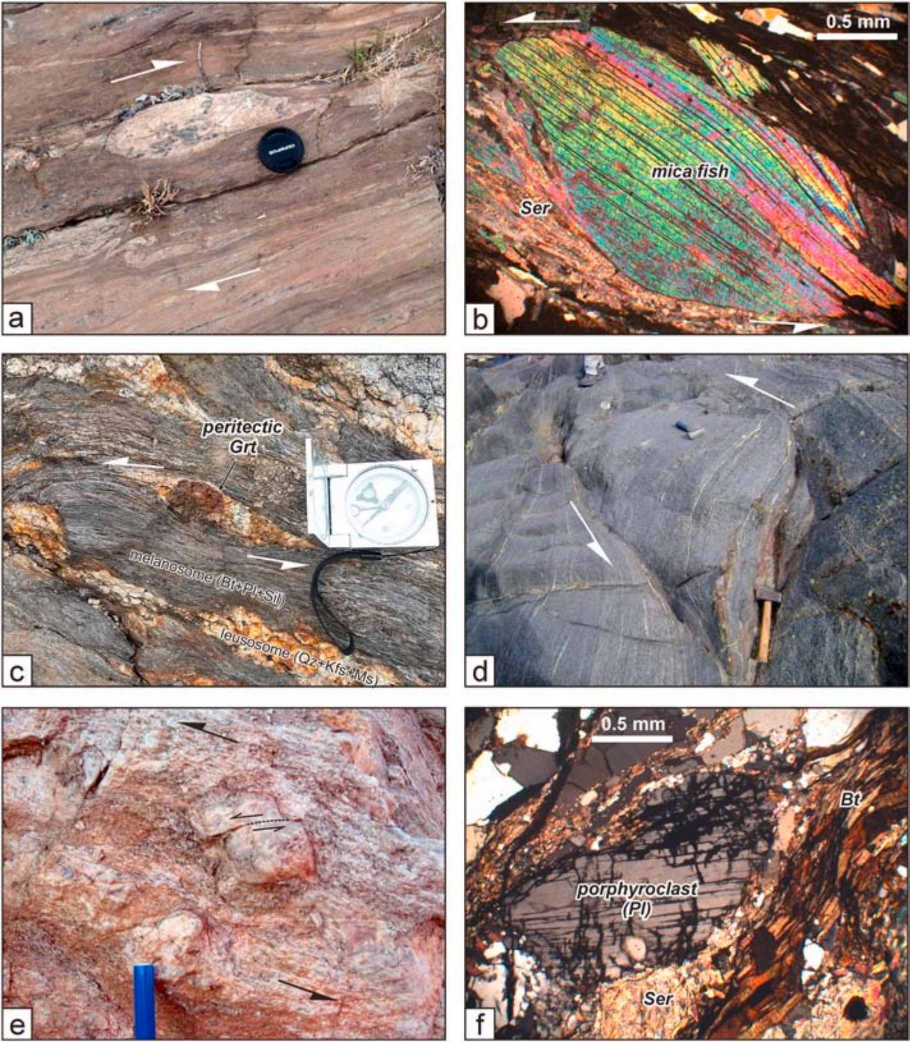
a
0.5 mm
mica fish
Ser
b
peritectic
Grt
melanosome (Bt+Pl+Sil)
leusosome (Qz+Kfs+Ms)
c
d
e
0.5 mm
Bt
porphyroclast
(Pl)
Ser
f

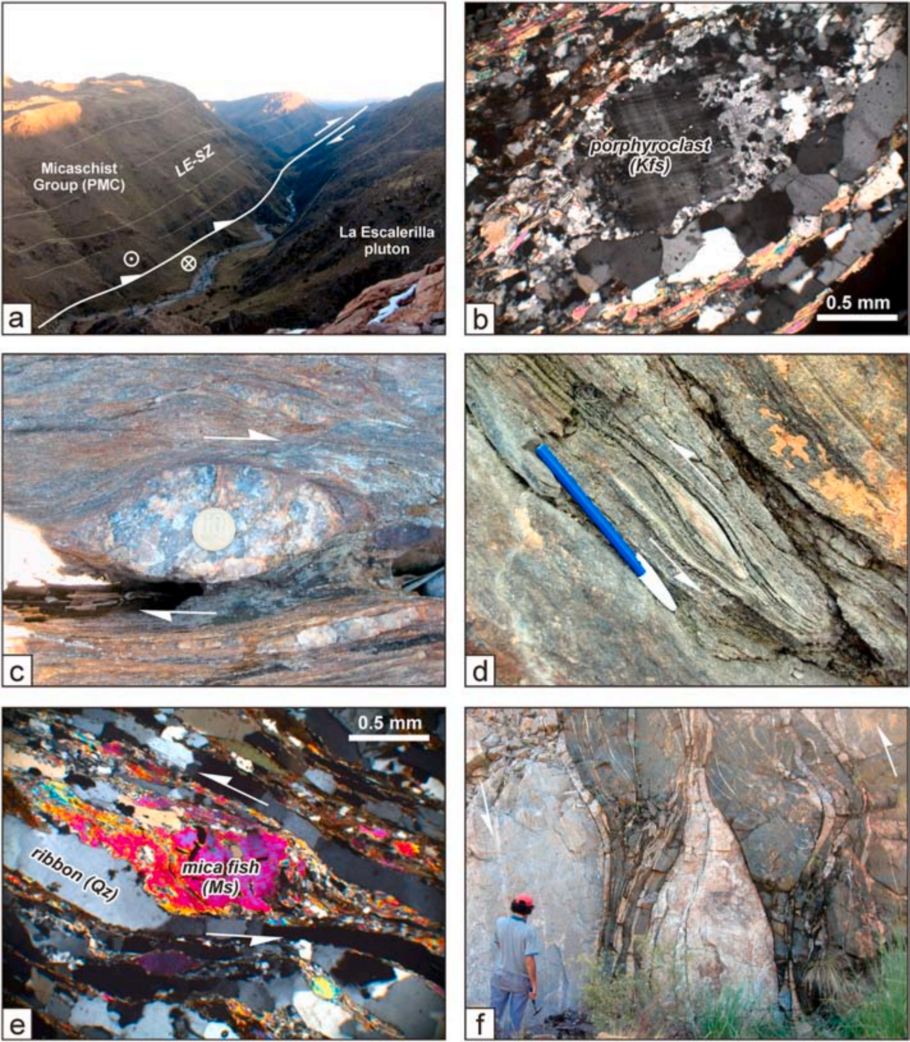
Micaschist Group (PMC)
LE-SZ
La Escalerilla pluton
a
porphyroclast (Kfs)
0.5 mm
b
c
d
0.5 mm
ribbon (Qz)
mica fish (Ms)
e
f

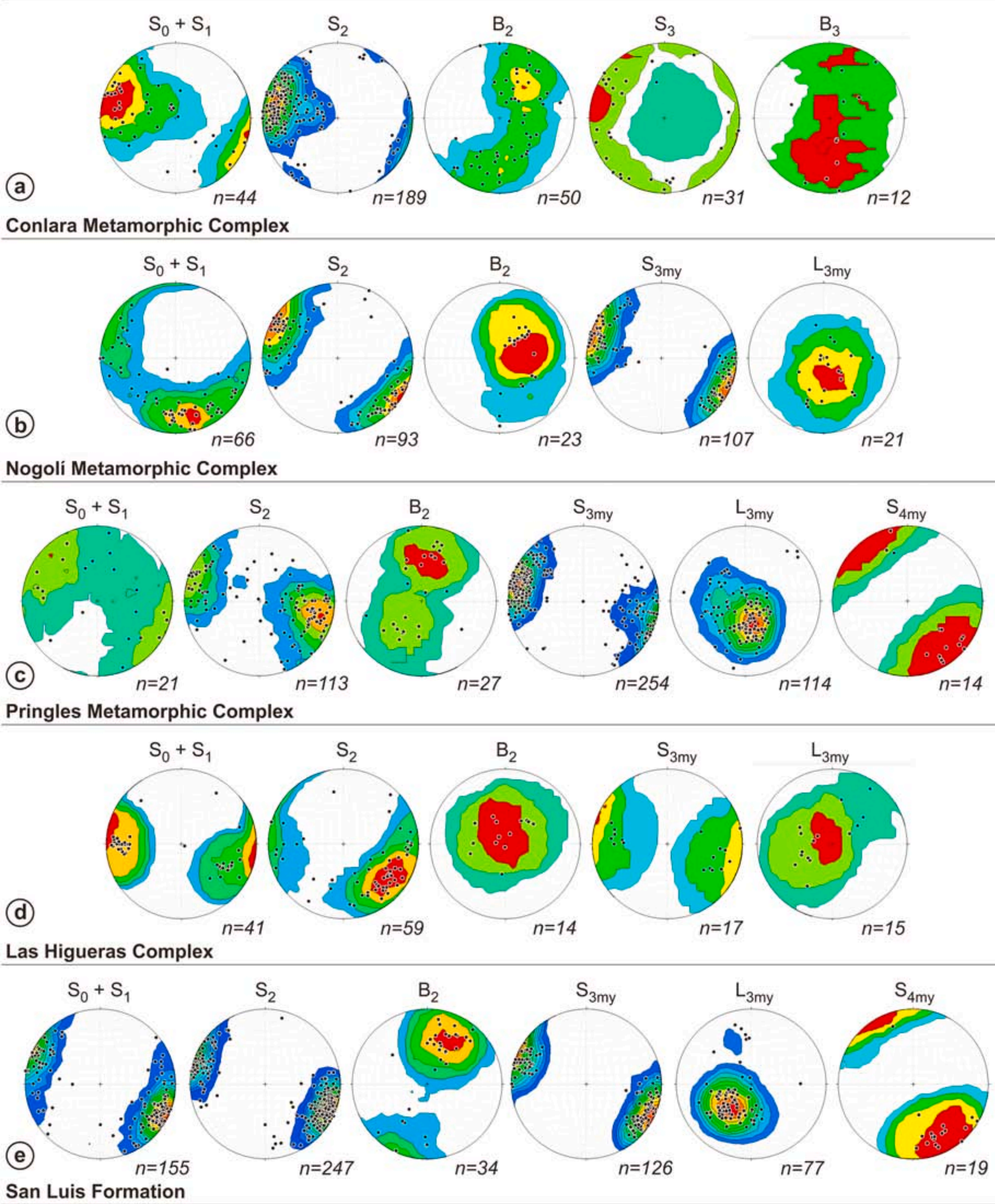

$S_0 + S_1$
S_2
B_2
S_3
B_3
a
n=44
n=189
n=50
n=31
n=12
Conlara Metamorphic Complex
$S_0 + S_1$
S_2
B_2
S_{3my}
L_{3my}
b
n=66
n=93
n=23
n=107
n=21
Nogolí Metamorphic Complex
$S_0 + S_1$
S_2
B_2
S_{3my}
L_{3my}
S_{4my}
c
n=21
n=113
n=27
n=254
n=114
n=14
Pringles Metamorphic Complex
$S_0 + S_1$
S_2
B_2
S_{3my}
L_{3my}
d
n=41
n=59
n=14
n=17
n=15
Las Higueras Complex
$S_0 + S_1$
S_2
B_2
S_{3my}
L_{3my}
S_{4my}
e
n=155
n=247
n=34
n=126
n=77
n=19
San Luis Formation

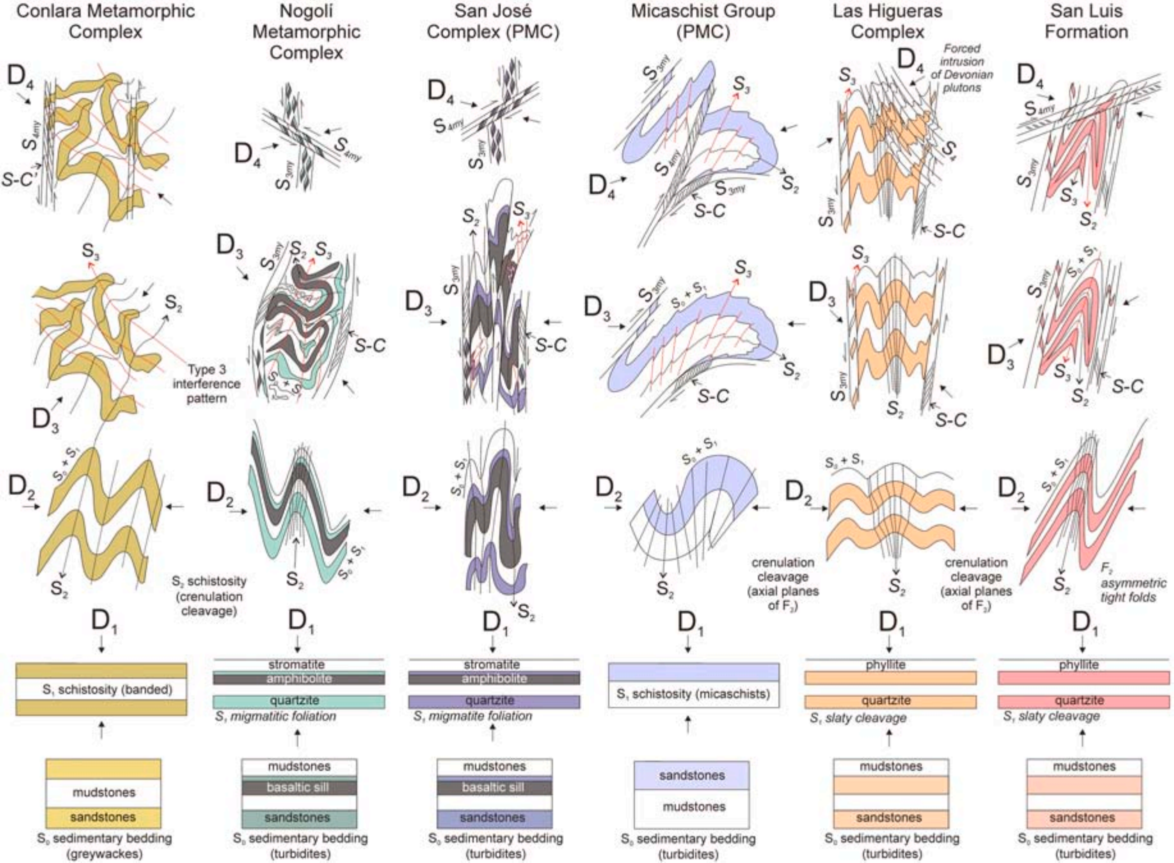

Conlara Metamorphic Complex
Nogolí Metamorphic Complex
San José Complex (PMC)
Micaschist Group (PMC)
Las Higueras Complex
San Luis Formation
D4
D3
D2
D1
S-C
Type 3 interference pattern
Forced intrusion of Devonian plutons
S2 schistosity (crenulation cleavage)
crenulation cleavage (axial planes of F2)
F2 asymmetric tight folds
S1 schistosity (banded)
stromatite
amphibolite
quartzite
S1 migmatitic foliation
S1 migmatite foliation
S1 schistosity (micaschists)
phyllite
S1 slaty cleavage
mudstones
sandstones
basaltic sill
S0 sedimentary bedding (greywackes)
S0 sedimentary bedding (turbidites)

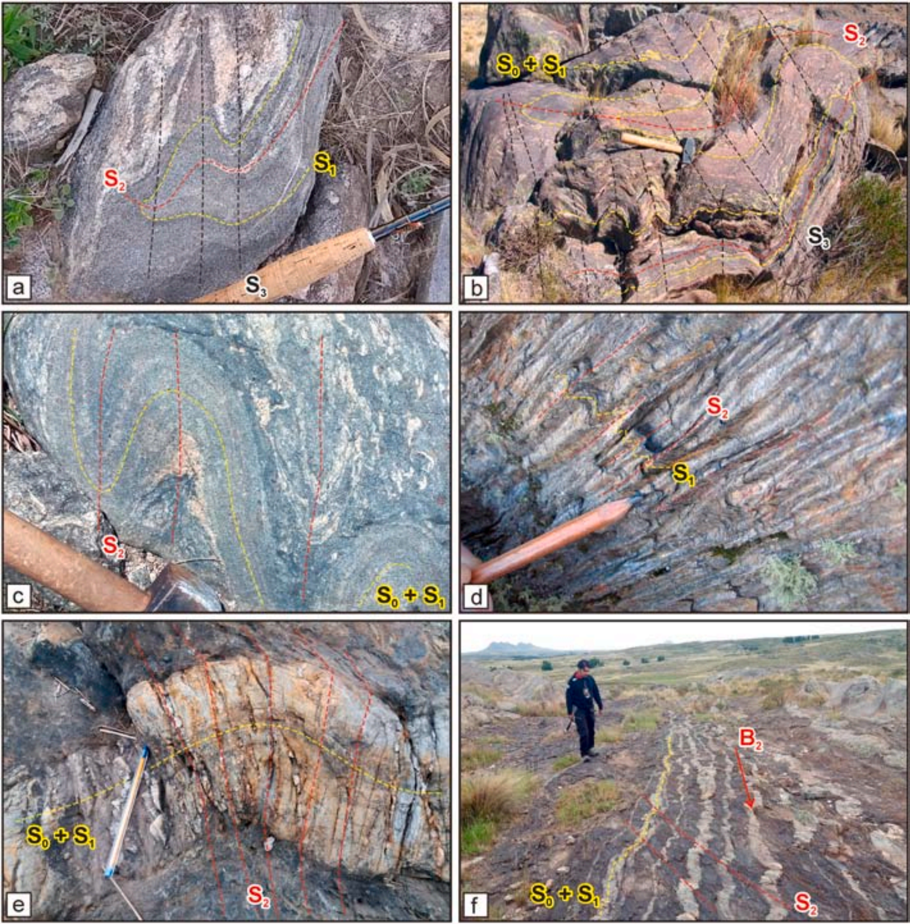
S2
S1
S3
a
S0 + S1
S2
S3
b
S2
S0 + S1
c
S2
S1
d
S0 + S1
S2
e
B2
S0 + S1
S2
f

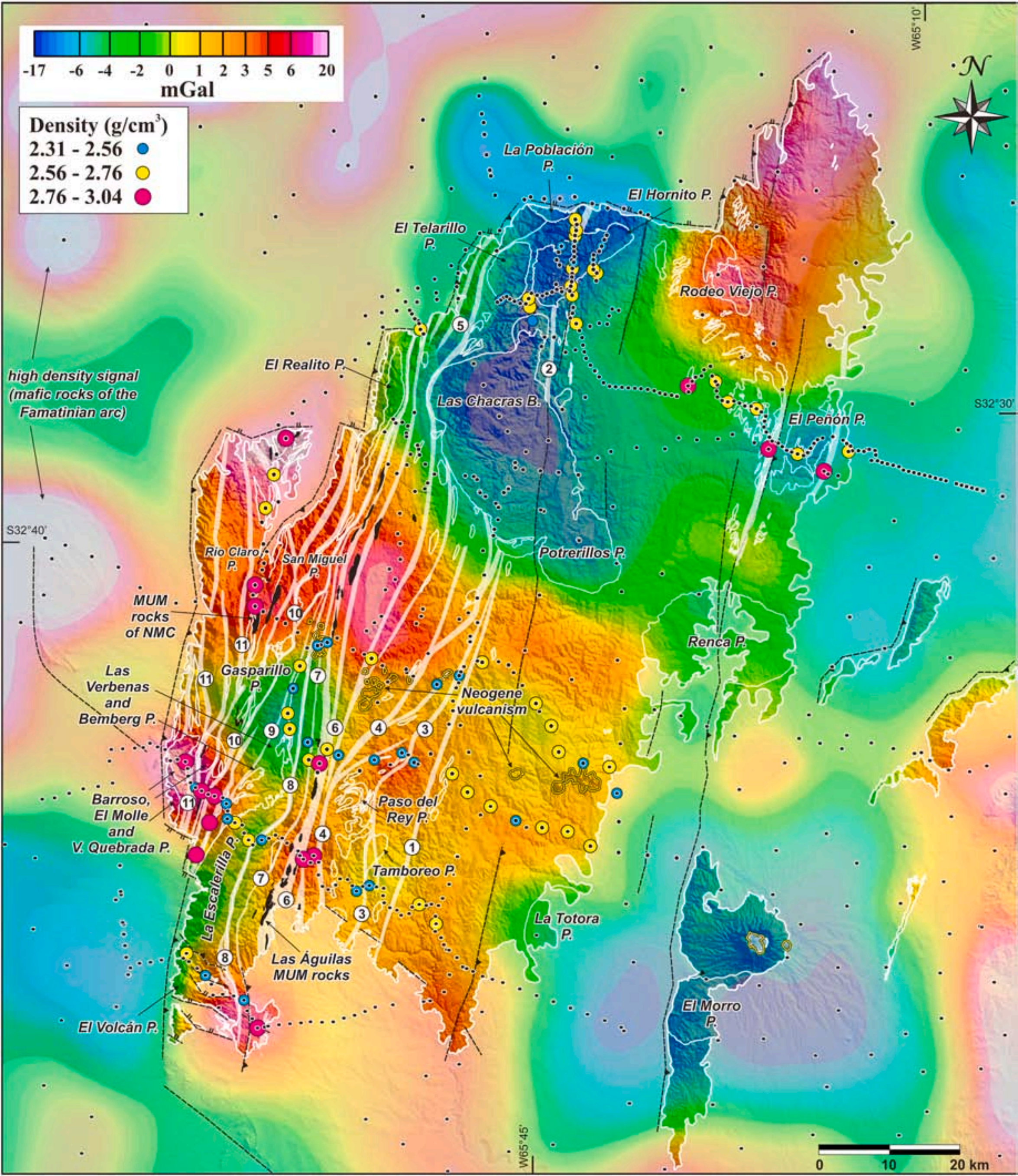

-17 -6 -4 -2 0 1 2 3 5 6 20
mGal
Density (g/cm^3)
2.31 - 2.56
2.56 - 2.76
2.76 - 3.04
W65°10'
S32°30'
S32°40'
W65°45'
high density signal (mafic rocks of the Famatinian arc)
La Población P.
El Hornito P.
El Telarillo P.
Rodeo Viejo P.
El Realito P.
Las Chacras B.
El Peñón P.
Río Claro P.
San Miguel P.
Potrerillos P.
MUM rocks of NMC
Renca P.
Gasparillo P.
Las Verbenas and Bemberg P.
Neogene vulcanism
Paso del Rey P.
Barroso, El Molle and V. Quebrada P.
Tamboreo P.
La Escalerilla P.
La Totora P.
Las Águilas MUM rocks
El Morro P.
El Volcán P.
0 10 20 km

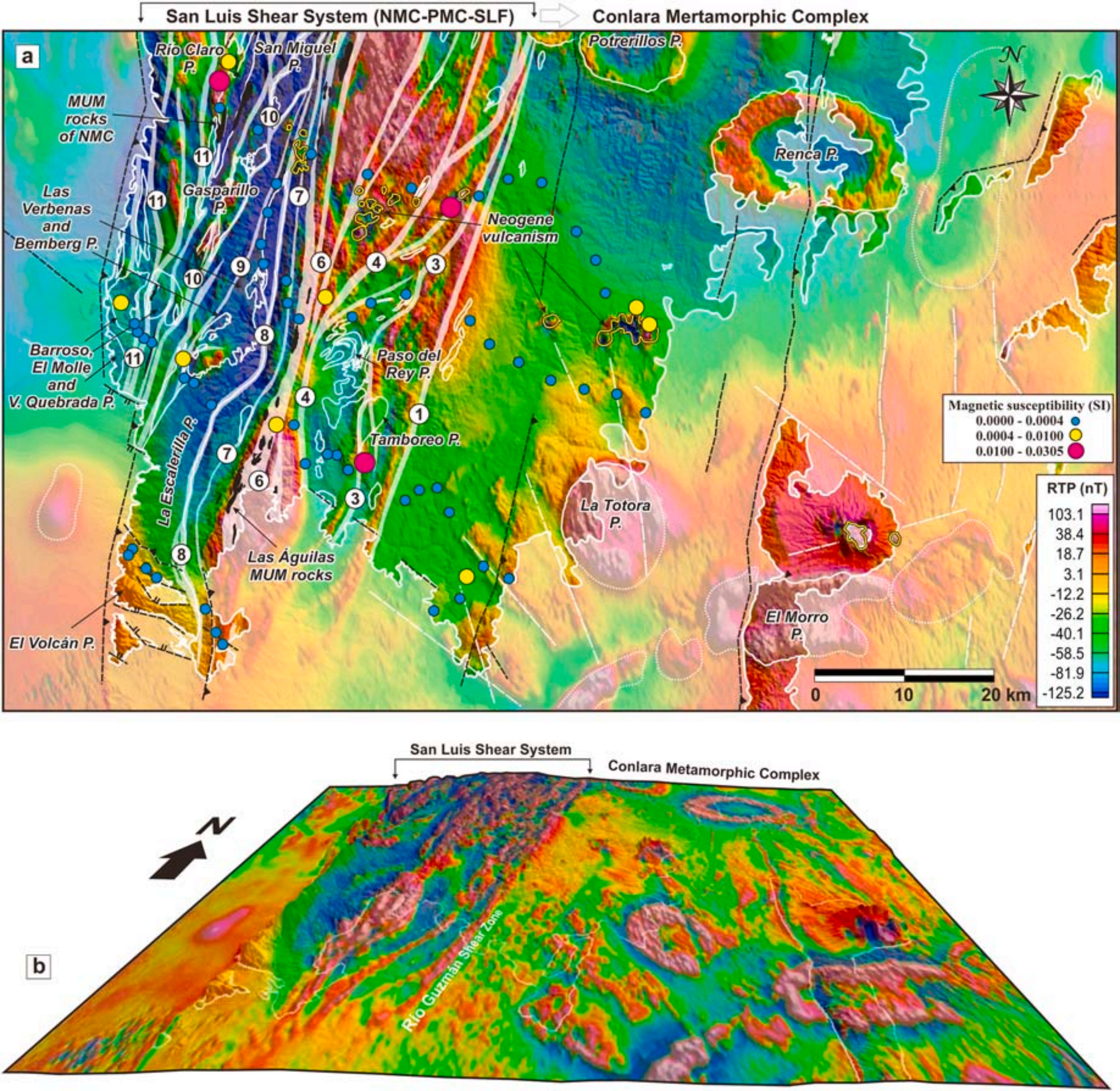
San Luis Shear System (NMC-PMC-SLF)
Conlara Mertamorphic Complex
a
Río Claro P.
San Miguel P.
Potrerillos P.
MUM rocks of NMC
Gasparillo P.
Las Verbenas and Bemberg P.
Neogene vulcanism
Renca P.
Barroso, El Molle and V. Quebrada P.
Paso del Rey P.
Tamboreo P.
La Escalerilla P.
Las Águilas MUM rocks
La Totora P.
El Morro P.
El Volcán P.
1
3
4
6
7
8
9
10
11
Magnetic susceptibility (SI)
0.0000 - 0.0004
0.0004 - 0.0100
0.0100 - 0.0305
RTP (nT)
103.1
38.4
18.7
3.1
-12.2
-26.2
-40.1
-58.5
-81.9
-125.2
0
10
20 km
b
San Luis Shear System
Conlara Metamorphic Complex
N
Río Guzmán Shear Zone

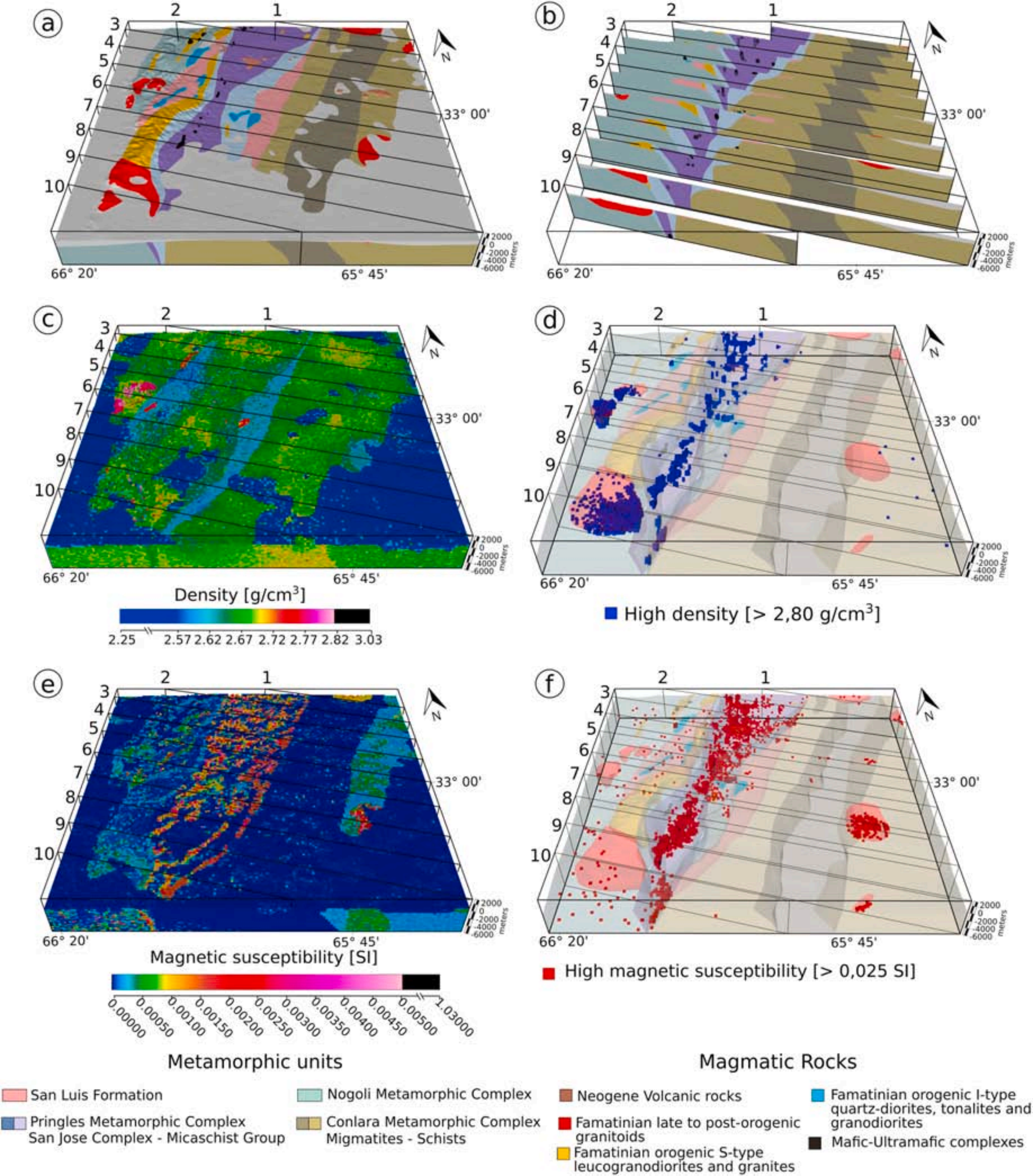
a
b
c
d
e
f
1
2
3
4
5
6
7
8
9
10
N
33° 00'
66° 20'
65° 45'
2000
0
-2000
-4000
-6000
meters
Density [g/cm3]
2.25
2.57
2.62
2.67
2.72
2.77
2.82
3.03
High density [> 2,80 g/cm3]
Magnetic susceptibility [SI]
0.00000
0.00050
0.00100
0.00150
0.00200
0.00250
0.00300
0.00350
0.00400
0.00450
0.00500
1.03000
High magnetic susceptibility [> 0,025 SI]
Metamorphic units
San Luis Formation
Pringles Metamorphic Complex
San Jose Complex - Micaschist Group
Nogoli Metamorphic Complex
Conlara Metamorphic Complex
Migmatites - Schists
Magmatic Rocks
Neogene Volcanic rocks
Famatinian late to post-orogenic granitoids
Famatinian orogenic S-type leucogranodiorites and granites
Famatinian orogenic I-type quartz-diorites, tonalites and granodiorites
Mafic-Ultramafic complexes

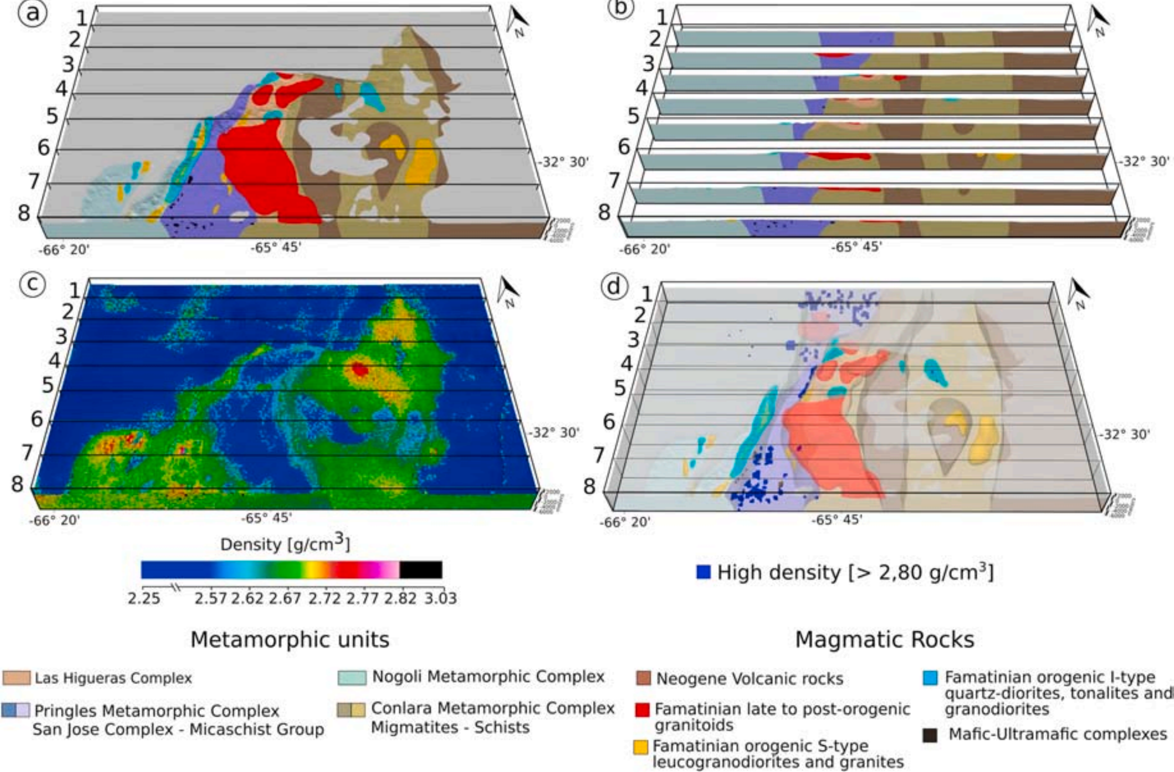

a
b
c
d
1
2
3
4
5
6
7
8
N
-32° 30'
-66° 20'
-65° 45'
Density [g/cm3]
2.25
2.57 2.62 2.67 2.72 2.77 2.82 3.03
High density [> 2,80 g/cm3]
Metamorphic units
Magmatic Rocks
Las Higueras Complex
Nogoli Metamorphic Complex
Pringles Metamorphic Complex
San Jose Complex - Micaschist Group
Conlara Metamorphic Complex
Migmatites - Schists
Neogene Volcanic rocks
Famatinian late to post-orogenic granitoids
Famatinian orogenic S-type leucogranodiorites and granites
Famatinian orogenic I-type quartz-diorites, tonalites and granodiorites
Mafic-Ultramafic complexes

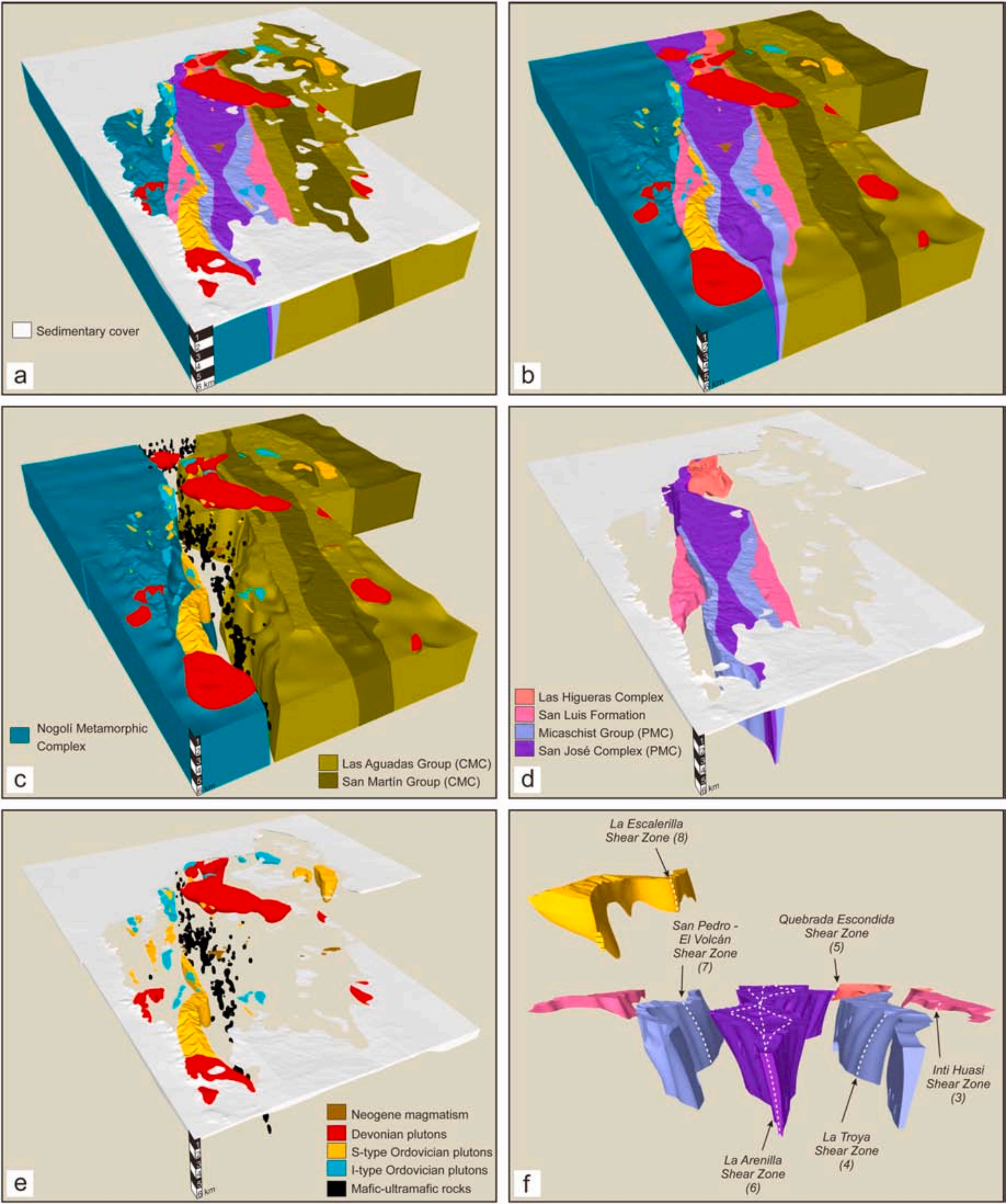

Sedimentary cover
a
b
Nogolí Metamorphic Complex
Las Aguadas Group (CMC)
San Martín Group (CMC)
c
Las Higueras Complex
San Luis Formation
Micaschist Group (PMC)
San José Complex (PMC)
d
Neogene magmatism
Devonian plutons
S-type Ordovician plutons
I-type Ordovician plutons
Mafic-ultramafic rocks
e
La Escalerilla Shear Zone (8)
San Pedro - El Volcán Shear Zone (7)
Quebrada Escondida Shear Zone (5)
Inti Huasi Shear Zone (3)
La Troya Shear Zone (4)
La Arenilla Shear Zone (6)
f
km

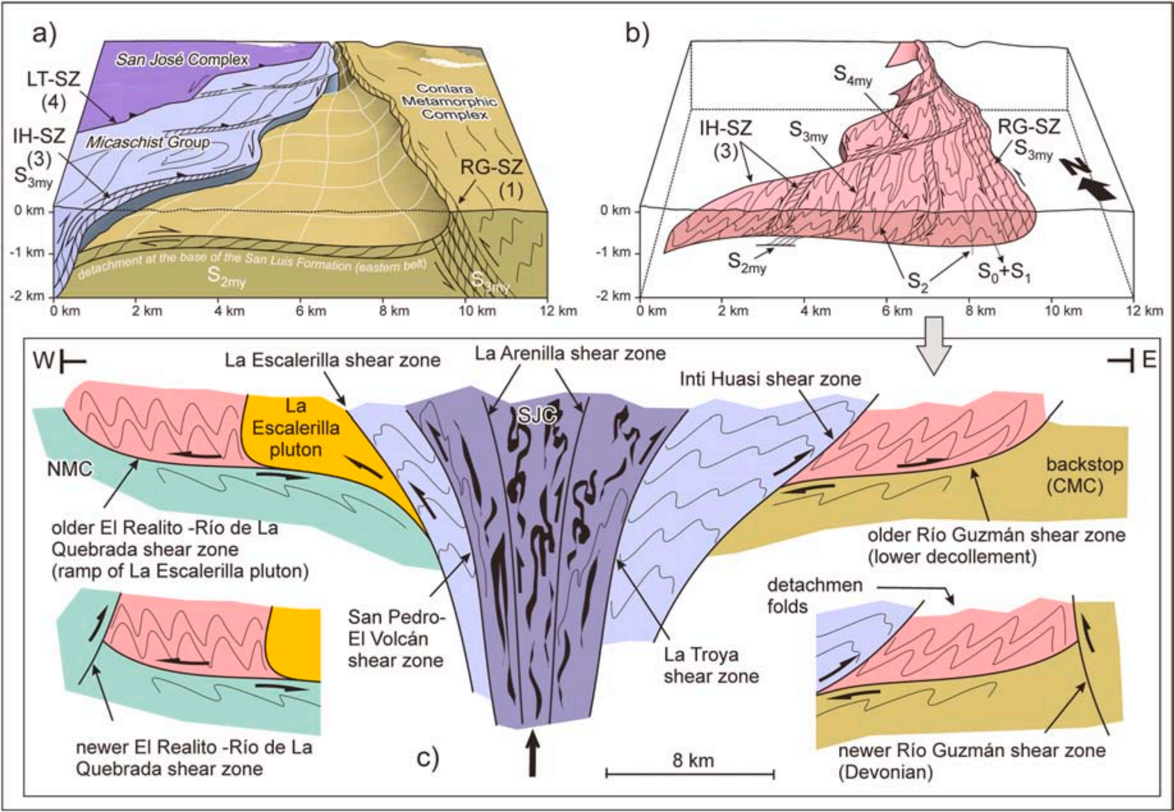

a)
San José Complex
LT-SZ
(4)
IH-SZ
(3)
S_{3my}
Micaschist Group
Conlara
Metamorphic
Complex
RG-SZ
(1)
0 km
-1 km
-2 km
detachment at the base of the San Luis Formation (eastern belt)
S_{2my}
S_{3my}
0 km
2 km
4 km
6 km
8 km
10 km
12 km
b)
S_{4my}
IH-SZ
(3)
S_{3my}
RG-SZ
S_{3my}
N
0 km
-1 km
-2 km
S_{2my}
S_2
S_0+S_1
0 km
2 km
4 km
6 km
8 km
10 km
12 km
W
E
La Escalerilla shear zone
La Arenilla shear zone
Inti Huasi shear zone
La Escalerilla pluton
SJC
NMC
backstop (CMC)
older El Realito -Río de La Quebrada shear zone (ramp of La Escalerilla pluton)
older Río Guzmán shear zone (lower decollement)
detachmen folds
San Pedro-El Volcán shear zone
La Troya shear zone
newer El Realito -Río de La Quebrada shear zone
c)
8 km
newer Río Guzmán shear zone (Devonian)

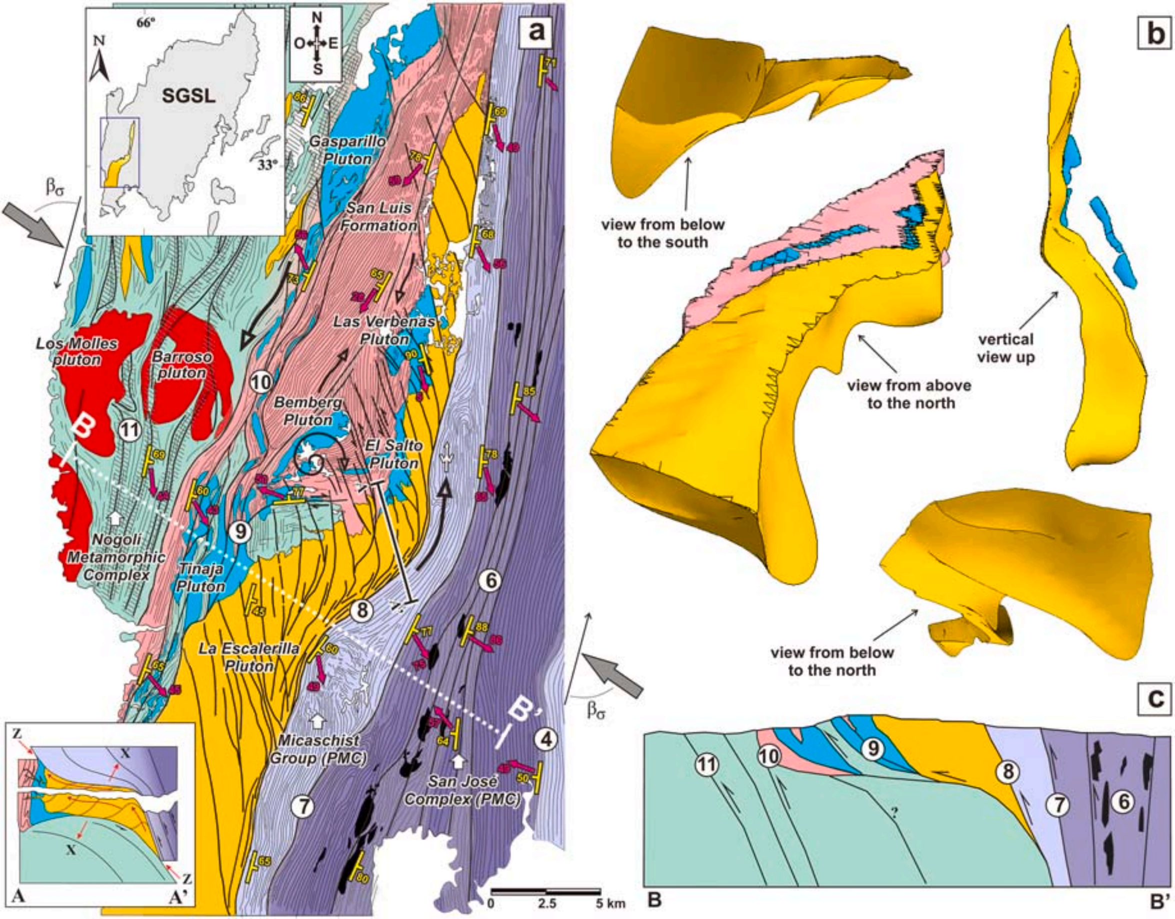

a
b
c
66°
33°
SGSL
N
O
E
S
Gasparillo Pluton
San Luis Formation
Las Verbenas Pluton
Los Molles pluton
Barroso pluton
Bemberg Pluton
El Salto Pluton
Nogolí Metamorphic Complex
Tinaja Pluton
La Escalerilla Pluton
Micaschist Group (PMC)
San José Complex (PMC)
B
B'
A
A'
Z
X
0
2.5
5 km
view from below to the south
view from above to the north
vertical view up
view from below to the north

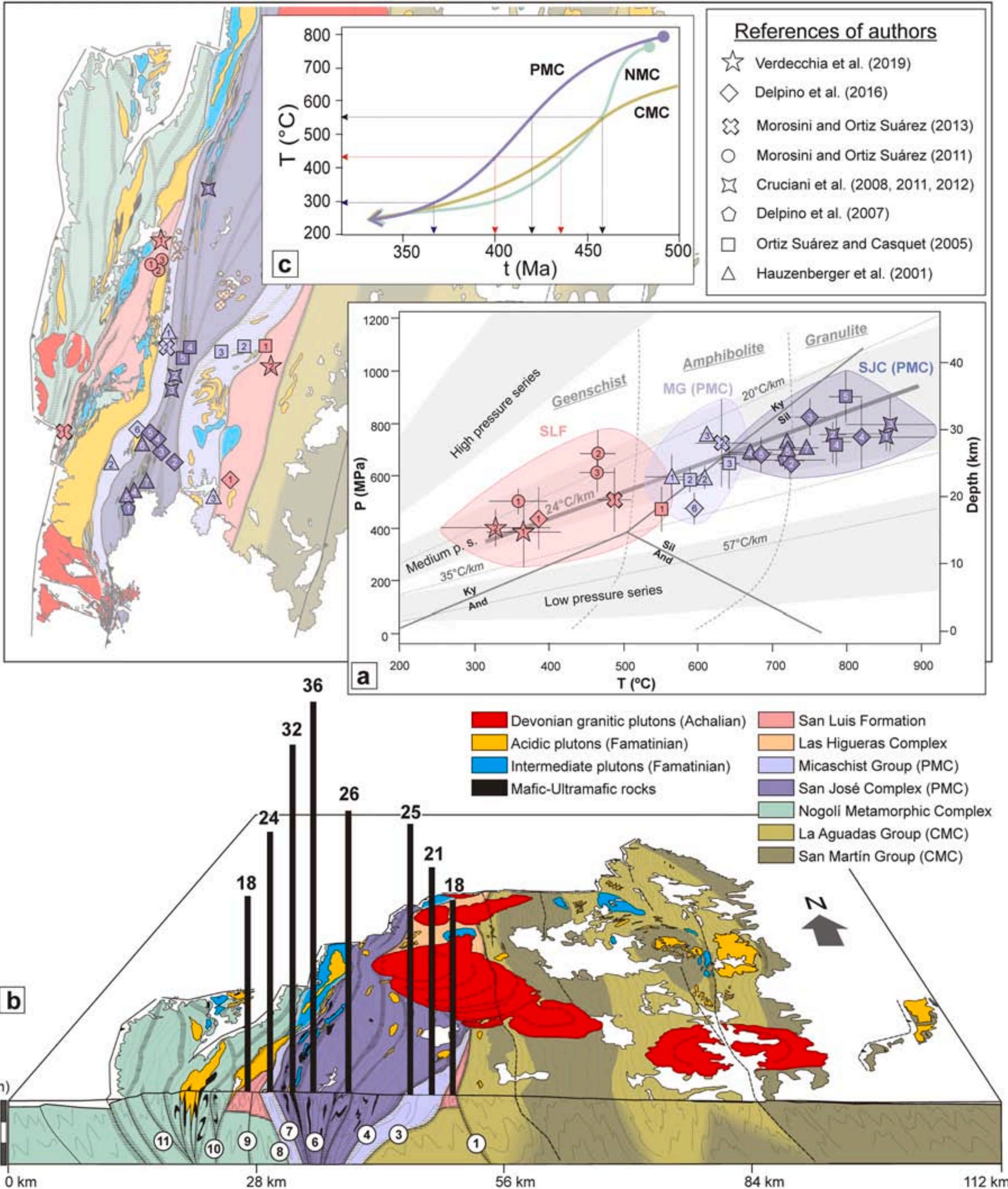

References of authors
Verdecchia et al. (2019)
Delpino et al. (2016)
Morosini and Ortiz Suárez (2013)
Morosini and Ortiz Suárez (2011)
Cruciani et al. (2008, 2011, 2012)
Delpino et al. (2007)
Ortiz Suárez and Casquet (2005)
Hauzenberger et al. (2001)
c
T (°C)
t (Ma)
PMC
NMC
CMC
a
P (MPa)
Depth (km)
T (ºC)
High pressure series
Geenschist
Amphibolite
Granulite
MG (PMC)
SJC (PMC)
SLF
20°C/km
24°C/km
35°C/km
57°C/km
Medium p. s.
Low pressure series
Ky
Sil
And
b
Devonian granitic plutons (Achalian)
Acidic plutons (Famatinian)
Intermediate plutons (Famatinian)
Mafic-Ultramafic rocks
San Luis Formation
Las Higueras Complex
Micaschist Group (PMC)
San José Complex (PMC)
Nogolí Metamorphic Complex
La Aguadas Group (CMC)
San Martín Group (CMC)
N
(km)
0 km
28 km
56 km
84 km
112 km

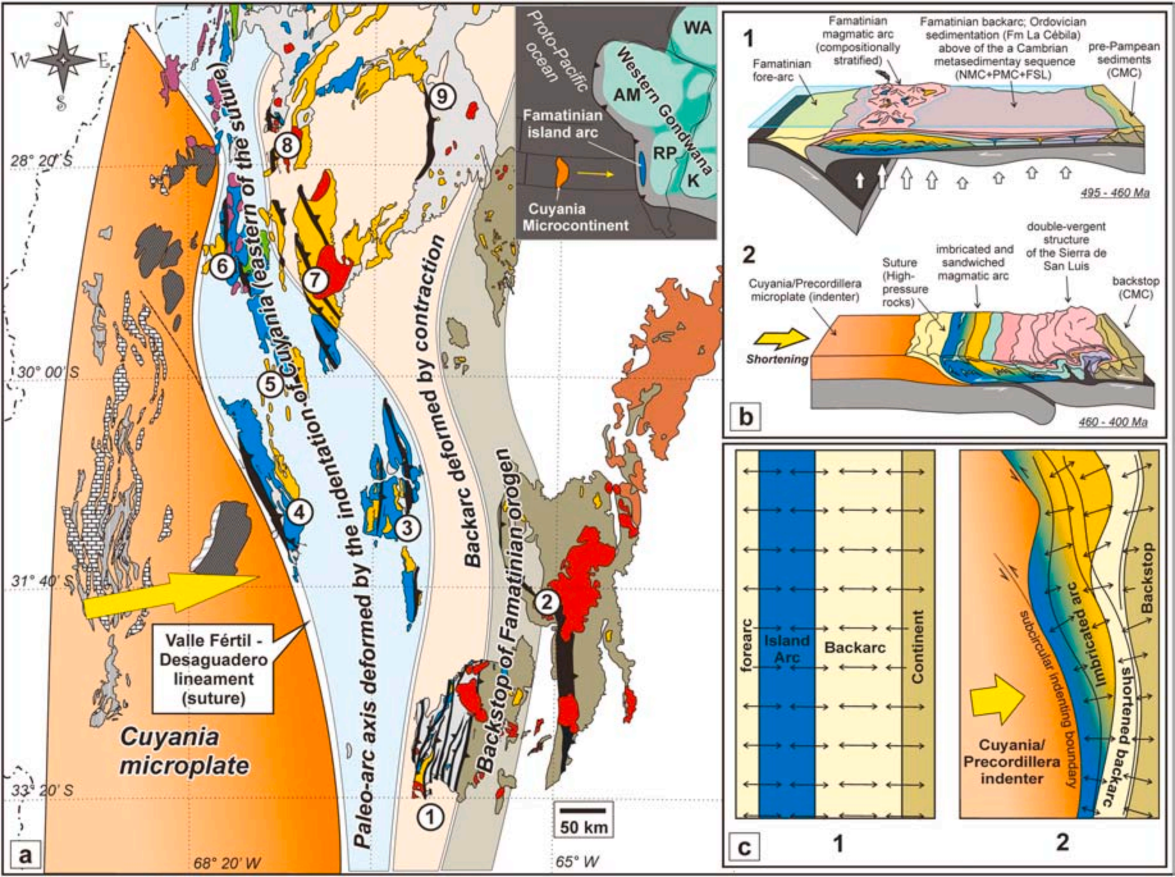

Proto-Pacific ocean
WA
Western Gondwana
AM
Famatinian island arc
RP
K
Cuyania Microcontinent
28° 20' S
30° 00' S
31° 40' S
33° 20' S
68° 20' W
65° W
Cuyania (eastern of the suture)
Paleo-arc axis deformed by the indentation of Cuyania
Backarc deformed by contraction
Backstop of Famatinian orogen
Valle Fértil - Desaguadero lineament (suture)
Cuyania microplate
50 km
a
1
Famatinian fore-arc
Famatinian magmatic arc (compositionally stratified)
Famatinian backarc; Ordovician sedimentation (Fm La Cébila) above of the a Cambrian metasedimentay sequence (NMC+PMC+FSL)
pre-Pampean sediments (CMC)
495 - 460 Ma
2
Cuyania/Precordillera microplate (indenter)
Suture (High-pressure rocks)
imbricated and sandwiched magmatic arc
double-vergent structure of the Sierra de San Luis
backstop (CMC)
Shortening
460 - 400 Ma
b
forearc
Island Arc
Backarc
Continent
subcircular indenting boundary
Imbricated arc
shortened backarc
Backstop
Cuyania/ Precordillera indenter
c
1
2

Highlights

- The main features of a shear system located in the Sierra de San Luis are detailed
- The results of a 3D litho-constrained geophysical model are presented
- Metamorphic conditions and deformation mechanisms on an orogenic scale are evaluated
- A double-vergent structure is produced by the backarc closing due to the push of an indenter

Declaration of interests

☒ The authors declare that they have no known competing financial interests or personal relationships that could have appeared to influence the work reported in this paper.

☐The authors declare the following financial interests/personal relationships which may be considered as potential competing interests: